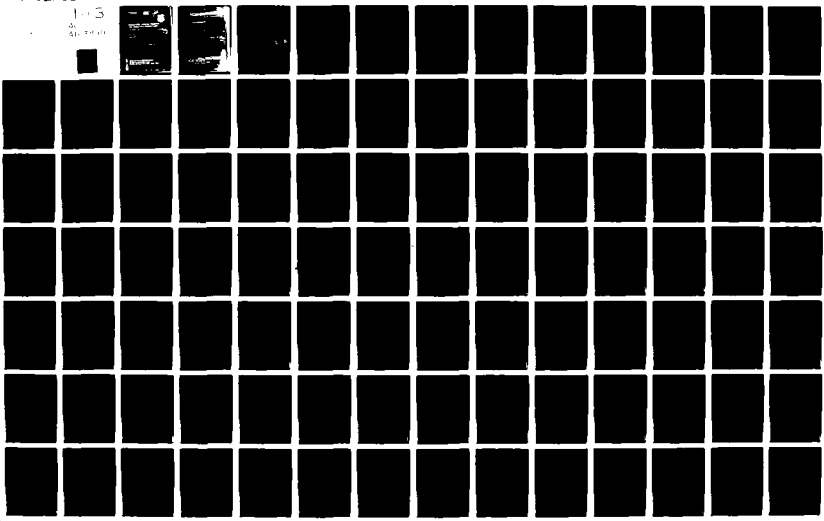


AD-A103 899

ATLANTIC RESEARCH CORP ALEXANDRIA VA  
INTRASYSTEM ANALYSIS PROGRAM (IAP) STRUCTURAL DESIGN STUDY.(U)  
JUN 81 W G DUFF, L D THOMPSON, H K SCHUMAN F30602-77-C-0150  
UNCLASSIFIED ARC-53-6111 RADC-TR-81-133 NL

F/G 20/3

103  
20  
NL



ADA103899

SEARCHED  
INDEXED  
SERIALIZED  
FILED  
FEB 27 1968  
FBI - MEMPHIS

1968-10000

## UNCLASSIFIED

SECURITY CLASSIFICATION OF THIS PAGE (When Data Entered)

19 REPORT DOCUMENTATION PAGE		READ INSTRUCTIONS BEFORE COMPLETING FORM
1. REPORT NUMBER <b>(18) RADC-TR-81-133</b>	2. GOVT ACCESSION NO. <b>AD-A103 899</b>	3. RECIPIENT'S CATALOG NUMBER
4. TITLE (and Subtitle) <b>INTRASYSTEM ANALYSIS PROGRAM (IAP) STRUCTURAL DESIGN STUDY.</b>	5. TYPE OF REPORT & PERIOD COVERED <b>Final Technical Report, 1977 - 1981,</b>	6. PERFORMING ORG. REPORT NUMBER <b>ARC 53-6111</b>
7. AUTHOR(s) <b>William G. Duff Harvey K. Schuman</b>	8. CONTRACTOR OR GRANT NUMBER(s) <b>F30602-77-C-0150 New</b>	9. CONTRACTOR OR GRANT NUMBER(s)
10. PERFORMING ORGANIZATION NAME AND ADDRESS <b>Atlantic Research Corporation Alexandria VA 22314</b>	11. PROGRAM ELEMENT, PROJECT, TASK AREA & WORK UNIT NUMBERS <b>62702F 23380309</b>	12. REPORT DATE <b>Jun 1981</b>
11. CONTROLLING OFFICE NAME AND ADDRESS <b>Rome Air Development Center (RBCT) Griffiss AFB NY 13441</b>	13. NUMBER OF PAGES <b>225</b>	14. SECURITY CLASS. (of this report) <b>UNCLASSIFIED</b>
14. MONITORING AGENCY NAME & ADDRESS (if different from Controlling Office) <b>Same</b>	15. DECLASSIFICATION/DOWNGRADING SCHEDULE <b>N/A</b>	16. DISTRIBUTION STATEMENT (of this Report)  <b>Approved for public release; distribution unlimited.</b>
17. DISTRIBUTION STATEMENT (of the abstract entered in Block 20, if different from Report)  <b>Same</b>	<b>DTIC SELECTED SEP 8 1981</b>	
18. SUPPLEMENTARY NOTES <b>RADC Project Engineer: Gerard T. Capraro (RBCT)</b>		
19. KEY WORDS (Continue on reverse side if necessary and identify by block number) <b>Electromagnetic Compatibility Method of Moments Geometrical Theory of Diffraction</b>	<b>Physical Theory of Diffraction Mathematical Models Radiation and Scattering</b>	
20. ABSTRACT (Continue on reverse side if necessary and identify by block number)  <b>The Intrasystem Analysis Program is a collection of computer codes used in analyzing the electromagnetic compatibility of aircraft, space/satellite, and ground-based systems. The IAP is reconsidered here in terms of an overriding framework. The concept of a procedure is introduced whereby emitter, receptor, and coupling models are grouped and interfaced for efficient use in EMC analysis. All aspects impacting the construction of a procedure are considered in detail. These include</b>		

045550

7

**UNCLASSIFIED**

**SECURITY CLASSIFICATION OF THIS PAGE(When Data Entered)**

data; task; systems equations; emitter, receptor, and coupling models; computer resources; accuracy; and intended user. The attributes of many existing, or soon to be available, coupling models are tabulated for ready reference during the construction of procedures. The wide range of problems amenable to these coupling models is made apparent through grouping into "basic" and "combined" categories.

Accession No.		
NTIS SP&I	<input checked="" type="checkbox"/>	
DTIC TIR	<input type="checkbox"/>	
Unnumbered	<input type="checkbox"/>	
Justification	<input type="checkbox"/>	
By _____		
Distribution/		
Availability Codes		
Avail and/or		
Dist	Special	
A		

**UNCLASSIFIED**

**SECURITY CLASSIFICATION OF THIS PAGE(When Data Entered)**

## TABLE OF CONTENTS

<u>Section</u>	<u>Title</u>	<u>Page</u>
1.0	INTRODUCTION . . . . .	1-1
2.0	CONCLUSIONS AND RECOMMENDED FUTURE DEVELOPMENT . . . . .	2-1
3.0	EMC PROCEDURE SYNTHESIS . . . . .	3-1
	3.1 Task . . . . .	3-2
	3.2 Available Data . . . . .	3-2
	3.3 Additional Constraints . . . . .	3-8
	3.3.1 Computer Resources . . . . .	3-9
	3.3.2 Accuracy . . . . .	3-16
	3.3.3 Usability . . . . .	3-17
	3.4 Guide to Procedure Construction. .	3-18
4.0	SYSTEMS EQUATIONS . . . . .	4-1
	4.1 Waveform Systems Equations . . . .	4-1
	4.2 Parameter Systems Equations. . . .	4-5
5.0	EMITTER MODELS . . . . .	5-1
	5.1 Frequency Domain Emitter Models. .	5-1
	5.1.1 Current IAP Models . . . . .	5-2
	5.1.2 Recommended Additional Models. .	5-2
	5.2 Time Domain . . . . .	5-6
	5.2.1 Current IAP Models . . . . .	5-7
	5.2.2 Recommended Additional Models. .	5-7
6.0	RECEPTOR MODELS . . . . .	6-1
	6.1 Present IAP Receptor Models. . . .	6-1
	6.2 Recommended Additional Models. . . .	6-1
	6.2.1 System Level Nonlinear Receptor Models . . . . .	6-1
	6.2.2 Time Domain Receptor Models. . . .	6-3
	6.2.3 User Defined Susceptibility. . . .	6-4
7.0	COUPLING MODELS . . . . .	7-1
	7.1 Basic and Combined Coupling Models	7-1
	7.2 Summary . . . . .	7-84

TABLE OF CONTENTS (CONTINUED)

<u>Section</u>	<u>Title</u>	<u>Page</u>
APPENDIX A	BASIC COUPLING MODELS . . . . .	A-1
A.1	FREQUENCY DOMAIN . . . . .	A-1
	A.1.1 Low to Medium Frequency Ratiation and Scattering . . . . .	A-1
	A.1.1.1 Thin Wires . . . . .	A-3
	A.1.1.2 Conducting Surfaces . . . . .	A-30
	A.1.1.3 Conducting Bodies of Revolution	A-38
	A.1.1.4 Material Bodies - Surface Current Formulation . . . . .	A-44
	A.1.1.5 Material Bodies of Revolution . .	A-45
	A.1.1.6 Material Bodies - Volume Current Formulation . . . . .	A-49
A.1.2	HIGH FREQUENCY . . . . .	A-51
	A.1.2.1 Free Space Transmission . . . . .	A-52
	A.1.2.2 Geometrical Optics . . . . .	A-54
	A.1.2.3 Geometrical Theory of Diffraction	A-60
	A.1.2.4 Physical Theory of Diffraction . .	A-63
A.1.3	TRANSMISSION LINE . . . . .	A-64
	A.1.3.1 Transmission Line Equations . . . .	A-65
	A.1.3.2 State Vector Representation of TML Equations . . . . .	A-65
	A.1.3.3 Multiconductor Transmission Lines	A-66
	A.1.3.4 Cross Coupling Within Transmission Line Bundles . . . . .	A-67
	A.1.3.5 Lumped Circuit TML . . . . .	A-69
	A.1.3.6 Weak Coupling TML . . . . .	A-70
	A.1.3.7 Transmission Line Per-Unit- Length Parameters . . . . .	A-71
A.2	TIME DOMAIN . . . . .	A-72
	A.2.1 Radiation and Scattering . . . . .	A-72
	A.2.1.1 Singularity Expansion Method . .	A-72
	A.2.1.2 Time Marching: Finite Difference	A-73
	A.2.1.3 Time Marching: Current Expansion	A-74
	A.2.2 Transmission Line . . . . .	A-74

TABLE OF CONTENTS (CONCLUDED)

<u>Section</u>	<u>Title</u>	<u>Page</u>
APPENDIX B	COMBINED COUPLING MODELS . . . . .	B-1
B.1	LOW TO MEDIUM FREQUENCY RADIATION AND SCATTERING . . . . .	B-1
	B.1.1 Thin Wires and Surfaces - Frequency Domain . . . . .	B-1
	B.1.2 Material Bodies - Frequency Domain	B-1
B.2	HIGH FREQUENCY . . . . .	B-9
	B.2.1 Curved Surfaces with Edges . . . . .	B-9
	B.2.2 Combined GTD Moment Methods . . . . .	B-11
B.3	TIME DOMAIN . . . . .	B-12
B.4	BRANCHED TRANSMISSION LINE . . . . .	B-13
APPENDIX C	SYSTEMS EQUATIONS - DERIVATIONS . . . . .	C-1
C.1	WAVEFORM SYSTEMS EQUATIONS . . . . .	C-1
	C.1.1 Continuous Spectrum . . . . .	C-1
	C.1.2 Discrete Spectrum . . . . .	C-4
C.2	PARAMETER SYSTEMS EQUATIONS . . . . .	C-5
	C.2.1 Average Power-Deterministic Waveform	C-5
	C.2.2 Average Power-Stochastic Waveform .	C-7
	C.2.3 Total Energy-Deterministic Waveform	C-7
	C.2.4 Total Energy-Stochastic Waveform .	C-9
	C.2.5 Peak Current-Deterministic Waveform	C-10
	C.2.6 Peak Current-Stochastic Waveform .	C-11
	C.2.7 Rise Time . . . . .	C-14
APPENDIX D	SYSTEM LEVEL AND IAP CODES . . . . .	D-1
APPENDIX E	REFERENCES . . . . .	E-1

#### ACKNOWLEDGEMENT

The authors gratefully acknowledge contributions and guidance from G. T. Capraro, RADC; C. R. Paul, University of Kentucky; D. D. Weiner, and P. B. Berra, Syracuse University; and T. W. Doeppner, Jr., Brown University.



## ABSTRACT

The Intrasystem Analysis Program is a collection of computer codes used in analyzing the electromagnetic compatibility of aircraft, space/satellite, and ground-based systems. The IAP is reconsidered here in terms of an overriding framework. The concept of a procedure is introduced whereby emitter, receptor, and coupling models are grouped and interfaced for efficient use in EMC analysis. All aspects impacting the construction of a procedure are considered in detail. These include data; task; systems equations; emitter, receptor, and coupling models; computer resources; accuracy; and intended user. The attributes of many existing, or soon to be available, coupling models are tabulated for ready reference during the construction of procedures. The wide range of problems amenable to these coupling models is made apparent through grouping into "basic" and "combined" categories.



## 1.0 INTRODUCTION

The Intrasystem Analysis Program (IAP) is a collection of computer codes used in analyzing electromagnetic compatibility (EMC) problems for aircraft, space/satellite, and ground-based systems. The IAP effort is directed by the Compatibility Branch (RADC/RBCT), Rome Air Development Center, Air Force Systems Command, Griffiss Air Force Base, New York. This report describes the framework within which a "second-generation" IAP is being developed. It contains an assessment of available methods that perhaps should be included in the IAP. Specific areas that must be developed further are indicated.

The underlying principle used throughout this document is the concept of a "procedure". A procedure is primarily a collection of emitter models (e.g., an incident plane wave), receptor models (e.g., the  $\tilde{E}$ -field at a point in space or the skin current induced on a metal box), and coupling models (e.g., antenna, transmission, and propagation models). These generalized definitions extend the IEMCAP (Section D.1.1) use of the terms to all of IAP.

The major aspects of a procedure are described in Section 3. An example of the process of constructing a procedure is described together with tables that facilitate the choice of coupling models. These tables refer to tables in Section 7, which conveniently summarize important attributes of the coupling models. More elaborate discussions of coupling models are contained in Appendices A and B.

IEMCAP is the current "system level" computer code in IAP. It comprises many relatively simple emitter, receptor, and coupling models and the mechanisms (systems equations) for grouping them to assess the EMC of a complex system. IEMCAP, a number of system level codes, and other IAP codes are described briefly in Appendix D.

## 2.0

CONCLUSIONS AND RECOMMENDED FUTURE DEVELOPMENT

The IAP designer\* must identify procedures with which an IAP analyst (user) can conduct intrasystem analyses. The designer must choose from many emitter, receptor, and coupling models and then group and interface them, taking into account task requirements, available structural and electrical data, receptor performance criteria, computer resources, accuracy constraints, and user competence.

This report is designed to serve as a guide in constructing procedures and identifying those aspects of the IAP that require further development. A summary of important coupling models comprises a major part. The often complex coupling medium (occasionally referred to as the "coupling path") necessitates careful modeling considerations. It often is necessary to model a complex structure by using relatively simple components; for example, an aircraft may be modeled with standard geometric shapes: cylinder (fuselage), cone (nose), and quadrilateral surfaces (wings and tail). It is not always clear which characteristics must be preserved during modeling to avoid significant differences between analytical and actual results.

Many coupling models are available that can accurately analyze complex structures; e.g. nonuniform transmission lines, inhomogeneous grounds, and odd-shaped aircraft. The applicability of these models can be increased significantly through use of presently available combining techniques and through further development of combining techniques. The concept of basic coupling models and combined coupling models thus is emphasized. Only coupling models of general applicability are considered. Many of these are found to be of the "moment method" or "geometrical theory of diffraction" types.

A general conclusion is that only "worst-case" analyses will be feasible for most near future EMC problems.

\* An IAP designer develops and maintains the IAP. An IAP analyst uses the IAP to solve EMC problems.

It often is difficult to preserve phase throughout a coupling path and, when more than one emitter is present or there are multiple coupling paths, preservation of phase is important. Under "worst-case" philosophy, as in IEMCAP, all responses at a receptor are assumed to add in phase. This results in an upper bound to interference prediction; thus, potential EMI problems are not likely to be missed. To avoid unnecessary analysis and experiment, or system "overhardening," an additional goal of an IAP improvement is to minimize overprediction.

Coupling models are discussed in Sections 3.4 and 7.0 and presented in detail in Appendices A and B. Some particular recommendations based upon these descriptions are given below.

A time-domain finite-difference or finite-element model (FE-TD) has the advantage of almost complete generality: media may be inhomogeneous, anisotropic, or nonlinear (Section A.2.1.2); however, the underlying method solves Maxwell's equations for  $E$ - and  $H$ -fields in time-stepping fashion. This results in a rapid increase in required computer memory and CPU time with structure size. The application to relatively small, yet highly complex, bodies suggests combining FE-TD with other models. This is being investigated through an RADC/RBCT contract.

A triangular  $E$ -field surface patch moment method model (SPE-FD) has been developed recently (Section A.1.1.2) and should be incorporated into the IAP, either alone or in combination with other computer codes such as GEMACS (Section D.2.1). The advantage of triangular patches over rectangular patches is that the former provides a better fit for curved surfaces with curved edges. The advantage of an  $E$ -field formulation over an  $H$ -field formulation is that the former can apply to thin surfaces; e.g., wings and solar panels. The AMP

[AMP, July 1972], NEC [Burke, July 1977], and GEMACS codes incorporates a surface H-field formulation; therefore, such conducting surfaces must be treated by wire gridding with many associated uncertainties, especially if induced surface current is desired.

High-frequency techniques based on ray theory (such as the geometrical theory of diffraction) have been developed and computer programmed with applicability to a limited number of scatterer types. These models now are sufficiently proven to begin including them in the IAP. Other theories, such as the physical theory of diffraction and the spectral theory of diffraction, should be considered in the future. These are of greater applicability than the ray theory methods; however, they presently are too complicated for implementation in a general computer code.

There are many transmission line models that should be included in the IAP. These include a twisted pair model (Section D.2.4), a model that accounts for cable clamps and ribs [Tesche, Dec. 1976; Coen, Sept. 1977], a branching and multiple termination model [Paul, Oct. 1979; Tesche, March 1979; Tesche, July 1975; Liu, Sept. 1977; Giri, Sept. 1978; Baum, Nov. 1978], and a stacked ribbon cable model [Paul, Feb. 1978; Paul, 1977]. However, more effort is needed in developing transmission line models that handle combinations of wire types (e.g., shielded wires, shielded groups, twisted pairs).

The successful application of a model generally requires a minimum knowledge of the system being modeled. That knowledge is not always at hand; for example, an RF circuit analysis of an audio circuit requires an understanding of circuit component behavior at RF. This behavior is often difficult to measure accurately or to obtain through theoretical

analysis [Whalen, Nov. 1979]. Out-of-band input and output impedances of many devices that terminate transmission lines can be crucial to accurate transmission line analyses. These impedances often are not known. As a third example, a coupling model that accurately predicts the scattering from a missile plume is of limited value if the electrical properties (conductivity, etc.) of the plume are not known accurately. Thus, realization of the full potential of coupling models requires, for example, further development of (1) theoretical and experimental models for analyzing the chemical nature of matter and (2) measurement techniques, especially "out-of-band."

Besides coupling models, a second major weakness within the IAP, and EMC modeling in general, is limited knowledge of receptor performance criteria. The input waveform parameters that most affect receptor performance are not always obvious. An even more difficult problem is judging the level of the parameters which, if exceeded, induce interference. A study of the performance criteria of many receptors, both analog and digital is, therefore, clearly warranted.

## 3.0

EMC Procedure Synthesis

A principal motivation for this work is the need for guidelines in constructing procedures applicable to the evaluation of the electromagnetic compatibility (EMC) of a myriad of electronic systems either ground based, aircraft, space/missile or simply an "equipment". The construction of such procedures is a principal task of the IAP designer. An EMC analysis of electronic systems is usually quite complicated. The large number of electronic components, irregular geometries, incomplete knowledge of system components, and usually limited time and money are among the reasons calling for powerful, versatile analytical tools at the EMC analyst's disposal. The application of these tools should require only an understanding of their underlying assumptions and limitations and not a detailed knowledge of their construction or theory. The analyst (as opposed to IAP designer) should not need to create new tools for each analysis.

These analytical tools are called procedures. A procedure is a combination of electromagnetic emitter, receptor, and coupling (transfer) models interfaced in accordance with systems equations. A procedure can be assembled in the form of computer codes to perform one or more tasks. An example of a "system level" code of this type is IEMCAP [Paul, A Summary of Models in IEMCAP]. However, new procedures are needed to satisfy the expanding reliance upon analysis. These new procedures must interface emerging analytical models with existing tested ones.

Considerations impacting the choice of a procedure are discussed in the following subsections. These are labeled task, available data, and additional constraints. Other factors - emitter models, receptor models, coupling models, and systems equations - are each treated in a separate subsequent section.

### **3.1      Task**

All components of an electronic system must operate in harmony with each other: 400 Hz power line emissions should not appear on logic circuits, digital signals flowing between logic circuits should not interact unintentionally with other logic circuits, radar signals should not unintentionally excite logic circuits or electro-explosive devices, etc. A major function of the EMC analyst, therefore, is to predict whether an emission is likely to induce interference at a receptor.

To perform this function, the EMC analyst must evaluate the electronic system by measurements and by analytical procedures. Each procedure is guided by a purpose or task to be performed. The analyst must identify these tasks. For example, a task can be "one-on-one" such as in determining the field at a desired location due to a single transmitter. A task can also be "many-on-one", e.g., the evaluation of the compatibility of a single receiver in an environment of many emitters. A third type of task is the frequency assignment of many receivers among many emitters.

### **3.2      Available Data**

The data available for analyzing an electronic system are generally a function of the system's life cycle. The various phases that comprise a life cycle will be discussed shortly. The availability of data impacts the selection and design of procedures chosen for EMC analyses appropriate to these phases. Some procedures, such as those containing moment method coupling models, usually require structure geometry specified to within fractions of a wavelength while other procedures require only approximate structural representations perhaps in terms of generic shapes. Also the electrical characteristics needed by procedures can be as detailed as time waveforms or as superficial as frequency bands of operation.

There are five phases to the life cycle of an electronic system [Freeman, December 1977]: conceptual, validation, full scale development, production, and deployment. The major aspects of each phase are summarized in Table 3.2-1. The available data increase as the system progresses through these phases. The extent of the data at each phase is dependent upon the degree to which "off the shelf" equipment is included in the electronic system. Table 3.2-2 is a summary of the types and/or complexity of data expected to be available at each phase.

Since the complexity of an EMC analysis is limited by the data available, the procedures at the EMC analyst's disposal must be correspondingly flexible in data input needs. This flexibility can be incorporated into procedures, constructed by an "IAP designer," by choosing and developing emitter, receptor, and coupling models which vary in complexity since complexity directly impacts data needs.

The electrical characteristics of a system are an important consideration in the construction and choice of a procedure. For example if equipment operating frequencies and bandwidths are available then a frequency allocation procedure is applicable. This procedure would include harmonic and intermodulation models and would be useful during any of the five life cycle phases. Furthermore, if power output and susceptibility levels are known then the frequency allocation could be expanded to include emitter and receptor models more representative than simple "step functions" in the frequency domain.

Also many coupling models require waveform source descriptions in terms of amplitude versus frequency. Other models require phase information as well or complete time waveforms. These more sophisticated models are likely to be less applicable during the early phases of a system's life cycle where phase or time waveform data are usually scarce.

Table 3.2-1  
Summary of 5 Phases of Acquisition Life Cycle [Freeman, Dec. 1977]

Conceptual Phase

- Required Operational Capability (ROC)
- Mission Analysis
- Tradeoff Studies
- Alternative Concepts
- Feasibility Studies
- Experimental Hardware Development and Evaluation
- Risk Assessments
- System Functional Baseline

Validation Phase

- Define Technical Objectives
- Define Operational Deployment Concepts
- Pinpoint and Resolve High Risk Areas
- Establish Performance Specifications
- Evaluate Tradeoffs
- Hardware Development and Evaluation
- Prototype Demonstration
- System Definition
- Category I Tests - Subsystem/System Level
- Prepare RFP

Full-Scale Development

- System and Equipment Design
- System and Equipment Fabrication
- System and Equipment Test and Evaluation
- Define Total System Configurations
- Define Equipments
- Output: Production System  
Documentation  
Test Results

Table 3.2-1 (Continued)

Production Phase

- Production and Development of All Principal and Support Equipment

Deployment Phase

- First Unit To Phase Out
- Overlaps Production Phase
- Evaluation of Hardware Performance and Operational Procedures

Table 3.2-2  
Data Available Versus Phases of Life Cycle

Conceptual

- System Component Function Definitions
- Organizations Responsible for Each System Component
- Generic System Component
  - Power Circuits
  - Communication Circuits
  - Telemetry Circuits
  - Data Processing Circuits
- Expected Geometry
  - Size
  - Weight
  - Generic Shape

Validation

- Characteristics of Individual Component
  - Power Requirements
  - Time Waveforms
  - Spectrum
  - Susceptibility
- Prototype Specifications
  - Geometric Data
  - Schematics and Diagrams
  - Material Characteristics
- Support Equipment Characteristics

Full Scale Development

- Geometric Data
  - Shape and Surface Information
  - Wire Routing
  - Component Locations
- Test Results

Table 3.2-2 (Continued)

Production

- Measured Data Production Sample
- Refined Data on Geometry and Electrical Characteristics
- Description of Equipment Down To Brand Names

Deployment

- Maintenance Statistics
- Modification Specifications

Transmission line models, as a third example, require termination impedance information. If these terminations are equipment ports then the termination impedance values are rarely known outside of the equipment's operating frequencies. In addition, the reactive component of these port impedances, due to parasitic capacitances, etc., is often not available at any frequency. Also additional concerns are introduced by logic circuits where impedances are a function of "state" as well as frequency. Thus, the choice of model to include within a procedure is highly dependent on the electrical, as well as structural, data available.

The performance criteria of system components are another type of data impacting the choice of models and systems equations and, hence, procedures. The performance criteria of a component are its characteristics when viewed as a receptor, such as performance degradation curves, performance degradation thresholds, etc., necessary for determining parameters pertinent to conducting EMC analyses. A performance criterion could, for example, relate the fluctuation of a fuel gauge to a time waveform impinging on the gauge sensor-to-meter cable. An EMC analysis might then require a procedure composed of emitter, receptor, and coupling models, each maintaining phase as well as amplitude waveform characteristics.

### 3.3      Additional Constraints

Considerations in constructing a procedure in addition to the "task" and available data are discussed below. These are the computer resources, accuracy, and "userability."

### 3.3.1 Computer Resources

Electromagnetic compatibility computer analyses of large electronic systems are limited by the user's computer resources: primarily processing time and main memory storage size. The computer processing time includes the time lost during I/O between secondary memory and main memory. The "average" user of IAP codes currently accesses computers with core sizes less than 100K decimal computer words and processing times somewhere between those obtainable on a PDP 11/45 and a CDC 7600. Processing time here refers to the CPU (central processing unit) time needed to execute a FORTRAN program.

Computer limitations restrict the accuracy of EMC analyses because of the necessity of resorting to relatively simple models and procedures with associated greater approximations. A relaxation of computer limitations will allow more accurate models to be implemented and more complex electronic systems to be analyzed with fewer approximations.

In recent years computer capabilities have been rapidly increasing due to continuing advances in the hardware/firmware (defined below) and software technologies. In future years computer capabilities are expected to expand by a few orders of magnitude. Described below is a survey of computer capabilities that has been assembled with regard to "scientific computing". This survey summarizes a) the latest products from several manufacturers and their projected usage over the next few years, b) the current work being performed in the area of standardization of programming languages and graphic packages, c) the present and expected future states of the technologies in computer memories and digital communications, and d) the typical computer environments for "scientific computing" in 1985.

The top-of-the-line minis (termed "mega-minis") [Weizer, 1978] offered by the prominent minicomputer manufacturers are examined first. DEC is currently producing the VAX-11 780 computer. With entry-level systems for less than \$150,000, this computer has more power than a CDC-6600 - a "super computer" of a decade ago. For approximately \$300,000 a VAX system can be purchased that will support over 75 concurrent time sharing users, operating in a scientific or academic environment, with 2 MB (megabites) of primary memory and over 500 MB of disk storage.

The PRIME computer company's P500 and P550 are similar in power to that of VAX. PRIME's intention is to design a MULTICS-type system around these minicomputers, using a specially tailored instruction set and multi-processing.

Unfortunately, with both DEC and PRIME (as well as with all other minicomputer manufacturers), software development is lagging behind hardware development. Currently there are few programming languages available on the aforementioned systems. Networking software, although under extensive development, is not yet at the stage where useful computer networks can be built with off-the-shelf hardware and software. However, independent industry observers feel that this situation will change in the next few years, as software will become available to make better use of today's hardware [Weizer, 1978].

In the near future (the next two to three years) it should become possible to connect geographically distributed VAXs into a network in which users can log onto any computer in the network, access files in scattered network locations, and do this with a simple command language so that the user need not be aware of the system's geographical distribution. Such a

distributed computer system is called a decentralized network, in that the control of the network does not reside at any one location, but is more or less uniformly distributed throughout the network. Hence, the operation of no one processor is critical to the functioning of the network.

Such networks will probably be particularly useful for scientific computing. Different research groups within an organization will be able to obtain their own computers, tying them into their organization's network. This will allow a group to control the use of its own processor, making it more available for long computations, while allowing them to use data and output devices at other groups' installations. If one group's processor goes down for some reason, it will not be difficult to log onto some other processor and continue operating until their own processor becomes available.

Most computers currently being built, as well as those in the foreseeable future, are and will be microprogrammable. This means that it is possible, at least in theory, for one to tailor a processor's instruction set to one's own needs. Microprograms, called "firmware", are more difficult to produce than software, and hence will typically be purchased from the manufacturer. Firmware will probably be marketed as optional "enhancements" to the standard instruction sets, allowing the purchaser to "pick and choose" what he needs.

DEC's VAX-11/780 is advertised as being designed for FORTRAN programming, i.e., its instruction set (firmware) is tailored for executing FORTRAN programs. The VAX instruction format has space available for thousands of additional op-codes. Hence, one can expect that DEC will offer enhancements to the standard firmware, possibly including such features as extended (quadruple) precision floating point instructions and FFT (Fast Fourier Transform) instructions.

IBM's current top offering is the 3033. This computer is ostensibly a 370 with higher performance at lower cost than a 370 model 168-III. There is speculation, however, that it may be the beginning of IBM's next generation of computers [Withington, July 1978].

About 400 concurrent time-sharing users can be supported running 370 software on a 3033 with 8 MB of memory. The cost of such an installation is probably in the \$4-5 million range.

How the 3033 (actually the 303x series) will evolve into the next generation of computers depends more on IBM's marketing strategy than on advances in technology. It appears that more and more operating system functions will be put into firmware, and that many such functions will be relegated to separate processors. Firmware will be designed for executing programs written in particular languages, and it appears likely that separate processors will be used for executing programs written in different languages, as well as for such functions as data base management and communications. One will tailor particular systems by purchasing hardware/firmware/software modules to add to a system. This form of modularization will probably begin in the early 80's with the introduction of new computers (believed to be called Series E and Series H) and upgrades to the 3033 [Withington, July 1978].

IBM is pushing what it calls System Network Architecture (SNA), which provides for a centralized form of computer networking [Gergland, February 1978; Moulton, March 1977]. The idea is that control of the network resides in some small number of large processors (mainframes), with communications and some data processing performed by possibly geographically distributed minicomputers. (IBM has recently entered the minicomputer market

with its Series/1). This form of distributed processing is called hierarchical, and will probably be the dominant form of computer network through the early 80's for general purpose applications.

As software costs increasingly dominate total computing costs, the need for good programming language standards becomes increasingly important. This would limit software dependence upon peculiarities of particular systems and, hence, increase its portability. With the recent announcement of the approval of ANSI 77 FORTRAN, portable scientific software may become a reality even if such "advanced" features as direct access files and character manipulation are used. Other programming languages such as COBOL, PL/I, and BASIC have already been standardized, but ANSI 77 FORTRAN will have the most impact on the scientific community. ANSI 82 FORTRAN is now in the planning stage, but one can assume that it will be compatible with ANSI 77 FORTRAN.

Currently there are a number of graphics packages that are portable in the sense that they are written in FORTRAN, can thus be installed on any computer with little difficulty, and produce graphical output for a variety of devices [Siggraph, June 1978]. With the feasibility of a portable graphics package thus demonstrated, a group is currently at work developing a standard graphics package. They have published a preliminary version of their standard [Siggraph, Fall 1977], and it appears that there will be an ANSI standard graphics package within five years.

Perhaps the technology that is advancing fastest is memory technology. The cost of MOS random access memory (RAM) has been decreasing at a rate in excess of 40% per year [Feth, June 1976]. Hewlett-Packard offers MOS RAM for one line of its

minicomputers at a price of \$30,000/MB. DEC and other mini-computer manufacturers will soon be offering such memory at competitive prices.

The cost of disk memory has been decreasing at a rate of about 20% per year [Feth, June 1976]. Today CDC offers 300 MB disk systems for \$16,000. It is interesting to note that at this rate by 1985 MOS RAM should be as cheap as disk memory will be.

There has long been a large "gap" in the access speeds of primary memory (e.g., MOS RAM) and secondary memory (e.g., disk) of computers. It appears that this gap may soon be closed with the development of charge coupled device (CCD) technology [Theis, January 1978]. With CCDs memory can be constructed with access times roughly midway between those of RAMs and disks. This technology will probably first be utilized as a buffer storage between disk systems and a computer's primary memory resulting in a faster effective transfer rate between disk and primary memory [Theis, January 1978; Withington, July 1978].

Beginning in the early 80's there will be a great decrease in the price of digital communications [Lecht, 1977]. This will come about through satellite communications systems. There will be at least two competitors in this business - AT&T and Satellite Business Systems (SBS) - a company formed by IBM, COMSAT, and Aetna. The costs of communication will be so low that it will be cheaper to send information electronically than through the mail. Where today one might mail a tape from one installation to another and spend considerable processing time converting the data from one tape format to another, in 1985 such information will be transferred quickly and cheaply through communications networks with any necessary conversions performed automatically by microprocessors. There probably will be standard encryption systems available that should make it possible to transmit classified information.

There should be dramatic changes occurring in computing six to ten years from now. Computers will become an integral part of the modern office where there will be a terminal at every desk. The cost of processors will be so low that it will be insignificant compared to software and firmware costs. With anticipated advances in very large scale integration, one can expect that processors with the power of for example an IBM 370/158 will be available on a single chip. In fact, it has been speculated that the current champion supercomputer, the CRAY-1, will be on a single chip in ten years [Isaacson, July 1978]. This may be overly optimistic, but the following passage from Datamation illustrates what IBM plans in the not-so-distant future\* [Datamation, July 1978].

"In a recent pitch to top dp (data processing) executives, IBM indicated that by the early 80's it would market a system with the power of one-third of a 370/158 with 512K of main storage and 5 megabytes of disc, all packaged under the cover of a single keyboard display. The mighty mainframer also projected that by the mid-80's no new office building would be built which didn't provide the capability to install a terminal for every employee. The company's prognostication for its distributed systems included a data base package which would be a 'little brother' of IMS."

In 1985 the scientific user who is not tied to IBM will be able to obtain, at the size and price of today's fancy typewriter, a computer with a processor with more power than a VAX-11/780 or an IBM 370/158, over 1 MB of memory and an appreciable amount of nonvolatile secondary storage. People will have incredible computer power at their fingertips, for essentially insignificant costs.

---

\* In March 1979 IBM announced its next generation of medium size computer which will replace the IBM 370/158 hardware at 1/10th the cost.

The expected increases in size and speed of future systems will allow present computer code main memory requirements to be increased by a factor of approximately 100. The expected elemental processing times will be decreased to sub-nanoseconds and the expected memory sizes will be increased to 10 million computer words.

### 3.3.2 Accuracy

An EMC problem is typically very complex. Hence, a theoretical analysis is rarely exact. The approximations that enter into an analysis generally arise from two sources:

a. Problem Idealization - This is where an actual problem is replaced with a simpler problem. For example the highly inhomogeneous earth around a ground based system may be considered a homogeneous flat half space, or an odd-shaped fuselage may be considered cylindrical, or at low frequencies the wings, tail, and fuselage of an entire aircraft may each be represented by a thin straight wire (stick model), or random cables might be considered uniform, etc.

b. Model Analysis - Here a model is applied to the idealized problem. The resulting errors in analysis arise from [Miller, June 1976]: 1) formulation, e.g., thin-wire approximation [Harrington, 1968], plane wave coefficient method [AMP, July 1972], etc.; 2) numerical, e.g., moment method reduction of an infinite dimensional integro-differential equation to a finite dimensional matrix equation; and 3) computational, e.g., moment method matrix factorization or inversion round-off errors.

An idealized problem should include all important aspects of the actual problem. Resulting inaccuracies can be gauged either by (1) comparison with experiment or other analysis if results from these exist, or (2) continuously increasing the complexity of the idealized problem until computer parameters such as driving point impedance, radiation pattern, or current

show little change. Gauge (2) is a convergence test.

An accurate model analysis, on the other hand, is not related to the relevance of the model, but rather to the accuracy with which an analytical tool predicts important model parameters.

### 3.3.3 Userability

The term "Userability" refers here to the level of competence assumed for an IAP analyst in need of a procedure. There are two aspects to userability: first regards an understanding of the implementation and execution of associated computer code(s), and second, regards the applicabilities and limitations of the procedure.

The first aspect is a function of the structure of a procedure's computer codes. This structure determines the level of effort required to execute a code. All IAP computer codes should include facilitating features such as modularity, free-field input formats, clear documentation, etc. This type of userability directly affects the "expense" in using any procedure but does not necessarily affect the accuracy of a resulting analysis.

The second aspect of procedure userability pertains to the required level of understanding necessary to assess the applicability and accuracy especially regarding many of the coupling models of Section 7. The electromagnetic theory behind these models is quite complex. As a result the models generally involve a great deal of approximation which may require years of experience to adequately understand. This is especially true regarding the higher frequency models such as the geometrical theory of diffraction. However, even "straight forward" moment method models require knowledge of convergence, optimum segment sizes, etc.

Thus when creating a procedure it is important to consider the intended user. As each model is chosen the level of understanding required of a user must be assessed and made known. If a user has a choice between a complicated but accurate procedure, the results from which he is not adequately trained to interpret, and a simplified procedure with more appropriate models that he adequately understands, the user should choose the latter procedure. In conclusion a variety of procedures need to be designed not only to cover a range of accuracies but also a range of users.

### 3.4 Guide to Procedure Construction

The choice of procedure by an IAP analyst is governed by the task, available data, and additional constraints. Each of these has been discussed in the previous subsections. The development of a procedure by an IAP designer must in addition consider emitter, receptor and coupling models and systems equations. These other factors are discussed in subsequent sections.

There is a logical sequence of steps involved in procedure construction. Figure 3.4-1 depicts the sequence of steps in this process and the following example illustrates how a designer may proceed. A number of tables are included which facilitate the choosing of a coupling model. These tables should prove helpful in procedure construction in the near future. Of course they will require updating as additional models are developed and presently available models are advanced.

Step 1. Task Definition - The task is to perform a system level analysis to establish a baseline for the EMC of all system components. The results of this analysis will provide a measure of degradation at the receptors' inputs due to the signals produced by all emitters within the system.

Step 2. Examine the performance criteria of all receptors to be included in the analysis. Based upon the task and

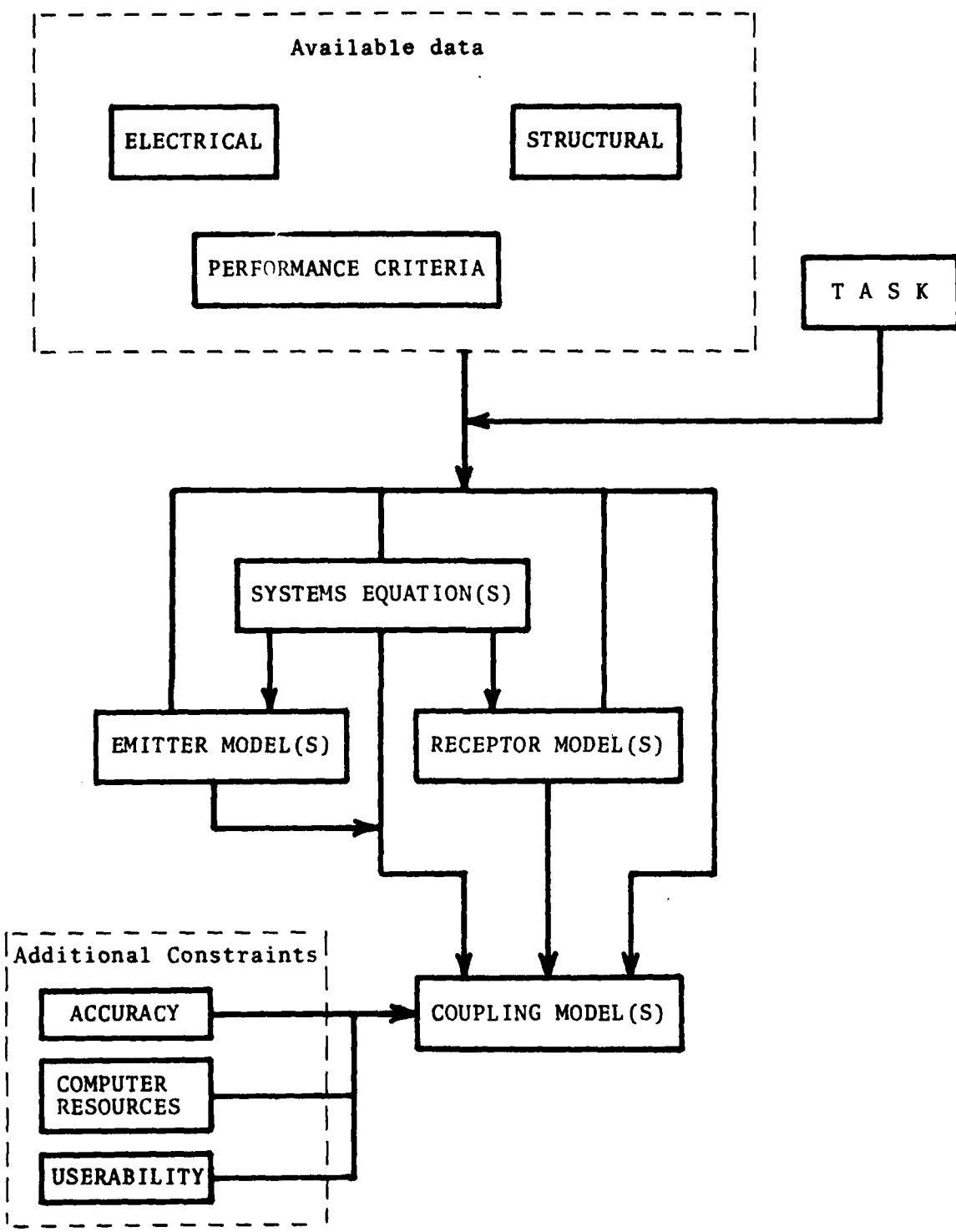


Figure 3.4-1. Driving elements in the construction of a procedure.

the performance criteria selections can be made as to the appropriate systems equations. The receptors included may be voltage or current threshold devices in which case the systems equations may include "peak" voltage and/or current margin calculations. For receptors that are average power sensitive the systems equations may be power margin calculations in terms of signal bandwidths.

Step 3. Select all the emitter and receptor models based upon the available data and the chosen systems equations. For example, if all that is known about a pulse producing equipment (e.g., pulsed radar) is its average power spectrum then the emitter model might be power versus frequency. In this case a time waveform model would not be appropriate. The receptor models are chosen in accordance with performance criteria and the way in which signals are combined by the systems equations.

Step 4. The remaining procedure components to be chosen are the coupling models. This choice is based on the data (structural, electrical, etc.) available, systems equations, and emitter and receptor models. The system structural data may include such things as antennas (their location, orientation and type), cables (type and routing), super-structure orientation or shape, etc. The electrical data include emission characteristics, such as peak or average power, pulse rise time, pulse width, pulse repetition rate, peak voltage or current, phase, frequency, amplitude envelope, etc., and the electrical characteristics of the coupling media (conductivity, permittivity, permeability, linearity, isotropy, timevariance etc.) The systems equations indicate whether the coupling models are to apply to linear or non-linear media, deterministic or stochastic emissions, time or frequency descriptive responses, etc.

Tables 3.4-1 through 3.4-5 conveniently categorize the coupling models summarized in Section 7. As an example of the use of these tables assume that the problem is coupling between

Table 3.4-1. Basic Coupling Models.

Symbol (Appropriate Section)	Name	Reference for Attribute Table (7.2-1)
TW-FD (A.1.1.1)	Thin Wire-Frequency Domain	B-1,2,3,4
SPH-FD(A.1.1.2)	Surface Patch ( $\tilde{H}$ -Field)-Frequency	B-5
SPE-FD(A.1.1.2)	Surface Patch ( $\tilde{E}$ -Field)-Frequency	B-6
BOR-FD(A.1.1.3)	Body of Revolution-Freq. Domain	B-7
FE-BOR-FD(A.1.1.5)	Finite Element-Body of Revolution - Frequency Domain	B-8
ESC-BOR-FD(A.1.1.5)	Equivalent Surface Current-Body of Revolution - Frequency Domain	B-9,10
ESC-SP-FD(A.1.1.4)	Equivalent Surface Current-Surface Patch-Frequency Domain	B-11
VC-FD(A.1.1.6)	Volume Current-Frequency Domain	B-12
SEM(A.2.1.1)	Singularity Expansion Method	B-13
FE-TD(A.2.1.2)	Finite Difference-Time Domain	B-14
TW-TD(A.2.1.3)	Thin Wire-Time Domain	B-15
SPE-TD(A.2.1.3)	Surface Patch ( $\tilde{E}$ -Field)-Time Domain	B-16
SPH-TD(A.2.1.3)	Surface Patch ( $\tilde{H}$ -Field)-Time Domain	B-17
TML-DP-FD(A.1.3.4)	Transmission Line-Distributed Parameter-Frequency Domain	B-18,19,20,21
TML-LC-FD(A.1.3.5)	Transmission Line-Lumped Circuit - Frequency Domain	B-22
TML-WC-FD(A.1.3.6)	Transmission Line-Lumped Circuit Weak Coupling-Frequency Domain	B-23
TML-DP-FW-FD(A.1.3.4)	Transmission Line-Distributed Parameter -Field to Wire-Frequency Domain	B-24
TML-WC-FW-FD(A.1.3.6)	Transmission Line-Lumped Circuit Weak Coupling-Field to Wire-Frequency Domain	B-25
TML-DP-TD(A.2.2)	Transmission Line-Distributed Parameter -Time Domain	B-26
FST(A.1.2.1)	Free Space Transmission	B-27
GO(A.1.2.2)	Geometrical Optics	B-28
GTD(A.1.2.3)	Geometrical Theory of Diffraction	B-29
PTD(A.1.2.4)	Physical Thoery of Diffraction	B-30

Table 3.4-2. Combined Coupling Models

Symbol (Appropriate Section)	Name	Reference for Attribute Table (7.2-2)
TW-FD/SPH-FD(B.1.1)	Thin Wire, Surface Patch ( <u>H</u> -Field) - Frequency Domain	C-1
TW-FD/SPE-FD(B.1.1)	Thin Wire, Surface Patch ( <u>E</u> -Field) - Frequency Domain	C-2,3
UM-BOR-FD(B.1.2)	Unimoment Method-Body of Revolution - Frequency Domain	C-4
TW-FD/BOR-FD(B.1.1)	Thin Wire, Body of Revolution - Frequency Domain	C-5
BOR-FD/ESC-BOR-FD(B.1.2)	Body of Revolution - Equiv. Surface Current - Freq. Domain	C-6
TW-FD/VC-FD(B.1.2)	Thin Wire-Volume Current - Frequency Domain	C-7
TW-TD/SPH-TD(B.3)	Thin Wire-Surface Patch ( <u>H</u> -Field) - Time Domain	C-8
SPE-TD-SPH-TD(B.3.)	Surface Patch E-Field and <u>H</u> -Field - Time Domain	C-9
TDA(B.3)	Time Domain Augmentation	C-10
TML-FD/N(B.4)	Transmission Line-Network- Frequency Domain	C-11
TML-WC-FD/S(B.4)	Transmission Line-Weak Coupling -Summation-Frequency Domain	C-12
GO/GTD(B.2.1)	Geometrical Optics, Geometrical Thoery of Diffraction	C-13
GTD/MOM(B.2.2)	Ray Methods, Moment Methods	C-14

Table 3.4-3. Coupling Models Grouped by Applicable Problem.

**Antenna-to-Field (Radiation)**

B-1,2,3,4,5<sup>(1)</sup>,6,7,13,14<sup>(1)</sup>,15,16,28,29,30

C-1,2,3,4<sup>(1)</sup>,5,6,7,8,9,10,13,14

**Field-to-Wire**

B-1,2,3,4,13,14,15,24,25,26

C-1,2,3,5,6,7,8,11,14

**Antenna-to-Antenna ("Coupling")**

B-1,2,3,4,6,7,13,15,16,27

C-1,2,3,5,6,7,8,9,10,14

**Wire-to-Wire ("Coupling")**

B-1,2,13,15,18,19,20,21,22,26

C-1,2,3,5,7,8,11,12,14

**Aperture Coupling (Field-to-Field Through an Aperture in a Conducting Shell)**

B-3<sup>(2)</sup>,4<sup>(2)</sup>,6<sup>(2)</sup>,7,13<sup>(2)</sup>,14<sup>(2)</sup>,15<sup>(2)</sup>,16<sup>(2)</sup>,28,29,30

C-2<sup>(2)</sup>,3<sup>(2)</sup>,4,5,6,9,10,13

**Scattering (Field-to-Field (Far))**

B-1,2,3,4,5,6,7,9,10,11,12,13,15,16,17,28,29,30

C-1,2,3,4,5,6,7,8,9,10,13,14

Notes:

- a) Refer to Tables 3.4-1 and 3.4-2 for model names and discussion sections. Refer to Tables 7.2-1 and 7.2.2 for model attributes.
- b) Antenna-to-field models also apply to field-to-antenna models via reciprocity (when coupling media is reciprocal). Same is true for field-to-wire and wire-to-field.

(1) Via reciprocity if media are reciprocal.

(2) Babinet's Principle may be required [Adams, June 1973].

TABLE 3.4-4  
Coupling Models Grouped by Applicability to Coupling Environment

GEOMETRY*	WIRE (e.g., Cable)	SURFACE (e.g. Aircraft Fuselage)	VOLUME (e.g. Missile Plume)
LINEAR, TIME-INVARIANT	B-1,2,13,15,18,19,20,21, 22,23,24,25,26 C-1,2,3,5,7,8,11,12,14	B-3,4,5,6,7, 13,15,16,17, 28,29,30 C-1,2,3,5,8,9, 10,13,14	B-8,9,10,11, 12,13,14 C-4,6,7,14
NON-LINEAR, TIME-INVARIANT	B-15 C-8	B-16,17 C-8,9	B-14
NON-LINEAR, TIME-VARIANT	B-15 C-8	B-16,17 C-8,9	B-14
NON-LINEAR, TIME-VARIANT	B-15 C-8	B-16,17 B-8,9	B-14

TABLE 3.4-5  
Coupling Models Grouped by Applicability to Scatterer Type and Size

GEOMETRY*	WIRE (e.g. Cable)	SURFACE (e.g. Aircraft Fuselage)	VOLUME (e.g. Missile Plume)
ELECTRICAL SIZE**			
<0.1	B-1,2,13,15,18,19,20,21, 22,23,24,25,26 C-1,2,3,5,7,8,11,12	B-3,4,5,6,7, 13,15,16,17 C-1,2,3,5,8,9	B-8,9,10,11, 12,13,14 C-4,6,7
>0.1	B-1,2,13,15,16,19,20,21 24,26	B-3,4,5,6,7, 13,15,16,17	B-8,9,10,11 12,13,14
<1.0	C-1,2,3,5,7,8,11	C-1,2,3,5,8,9	C-4,6,7
>1.0	B-1,2,13,15,18,19,20,21, 24,26	C-3,4,5,6,7, 13,15,16,17,	B-8,9,10,11, 12,13,14
<10.0	C-1,2,3,5,7,8,11	28,29,30	C-4,6,7,14
C-1,2,3,5,7,8,11	C-1,2,3,5,8,9, 13,14	C-1,2,3,5,8,9, 13,14	C-4,6,7,14
>10.0	C-14	B-28,29,30	C-14
	C-14	C-10,13,14	

\* Refers to major type of scattering or transmission structure or medium.

\*\* Refers roughly to the diameter, in a wavelengths at highest significant frequency in source waveform, of smallest sphere which can enclose structure.

Note: Refer to Tables 3.4-1 and 3.4-2 for model names and discussion sections.  
Refer to Tables 7.2-1 and 7.2-2 for model attributes.

two antennas on the fuselage of an aircraft. Table 3.4-3 (see Tables 3.4-1 and 3.4-2 for model names) lists many models which apply to the antenna-to-antenna coupling problem. If this antenna-to-antenna problem is time variant then the group of applicable models is reduced to B-15 and 16 and C-8 and 9 in accordance with Table 3.4-4. If, in addition, the frequency range is such that the dimensions of the problem exceed 10 wavelengths, then Table 3.4-5 indicates an absence of models for this problem (indicating an area in need of development). As a second example assume that the procedure is to include wire-to-wire analysis. The wire lengths are small relative to a wavelength and are located in bundles forcing wires close together and parallel. If the coupling is linear and time-invariant Table 3.4-4 shows that all models listed in Table 3.4-3 under wire-to-wire apply. Furthermore, Table 3.4-5, due to the low frequency, excludes only model C-14 (a high frequency technique).

Step 5. A list of coupling models has now been assembled. A choice is made among this list in accordance with trade-offs defined by the task and the additional constraints of computer resources, "userability", and accuracy. The more accurate the model generally the more costly the implementation and the more experience needed to interpret the results. As an aid in this decision the model attribute tables provided in Section 7 can be consulted. The final selection of coupling models is usually the choice of models providing the best accuracy within the computer limitations that can be properly implemented by the intended user.

The procedure construction is complete when all models have been identified, interface specifications have been defined, limitations and expected inaccuracies documented, and computer codes designed.

## 4.0

SYSTEMS EQUATIONS

Systems equations relate appropriate electromagnetic source (emitter output) characteristics to appropriate responses. These responses might be 1) waveforms such as time varying voltages at receptor inputs, 2) waveform parameters such as average power, or 3) interference indicators such as average power susceptibility margins.

The principal purpose for identifying systems equations is that they formulate a problem by relating input (sources, emitters) to output (receptor response parameter) within the constraints of the problem. This formulation is usually expressible in mathematical form with emitter, receptor, and coupling terms explicit. Thus pertinent attributes of emitter, receptor, and coupling models are readily apparent from systems equations. For example an average power susceptible receptor and linear media may be evidenced in a systems equation given in terms of frequency domain transfer functions. These attributes, in turn, provide a guide to choosing appropriate emitter models such as an average power density description or a waveform description. They also guide the choice of coupling models with regard to computing desired receptor parameters or margins and with regard to the type of media be it linear, nonlinear, time-variant, etc.

Two categories of systems equations are considered here: 1) "waveform systems equations", defined as those relating arbitrary time waveforms between emitters and receptors, and 2) "parameter systems equations", defined as those relating emitter outputs to receptor waveform parameters or interference indicators.

## 4.1

Waveform Systems Equations

In considering the interactions between emitters and potentially susceptible devices, it is important to recognize that there are different types of emissions and each may produce

different interference effects and may require different analysis methods. For the purpose of classifying waveform systems equations, emissions are considered to be aperiodic, periodic, or random. It is felt that this is a sufficiently general method of classifying emissions.

Aperiodic emissions are, with relatively few exceptions, of finite energy and can be represented in terms of their time waveforms or continuous frequency spectra. They are assumed to be deterministic here. Periodic emissions can be represented in terms of their time waveforms or discrete frequency spectra. Fourier analysis methods may be applied to either of these two types of waveforms. Random processes must in general be represented by their N-dimensional joint probability distribution functions. However, for certain situations (e.g., stationary Gaussian processes) they may be represented by their autocorrelation functions or power spectral densities.

The transfer of energy from an emitter to a potentially susceptible device may, in general, involve a nonlinear, time-varying, dispersive, and even random process. The randomness generally reflects a lack of precise information about the system. For example, relative wire positions within a cable bundle may either be impractical to obtain for a given system or so varied between systems of a given type that only a statistical representation is meaningful [Morgan, Feb. 1978].

The general type of transfer process is very difficult to treat analytically. However, in many cases of practical interest, it is possible to assume that the process is deterministic and time-invariant or to separate the time-variant process from the remainder of the transfer process. Furthermore, in some cases, it is possible to assume that the process is deterministic and linear, or to separate the nonlinearity from the remainder of the transfer process. Each of these assumptions results in certain limitations. A matrix, Table 4.1-1, has been constructed which shows the basic systems equations which result for each of the cases of interest.

Table 4.1-1. Waveform Systems Equations.

Transfer Relation	NONLINEAR	RANDOM	LINEAR AND DETERMINISTIC	
			GENERAL	TIME VARIANT (Time & Frequency Separable)
APERIODIC (Continuous Spectrum)	General solution not available. Time-domain analysis methods are available for special cases that may be considered as piecewise linear (e.g., hard limiting, mixing, etc.). Effort should be directed toward development of computer programs for these special cases. Volterra analysis may be used for periodic signals that have limited number of frequency components. Aperiodic or periodic signals may be represented in either time domain or frequency domain and Fourier transforms may be used. In general, random signals must be described in terms of their M-dimensional joint probability distribution functions.	Monte Carlo method offers general solution. Methods for solving cable bundle problems where relative wire locations and terminal loads are random, are discussed in (Morse, Feb. 1978).	$v_o(t) = \int_{-\infty}^t v_1(\tau) h_g(t-\tau, t) d\tau$	$v_o(t) = \int_{-\infty}^t v_1(\tau) h(t-\tau) d\tau$ $v_o(t) = v_1(t) h(t)$
PERIODIC (Discrete Spectrum)	General solution not available. Signals that have limited number of frequency components may be represented in either time domain or frequency domain and Fourier transforms may be used. In general, random signals must be described in terms of their M-dimensional joint probability distribution functions. Gaussian random processes may be described in terms of the autocorrelation function or power spectral density.		$v_o(t) = \int_{-\infty}^t v_1(t') R_{qq}(t', t-t') dt'$	$v_o(t) = A(t) \circ v_1(t) H(t)$ $v_o(t) = \frac{1}{T} \sum_{n=-\infty}^{\infty} R_q\left(\frac{n}{T}, t\right) v_n^1 e^{j \frac{2 \pi n}{T} t}$ $v_o(t) = \frac{1}{T} \sum_{n=-\infty}^{\infty} v_n^1 R_{qq}\left(\frac{n}{T}, t-\frac{n}{T}\right)$
RANDOM				General solution not available. Solution may be obtained for special case of a Gaussian Random Process.

In these equations

- $v_i(t)$  = time dependent emission
- $v_o(t)$  = time dependent response
- $h(t)$  = response measured at time  $t$  to a unit impulse applied at time 0 for a time invariant system
- $a(t)h(t-\tau)$  = response measured at time  $t$  to a unit impulse applied at time  $\tau$  for a time and frequency separable process.
- $h_g(y, t)$  = response measured at time  $t$  to a unit impulse applied at time  $t-y$  for a general time variant process
- $V_i(f)$  = Fourier transform of  $v_i(t)$
- $V_o(f)$  = Fourier transform of  $v_o(t)$
- $A(f)$  = Fourier transform of  $a(t)$
- $H(f)$  = Fourier transform of  $h(t)$
- = response of time invariant process to  $e^{j2\pi ft}$

$$H_g(f, t) = \frac{\text{response of general time variant process to } e^{j2\pi ft}}{e^{j2\pi ft}}$$

- $H_{gg}(f', f)$  = Fourier transform of  $H_g(f', t)$
- $T$  = period of periodic emission

$$V_n^i(T) = \int_{-T/2}^{T/2} v_i(t) e^{-j\frac{2\pi n}{T} t} dt$$

where the Fourier transform is defined by

$$X(f) = \int_{-\infty}^{\infty} x(t) e^{-j2\pi ft} dt \quad (4.1-1)$$

General equations are provided only for the linear, deterministic transfer process. They are given for three different types of temporal dependences and for both continuous and discrete spectrum emissions. Their derivations appear in Appendix C.1.

#### 4.2 Parameter Systems Equations

Some waveform parameters that receptors may be sensitive to include:

- average power
- total energy
- peak current (or voltage)
- rise time

For example certain explosive devices are triggered by the burning away of a wire (resistive heating). This is a total energy susceptibility. Also many digital devices are susceptible to instantaneous waveform level ("peak" sensitivity).

This parameter list is far from complete, of course, and one could conceive of many other parameters that a device may be sensitive to. For example pulse width or pulse repetition frequency. There are an infinity of conceivable parameters. However, the characteristics of almost all known receptors are likely to warrant consideration of only the above four.

The above four parameters are often related to corresponding interference indicators such as "susceptibility margins". These margins are numbers which indicate the level to which specified unwanted emissions cause unacceptable receptor performance. In IEMCAP, for example, the susceptibility margins [Pearlman, Sept 1977] are defined only in terms of average power. Also IEMCAP assumes the general receptor model as indicated in Figure 4.2-1. This receptor model has a linear input stage with transfer function  $B_r(f)$ , followed by a nonlinear detector. The IEMCAP susceptibility margin is then defined as the ratio of average power induced at the detector input to the interference threshold average power level at the detector input. The latter is

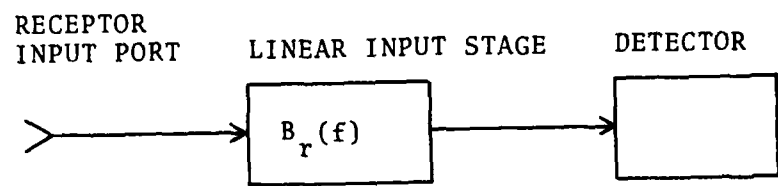


Figure 4.2-1. General IEMCAP Receptor Model.

assumed to be independent of frequency. The IEMCAP margins are actually computed, however, in terms of receptor input parameters where measurements are more readily performed [Pearlman, Sept. 1977].

In Table 4.2-1 susceptibility margins are given which generally are in accordance with the aforementioned IEMCAP philosophy. However, in addition to average power, receptors sensitive to total energy, peak current, and bandwidth (inversely proportional to rise time) of deterministic and stochastic waveforms are included. Although the margins are in terms of current waveforms corresponding voltage waveform margins would be similar. Also, referring to Figure 4.2-1, the receptor and detector input impedances are assumed 1-ohm each. Only minor changes in the tabulated margins would result if the impedances were arbitrary.

The definitions of all quantities in Table 4.2-1 are included in the list below. The term "switched stationary" as a susceptibility margin for total energy sensitive receptors indicates that the input waveform is an otherwise stationary process that is "turned" on and off at regular intervals. The derivations of the margins in Table 4.2-1, with further clarification, are given in Appendix C.2.

$P_d$	=	average power at input to detector
$P_r$	=	average power at input to receptor
$E_d$	=	total energy at input to detector
$i_d(t)$	=	detector input current
$i_r(t)$	=	receptor input current
$I_d(f)$	=	Fourier transform of $i_d(t)$ (finite energy) Phasor as defined by $i_d(t) = 2 \operatorname{Re}(I_d(f)e^{j\omega t})$ (sinusoid)
$I_r(f)$	=	Fourier transform of $i_r(t)$ (finite energy) Phasor as defined by $i_r(t) = 2 \operatorname{Re}(I_r(f)e^{j\omega t})$ (sinusoid)

Table 4.2-1. Susceptibility Margins.

	DETERMINISTIC	STOCHASTIC
AVERAGE POWER	$\int_{f_a}^{f_b} \frac{G_r(f)}{ I_r^s(f) ^2} df$	$\int_{f_a}^{f_b} \frac{G_r(f)}{ I_r^s(f) ^2} df$
TOTAL ENERGY	PERIODIC: Use average power margin APERIODIC: $\frac{1}{\Delta_r} \int_{f_a}^{f_b} \frac{ I_r(f) ^2}{ I_r^s(f) ^2} df$	STATIONARY: Use average power margin "SWITCHED" STATIONARY: $\frac{\Delta}{\Delta_r} \int_{f_a}^{f_b} \frac{G_r(f)}{ I_r^s(f) ^2} df$
PEAK CURRENT	$\int_{f_a}^{f_b} \frac{ I_r(f) }{ I_r^s(f) } df$	STATIONARY: $\frac{\sigma_r}{4\pi I_r^s(f) ^2}$ NORMAL, ZERO-MEAN STATIONARY: $\frac{\sqrt{2}}{\sigma_r} \int_{-\infty}^{\infty} \frac{1}{\sigma_r \sqrt{\pi}} e^{-x^2/(2\sigma_r^2)} dx$ $2 I_r^s(f_p) $ NARROWBAND GAUSSIAN: $\frac{1}{\sigma_r} \int_{-\infty}^{\infty} \frac{x}{\sigma_r^2} e^{-x^2/(2\sigma_r^2)} dx$ $2 I_r^s(f_o) $ NARROWBAND GAUSSIAN PLUS SINUSOID: $\frac{1}{\sigma_r} \int_{-\infty}^{\infty} \frac{x}{\sigma_r^2} e^{-(x^2+s^2)/(2\sigma_r^2)} J_0(\frac{xs}{\sigma_r}) dx$ $2 I_r^s(f_o) $
BANDWIDTH	$\beta_r / \beta_r^s$	$\beta_r / \beta_r^s$

$I_r^s(f)$	=	level of $I_r(f)$ which induces the interference threshold level at the detector
$K^P$	=	detector interference threshold power level
$K^E$	=	detector interference threshold energy level
$K$	=	detector interference threshold peak current level
$K^B$	=	detector interference threshold bandwidth
$G_r(f)$	=	spectral power density at receptor input (Note: $G_r(f)$ is defined for negative $f$ .)
$B_r(f)$	=	receptor input-to-detector linear transfer function
$\Delta_r$	=	time interval assigned to an energy sensitive receptor ( $\Delta_r$ defines $ I_r^s(f) $ according to $K^E = 2\Delta_r  B_r(f) ^2  I_r^s(f) ^2$ )
$\Delta$	=	duration of interference on receptor
$\sigma_d^2$	=	variance of detector input waveform
$\sigma_r^2$	=	variance of receptor input waveform = $2 \int_{f_a}^{f_b} G_r(f) df$
$\alpha$	=	fraction of time that a stochastic waveform peak at detector input must exceed $K$ to trigger interference
$f_p$	=	frequency for which $B_r(f)$ is maximum
$f_o$	=	center frequency of a narrowband Gaussian process
$f_a, f_b$	=	lower, upper frequencies defining common frequency band between interferer and receptor
$s$	=	amplitude of the sinusoid in a narrowband - Gaussian - plus - sinusoid process
$\tau$	=	pulse width of a pulse interfering waveform
$\beta$	=	3 dB point bandwidth of $B(f)$
$\beta_r^s$	=	receptor input waveform bandwidth which induces the interference threshold bandwidth at the detector
$\beta_r$	=	portion of the receptor input waveform bandwidth within the pass band of $B_r(f)$
$J_0(x)$	=	modified Bessel function of zero order

## 5.0 EMITTER MODELS

In order that the IAP meet user requirements for the system analysis of the 1980's, sufficient flexibility in modeling a system accurately and quickly must be included. As such, the system model typically begins with an input which is an emitter in the present IAP structure. The user must have the flexibility of modeling in the frequency domain, as has been traditional, or in the time domain, which allows modeling of transient and signal waveform inputs to a system. Further, because emitters have out of band emissions, the capability of modeling these emanations must be provided. To these ends, the section on emitters has been divided into two subsections, commencing with frequency domain emitter models that are currently existent in IAP (specifically IEMCAP) and following with the time domain models.

### 5.1 Frequency Domain Emitter Models

In developing frequency domain representations for emitters, it is important to recognize that there are different types of emission, and each may require different analysis methods. For the purpose of developing the IAP systems equation, emissions were considered to be aperiodic, periodic, random or some combination of these three. It is felt that this is a completely general method of classifying emission, and the systems equations resulting from this classification scheme have been presented in Section 4.

Each of the different types of emissions described above requires a different representation in the frequency domain. Aperiodic emissions are represented in terms of a continuous frequency spectrum. Periodic emissions are represented in terms of a discrete frequency spectrum. Fourier analysis methods may be applied to either of these two types of waveforms. Random processes are in general represented by an N-dimensional joint probability distribution function. However, for certain situations (e.g., stationary Gaussian processes) they may be represented

by autocorrelation functions or power spectral densities. The emitter models used in the current IAP (specifically IEMCAP) exclusively use power spectral density representations.

#### 5.1.1     Current IAP Models

While complete descriptions of the emitter models utilized by IAP are available [Paul, no date], the existing emitter models have been summarized in Table 5.1-1 in groupings according to signal characteristics. Table 5.1-2 illustrates the attributes or input parameters necessary for the utilization of these current IAP system level models. Although the current IAP emitter models cover a wide range of equipment outputs available in avionic systems, the evolution of technology requires that additional emitter models be included in future releases of the IAP codes.

#### 5.1.2     Recommended Additional Models

There are several types of emissions that are typically encountered in intrasystem design that are not presently modeled in IEMCAP. It is recommended that future effort be directed toward developing models for the following types of emissions.

##### 5.1.2.1   Noise

In certain cases, emissions are random and can best be described as "noise". Effort needs to be directed toward formulating frequency domain models to represent these types of emissions. Certain noise models are relatively easy to formulate in the frequency domain. For example, white Gaussian noise can be represented as a uniform power spectrum. Further, select models for nonwhite noise such as shot noise have been formulated in the frequency domain and could be easily included in an IAP. Currently the only method available for representing noise in an analysis is by utilizing the user specified spectrum option which, at best, is limited by the present IEMCAP limit of 90 frequencies per equipment.

Table 5.1-1. Current IAP Frequency Domain Emitter Models.

Signal & Control Modulation		Radio Frequency Modulation	
Periodic		Periodic	
ESPIKE	$\Delta$ exponential spike pulse train	CW	$\Delta$ continuous wave
RECTPL	$\Delta$ rectangular pulse train	RECTPL RADAR	$\Delta$ rectangle pulse radar
TRAP	$\Delta$ trapezoidal pulse train	TP2D RADAR	$\Delta$ trapezoidal pulse radar
TRIANG	$\Delta$ triangular pulse train	COSQD RADAR	$\Delta$ cosine squared pulse radar
SAWTH	$\Delta$ sawtooth pulse train	GAUSS RADAR	$\Delta$ gaussian pulse radar
DMPSSIN	$\Delta$ damped sinusoidal train	CHIRP RADAR	$\Delta$ chirp pulse radar
Random Modulation		Random Modulation	
PDM	$\Delta$ pulse duration modulation	PDM	
NRZPCM	$\Delta$ non-return to zero pulse code modulation	NRZPCM	
BPPCM	$\Delta$ biphasic pulse code modulation	BPPCM	
PPM	$\Delta$ pulse position modulation	PPM	
TELEG	$\Delta$ telegraphy	TELEG	
PAM	$\Delta$ pulse amplitude modulation	FSK	$\Delta$ frequency shift keying
VOICE	$\Delta$ clipped voice	PAMFM	$\Delta$ pulse amplitude modulation/frequency modulation
CVOICE	$\Delta$ user specified spectrum	AM(VOICE)	$\Delta$ amplitude modulation, voice
SPECT	$\Delta$ user specified spectrum	(CVOICE)	• chirped voice
		(NONVCE)	• non-voice
Non-Required Spectra		DSBSC (VOICE)	$\Delta$ double sideband suppressed carrier
MIL-STD-461		(CVOICE)	
RF Ports		(NONVCE)	
Equipment Case		LSSB (VOICE)	$\Delta$ 1 lower sideband
Power, Signal or Control Parts		(CVOICE)	
MIL-STD-6181		(NONVCE)	
RF Ports		USSB (VOICE)	$\Delta$ upper sideband
Equipment Case		(CVOICE)	
Power, Signal or Control Parts		(NONVCE)	
MIL-STD-704		FM (VOICE)	$\Delta$ frequency modulation
Power Line Emission		(CVOICE)	
LOLKG	$\Delta$ local oscillator leakage	(NONVCE)	
		SPECT	

Source Parameter		Parameter Description		Units		Control		Signal & Control	
$f_h$	* highest required frequency (para)			Hz					
$f_l$	* lowest required frequency (para)			Hz					
$V_{UNIS}$	= volts/amp. (para)			volts/amp.					
$b_w$	* information bandwidth (para)			Hz					
$A$	* amplitude in UNITS (para)			volts/amps.					
$f_1$	* decay freq. of damped sin (subpara)			Hz					
$f_2$	* one, freq. of damped sin (subpara)			Hz					
$n_{phase}$	* number phases (para)								
$n_{bh}$	* highest harmonic (para)								
$f$	* frequency (para)			Hz					
$V$	* line voltage (para)			volt					
$\epsilon_n$	* user modulation level (subpara)								
$f_m$	* user modulation frequency (subpara)			Hz					
$T_{ohb}$	* broadband local osc. leakage (subpara)			dBm/MHz					
$T_{onb}$	* narrowband local osc. leakage (subpara)			dBm					
$b$	* b-dB nonvoice bandwidth (subpara)			Hz					
$c_m$	* modulation index (subpara)								
$PCR$	* pulse compression ratio (subpara)								
$t_f$	* falltime (subpara)			sec					
$t_r$	* risetime (subpara)			sec					
$df$	* maximum frequency deviation (subpara)			Hz					
$diff$	* upper & lower osc. freq. difference (subpara)			Hz					
$f_{tone}$	* tone frequency (subpara)								
$wpm$	* words per minute (subpara)								
$t$	* pulse width (subpara)			sec					
$r_b$	* bit rate (subpara)			bits/sec					
$CW$	* carrier frequency (para)			Hz					
$h_n$	* harmonic level (para)			dB					
$h_{ac}$	* -6-dB channel bandwidth (para)			Hz					
$P$	* maximum output power (para)			Watts					
$f_h$	* highest carrier frequency (para)			Hz					
$f_l$	* lowest carrier frequency (para)			Hz					

**Table 5.1-2.** Attribute Table for Frequency Domain IEMCAP Emitter Models.

**NOTE:** Units in dBm/MHz for RF, dBm/Hz for power, or dBuv/MHz or dBuA/MHz for S & C.

### 5.1.2.2 Signal/Control and RF Modulation

Additional emitter models in the frequency domain should reflect current trends in technology. Increased communication capacity through multiplexing techniques is becoming a common scenario and since time domain models have been studied for FDM and TDM, the frequency domain models which described these multiplexing techniques should be formulated and include in an IAP. Other time domain models that have been studied and should be included in an IAP are PSK, MPS, and delta modulation (DM). To ensure secure, jam-resistant communications, advanced techniques (such as spread spectrum) and associated subsets (such as frequency hopping) should be studied and included in an IAP. Spread spectrum techniques most closely resemble noise in the frequency domain and further represent a very broad spectrum which in the current IAP may present implementation problems. Future IAP codes should be structured to accommodate these types of emitter models.

### 5.1.2.3 Spectrum Modeling and Complex Modulation

Flexibility in spectrum modeling is necessary in an IAP to allow the user the ability to accurately define the total emitter spectrum, required and nonrequired. Additional capability in spectrum modeling should, as a minimum, take the form of default harmonic models unless the user does not wish to incorporate this additional information. The exact amount of flexibility along these lines needs to be determined.

In addition to modeling the spectrum in terms of carrier harmonics, the user should be afforded the opportunity of specifying the level in between these harmonics. This could be accomplished by allowing the user to specify two or more models simultaneously (in this case the two models for harmonics and noise). This specification would also allow complex modulation techniques to be employed (modulation of a CW signal with an ESPIKE, for example). This multiple specification is inherently simple, yet affords great flexibility to the user.

#### 5.1.2.4 Modulation Products

Intermodulation, cross-modulation and nonlinearities can cause severe problems. However for the purpose of this report, these effects are incorporated into the coupling models, and the system level nonlinear receptor models.

#### 5.1.2.5 User Specified Spectrum

To round out IAP flexibility in spectrum modeling, additional capability should be allowed the user in terms of a user specified spectrum. It is suggested that it may be more useful to represent an emission spectrum in the form of "Bode" plots where it is necessary for the user to specify only break-point frequencies and rolloffs of the spectrum envelope in dB per octave or dB per decade.

### 5.2 Time Domain

Emitter models for most EMC analysis routines have traditionally operated in the frequency domain. With the advent of the large scale use of digital electronics, however, it has become desirable to model the transient phenomena which occur in such electronic equipment. Accurate modeling of these phenomena cannot be accomplished in the frequency domain, however, necessitating the development of time domain representations of the frequency domain models discussed previously. These time domain models, will not only accurately represent these transient phenomena, but will also model threshold devices common in digital electronics, a feature which should prove invaluable to the EMC engineer. The great usefulness of time domain models for describing these effects makes their inclusion in an IAP very desirable, and as such, they are discussed in some detail in this section.

### 5.2.1 Current IAP Models

While the emitter models in IAP are currently all represented in the frequency domain, those emitter models that do have a time domain representation have been studied and are summarized in Table 5-2-1. Graphical representations of these models are presented in Figure 5.2-1. Where a model may represent a signal or a modulation, the dependent variable will be denoted as both  $m(t)$  and  $v(t)$ . The attributes associated with these time domain models are compiled in Table 5.2-2. The emitter models are divided into periodic functions and random modulation of periodic functions. The models have as a common functional form the general equation,

$$v(t) = \sum_{n=0}^N A_n m(t) \cos[n\omega t + \phi_n(t) + \theta_n]$$

where  $A_n$  is the amplitude as a function of  $n$ ,  $m(t)$  is the amplitude modulation which may be a stochastic process,  $\omega$  is typically the carrier frequency,  $\phi_n(t)$  is the frequency or phase modulation and as such may be a stochastic process,  $\theta_n$  is a phase constant and  $n$  is an integer value from 0 to  $N$ , where  $N$  is the total number of signals. The models shall use this notational convention with some exceptions which will be noted with the model. Currently, no attempt has been made to characterize  $m(t)$ , the stochastic process in the time domain. This will be discussed further for several specific representations of  $m(t)$  in future sections. The general characteristics of  $m(t)$  will require additional study prior to inclusion in an IAP.

### 5.2.2 Recommended Additional Models

With the arrival of large amounts of digital avionics in complex electromagnetic environments, additional types of emitter modulation models and capabilities may be required in the EMC analysis. While only the time domain representations may be given, a corresponding frequency domain model, if possible, needs to be generated.

Figure 5.2-1. Time Domain Emitter Models

SIGNAL/CONTROL

ESPIKE

exponential spike train

$$v(t) = A e^{-t/\tau}, \text{ is the pulse form,}$$

which repeats each  $T$  seconds.  $\tau$  is the time required to reach a value of  $v = A/e$ .

RECTPL

rectangular pulse train

$v(t)$  is a rectangular pulse of constant amplitude  $A$ , and duration  $\tau$  which repeats each  $T$  seconds.

TRAP

trapezoidal pulse train

$v(t)$  is a pulse of the form defined by the line segments seen in Figure 5.2-1.

TRIANG

triangular pulse train

$v(t)$  is an isosceles triangle with height  $A$  and base  $\tau$  occurring each  $T$  seconds.

SAWTOOTH

sawtooth pulse train

$v(t)$  is a right triangle with height  $A$  and base  $\tau$ , occurring each  $T$  seconds.

DMPSIN

damped sine wave pulse train

$v(t)$  is a pulse of the form  $A e^{-t/\tau} \sin \omega_0 t$ , where  $\tau$  is the decay constant and  $\omega_0$  is the oscillatory frequency. The pulse repeats each  $T$  seconds.

PDM

pulse duration modulation

$v(t)$  is a rectangular pulse of constant height  $A$ , with an arbitrary duration. The pulses occur every  $T$  seconds.

NRZPCM

non return to zero pulse code modulation

$v(t)$  is a rectangular pulse of the form  $A/2[1+m(t)]$  where  $m(t)$  takes the value of 1 or -1 randomly in each interval of  $T$  duration.

BPPCM

biphase pulse code modulation

$v(t)$  is a series of pulses of duration  $T$  which occur randomly and are of the form seen in Figure 5.2-1.

PPM

pulse position modulation

$v(t)$  are rectangular pulses of height  $A$  and duration  $\tau$ , one of which occurs at random spots in each interval of length  $T$ .

Table 5.2-1 (Continued)

RF  
PAM

pulse amplitude modulation

$v(t)$  are rectangular pulses of duration  $\tau$  and random amplitude occurring each  $T$  seconds.

CW

continuous wave

$$v(t) = A \cos(\omega_c t + \phi)$$

RECTPL RADAR

$v(t)$  is of the form  $m(t)\cos(\omega_c t + \theta)$  where  $m(t)$  is the rectangular pulse train discussed earlier.

TRAD RADAR

trapezoidal pulse train radar

$v(t)$  is of the form  $m(t)\cos(\omega_c t + \theta)$  where  $m(t)$  is the trapezoidal pulse train.

GAUSS RADAR

Gaussian pulse train radar

$v(t) = A \exp(-t^2/2\sigma^2) \cos\omega_c t$ , a pulse of amplitude  $A$  which occurs each  $T$  seconds, where  $\sigma$  is the standard deviation of the Gaussian.

COSQD RADAR

cosine squared pulse train radar

$v(t) = A \cos^2 \frac{nt}{T} \cos\omega_c t$ , a pulse which occurs each  $T$  seconds.

CHIRP RADAR

chirp pulse train radar

$v(t) = m(t)\cos\omega_c t$ , where  $m(t)$  is a string of trapezoidal pulses with unequal rise and fall times.

PDM

pulse duration modulation

$v(t) = m(t)\cos(\omega_c t + \theta)$ , where  $m(t)$  is the pulse duration modulation discussed earlier.

NRZPCM

nonreturn to zero pulse code modulation

$v(t) = A/2[1+m(t)]\cos\omega_c t$  where as before  $m(t)=1$  or  $-1$  in each interval of length  $T$ .

BPPCM

biphase pulse code modulation

$v(t) = m(t)\cos\omega_c t$   $m(t)$  is as discussed previously.

PPM

pulse position modulation

$v(t) = m(t)\cos\omega_c t$   $m(t)$  is as discussed previously.

FSK

frequency shift keying

$v(t)$  is either  $A\cos\omega_1 t$  or  $A\cos\omega_2 t$  for each interval  $T$ .

Table 5.2-1 (Continued)

AM

amplitude modulation

$$v(t) = A[1+\beta m(t)] \cos[\omega_c t + \phi(t)]$$

A is constant amplitude  
 $\beta$  is modulation index  
 $m(t)$  is stochastic process  
 $\omega_c$  is carrier frequency  
 $\phi(t)$  is random phase  $0 < \phi < 2\pi$

DSB SC

double sideband suppressed carrier

$$v(t) = 2 \operatorname{Re}[A m(t) \exp(j\omega_c t)]$$

$m(t)$  is stochastic process  
 $\operatorname{Re}$  denotes real part of expression

LSSB

lower sideband

$$v(t) = \operatorname{Re}[A(m(t)-jm(t)) \exp(j\omega_c t)]$$

$m(t)$  is stochastic process  
 $\operatorname{Re}$  denotes real part of expression

USSB

upper sideband

$$v(t) = \operatorname{Re}[A(m(t)+jm(t)) \exp(j\omega_c t)]$$

FM(& PM)

frequency modulation (and phase modulation)

$$v(t) = A \cos(\omega_c t + \phi(t) + \theta)$$

$\theta$  is random frequency modulation  
 $m(t)$  is constant phase

for phase modulation  $m(t)=m(t)dt$

LOLKG

local oscillator leakage

$$v(t) = A \cos(\omega_c t + m(t) + \theta)$$

$m(t)$  is random drift characteristic

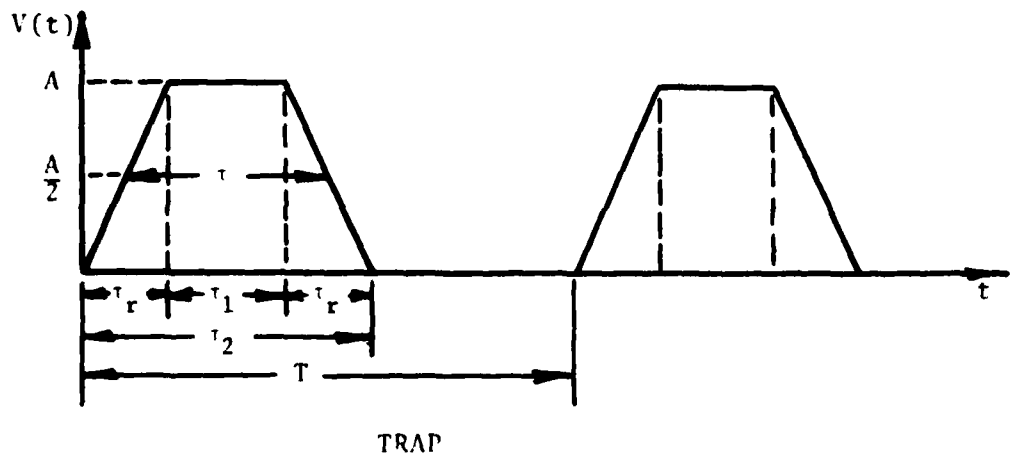
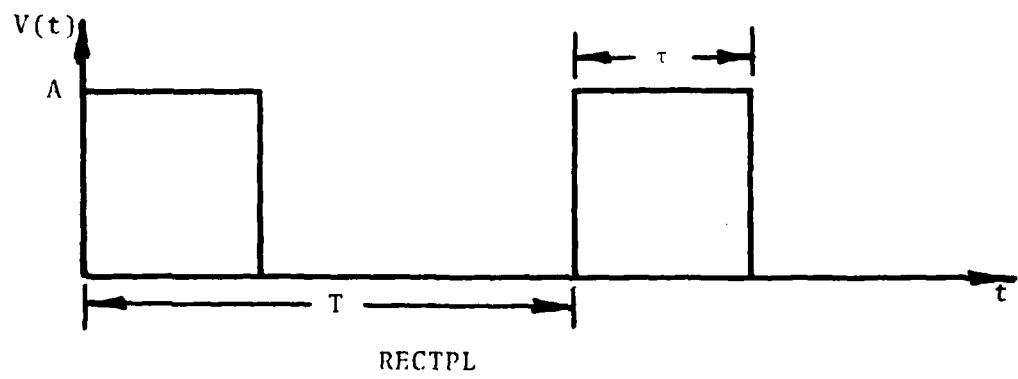
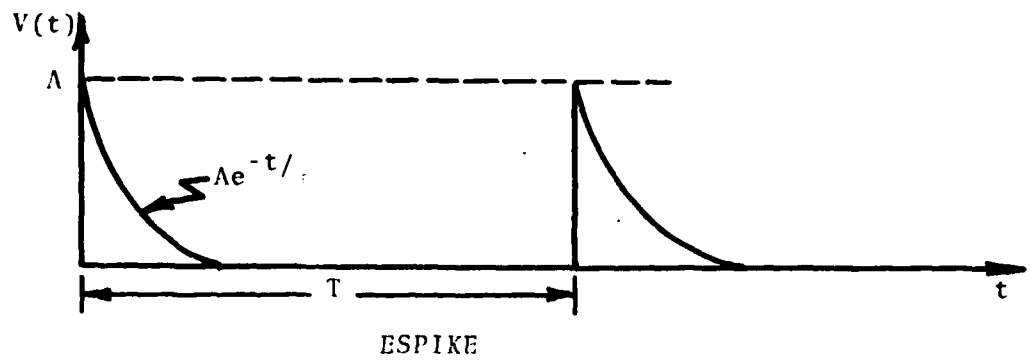
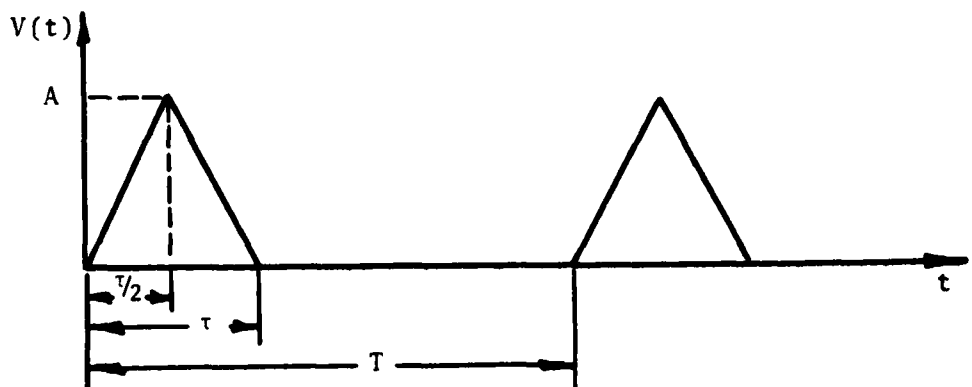
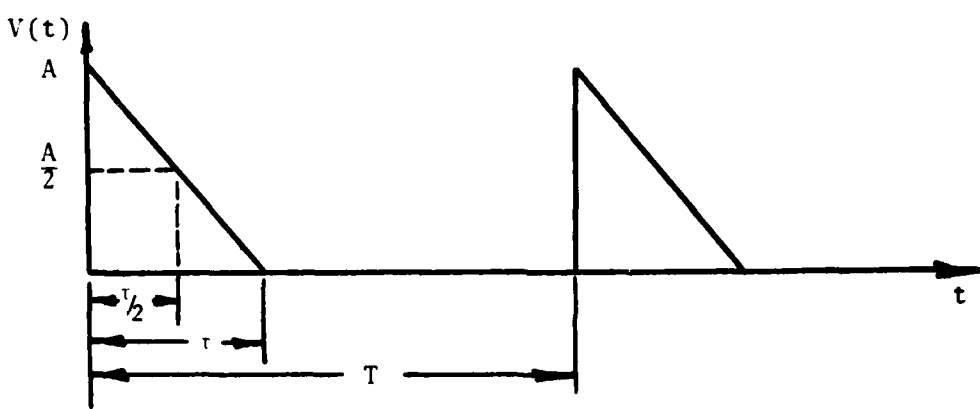


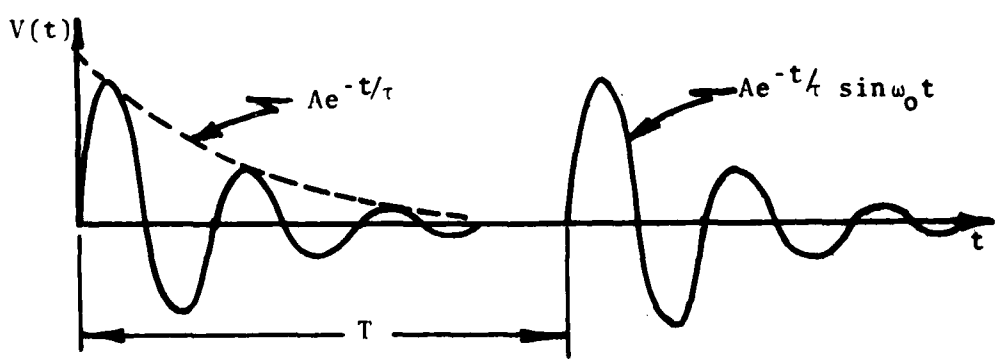
Figure 5.2-1. Emitter Models



TRIANG

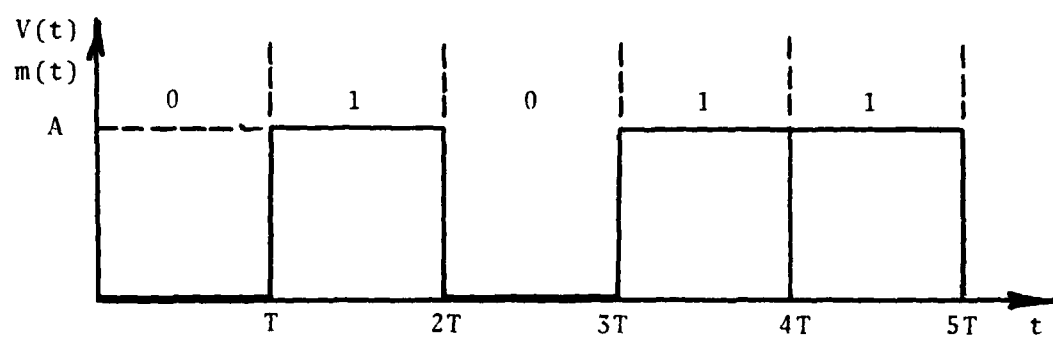
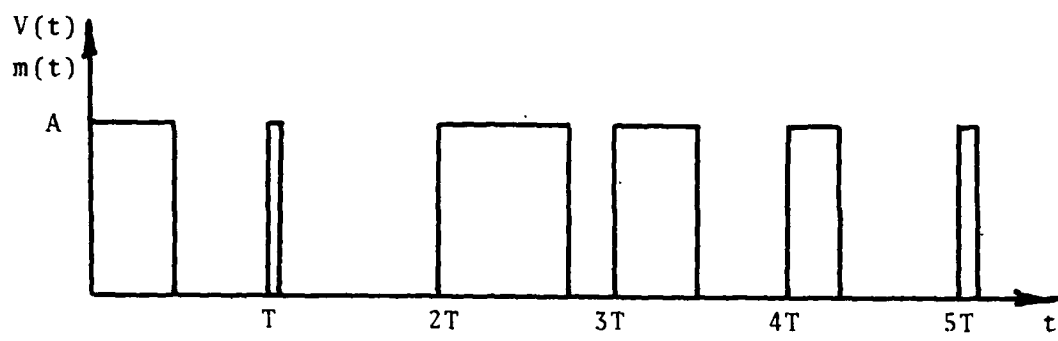


SAWTOOTH

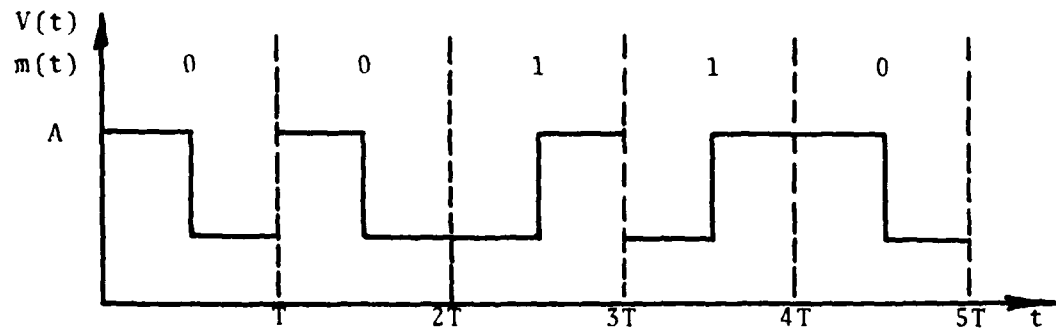


DMPSIM

Figure 5.2-1. (Continued)

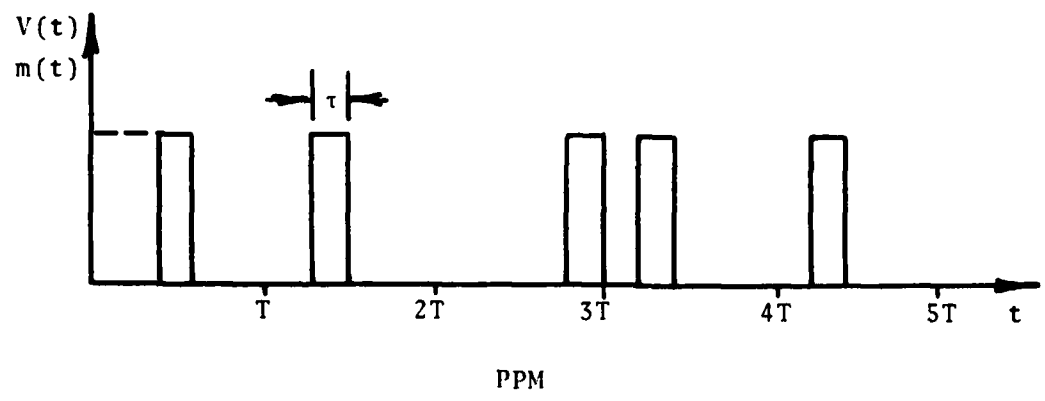


NRZPCM

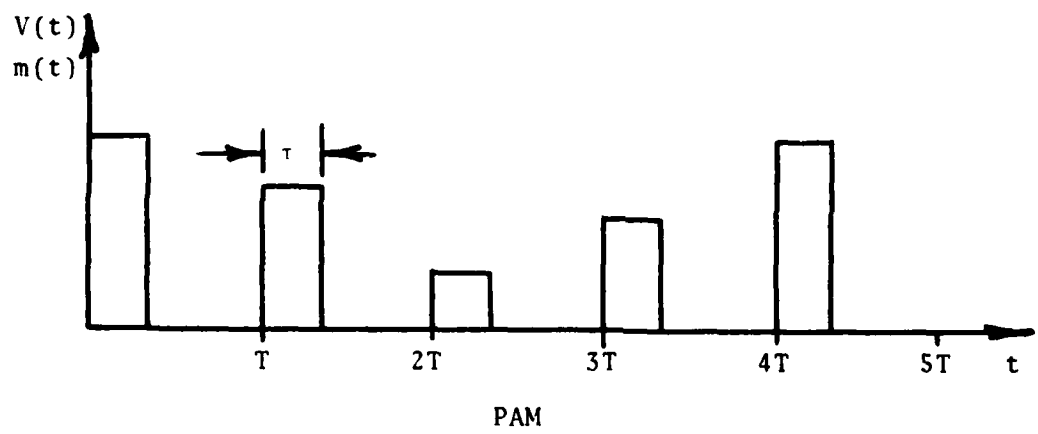


BPPCM

Figure 5.2-1. (Continued)

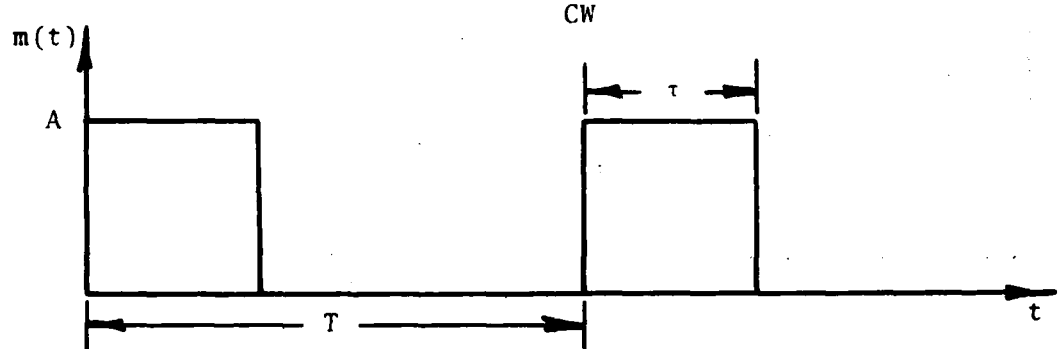
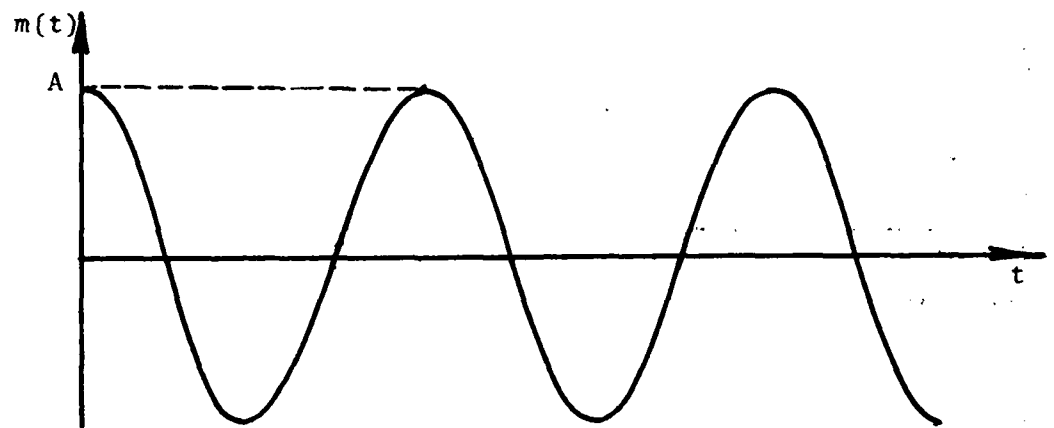


PPM

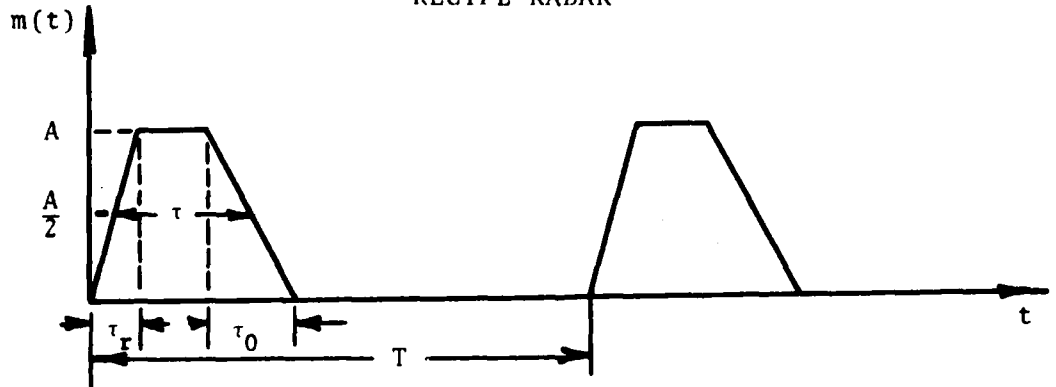


PAM

Figure 5.2-1. (Continued)



RECTPL RADAR



TRED RADAR

Figure 5.2-1. (Continued)

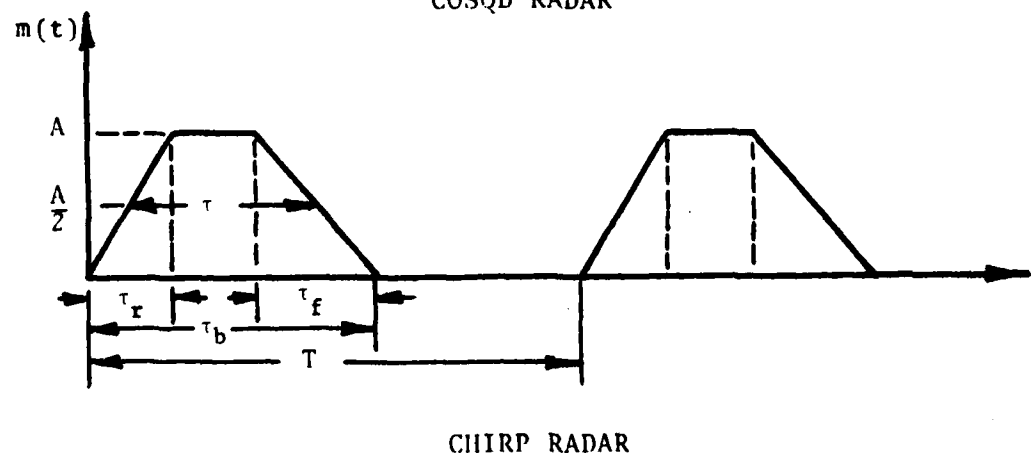
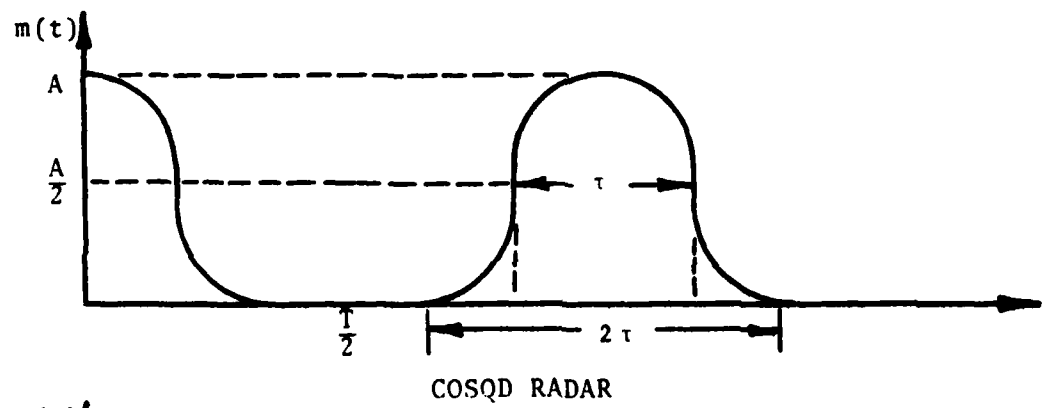
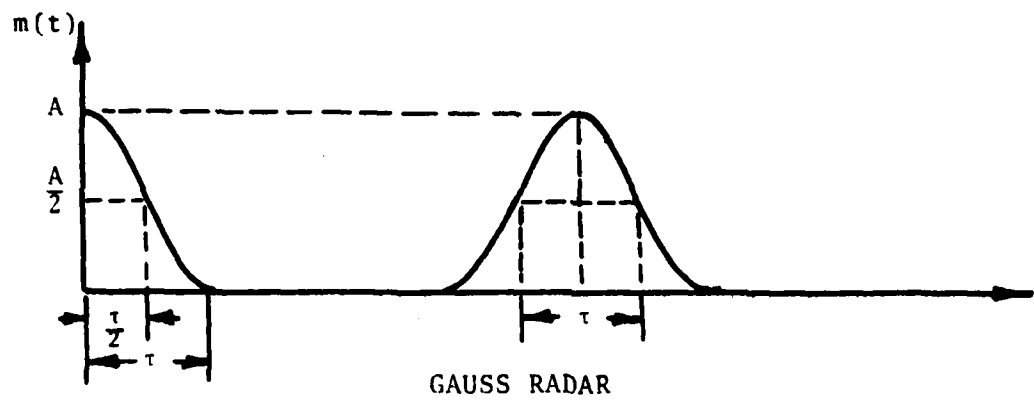


Figure 5.2-1. (Continued)

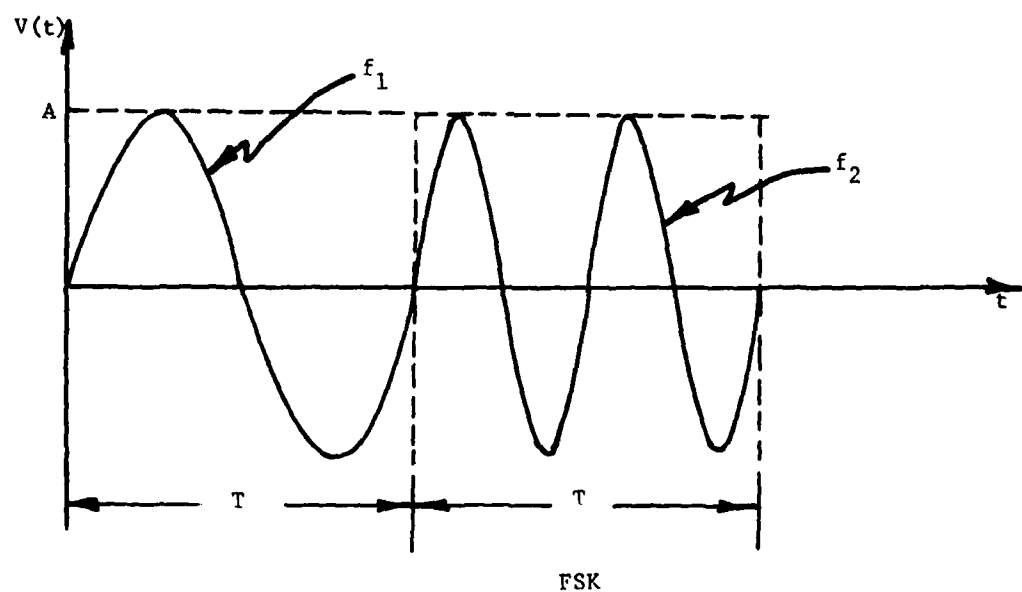
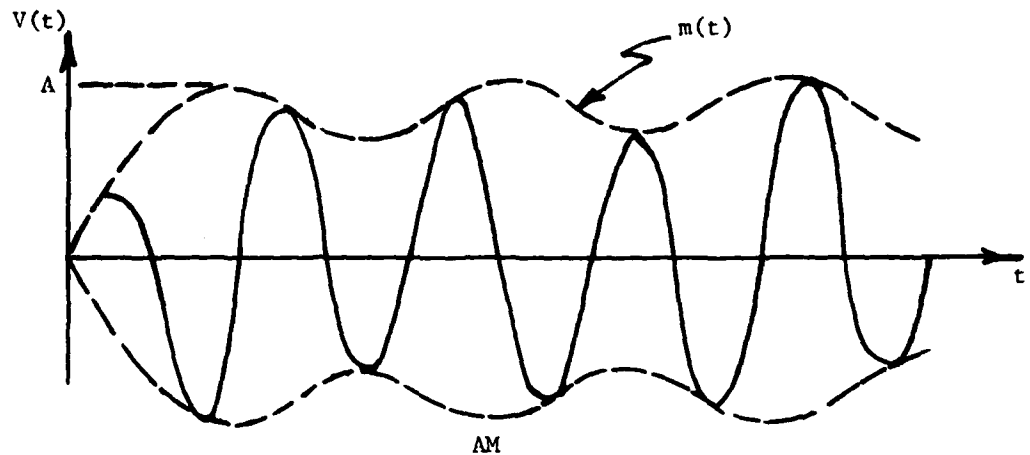


Figure 5.2-1. (Continued)

PARAMETER DESCRIPTION		UNITS
$\{A\}$	constant amplitude	volt
$\{A_i\}$	constant amplitude for $i \in \{1, 2, \dots, n\}$	volt
$\{A_{ij}\}$	constant amplitude for $i \in \{1, 2, \dots, n\}$ & $j \in \{1, 2, \dots, m\}$	volt
$\{A_{ijk}\}$	constant amplitude for $i \in \{1, 2, \dots, n\}$ , $j \in \{1, 2, \dots, m\}$ & $k \in \{1, 2, \dots, l\}$	volt
$\{A(t)\}$	stochastic process, $A(t) = \{A_i(t)\}_{i=1}^n$	radians
$\{A_m(t)\}$	stochastic process, $A_m(t) = \{A_{ij}(t)\}_{j=1}^m$	radians
$\{A_{mj}(t)\}$	stochastic process, $A_{mj}(t) = \{A_{ijk}(t)\}_{k=1}^l$	radians
$\{A_{mj}(t)\}_{j=1}^m$	stochastic process, $\{A_{mj}(t)\}_{j=1}^m$	radians
$\{A_{mj}(t)\}_{j=1}^m$	random drift	radians
$\{A_{mj}(t)\}_{j=1}^m$	constant amplitude pulse train	
$\{A_{mj}(t)\}_{j=1}^m$	normalized square wave $\omega/T$	
$\{T\}$	continuous time, $t_{20}$	sec
$\{T\}$	waveform period	sec
$\{T_i\}$	$i^{\text{th}}$ period	sec
$t_p$	time to peak	sec
$t_d$	pulse duration, $t_1 - t_2$	sec
$t_r$	risetime	sec
$t_s$	time to slope change	sec
$t_f$	falltime	sec
$\sigma$	standard deviation time	sec
$\omega_m/\omega_n$	= mark & space frequency	rad/sec
$\omega_c$	carrier frequency	rad/sec
$\theta$	modulation index, $0 \leq \theta \leq 1$	rad/sec
$B$	chirp bandwidth	rad/sec
$\phi(t)$	random phase angle, $0 \leq \phi \leq 2\pi$ (or freq.)	radian
$\phi_0$	constant phase angle	radian

Table 5.2-2. Attribute Table for Time Domain Emitter.

### 5.2.2.1 Noise

Long a concern in electronic systems, noise is a process which is not necessarily well-behaved in the time domain and as such may be modeled in only a few mathematically practical cases, most notably the Gaussian process. The prime difficulties arise not only in characterizing the time domain waveforms but in the prediction of coupling effects on the waveform. In that these problems are not restricted to the specification of noise waveform but are also affected by the stochastic modulation processes in the time domain, this subject area requires more study to adequately define the models which should be included in an IAP.

### 5.2.2.2 Signal/Control and RF Modulation

Additional signal/control and RF emitter modulation models that have been studied and which could be included in an IAP are presented in Tables 5.2-3 and 5.2-4. PSK, M-ary (MPSK), TDM and FDM comprise the new models to be included in an IAP with a variation in the BPPCM stochastic process modulation giving rise to the best additional model, delta modulation (DM). Further flexibility in an IAP could be realized by allowing the user the option of filtering the time domain waveforms in a manner similar to the SEMCAP approach.\* However, this will be discussed further in the next section on wave shaping.

### 5.2.2.3 Waveform Specification and Complex Modulation

In addition to the incorporation of energy spectra time domain modeling, the user should be afforded the opportunity of specifying a unique waveform or waveshape. In the time domain, this may take a simple form such as filtering of a predetermined "standard" model by a specified filter type, as in SEMCAP. A minimum filter choice should include low, bandpass or high pass filters or any combinations of these with the user specifying the filter parameters.

\* See Section D.1.2 for a description of SEMCAP.

Table 5.2-3.

**PSK**

**Phase Shift Keying**

$$v(t) = A \cos(\omega_c t + \theta)$$

(not general see m-ary)  
where  $\theta$  varies between  
discrete values of  $0 & n$

**M-ary (MPSK)**

**Multiple Level PCM/PSK**

$$v(t) = A \cos(\omega_c t + \theta_j); \quad \theta_j = \frac{2\pi(j-1)}{m} \quad j = 1, 2, 3 \dots m$$

m is number states being transmitted

**FDM**

**Frequency Duration Multiplexing**

$$v_c(t) = \sum_{i=1}^M c_i(t) m_i(t)$$

for M channels where  
 $c_i(t)$  is the modulation  
carrier for AM  
 $m_i(t)$  is a stochastic process

**TDM**

**Time Duration Multiplexing**

$$v_i(t) = \sum_{n=0}^{\infty} A m_i((n + \frac{i-1}{m})T) g(t - (n + \frac{i-1}{m})T) \quad i^{\text{th}} \text{ channel for } m \text{ channels}$$

If synchronizing signal  $c_s(t) = A \cos \omega_s t$  added then,

$$v_i(t) = v_i(t) + c_s(t)$$

**Delta Modulation:** Same basic model as BPPCM with stochastic process parameter variation.

Table 5.2-4. Attribute Table for Additional Time Domain Models.

	A	$\checkmark$	A	M	$g(F(t))$	$M_i(t)$	$c_i(t)$	t	$nT$	$\left[\frac{i-1}{M}\right]_T$	$w_s$	$w_c$	$\theta$	$\theta_j$	
	$\checkmark$		$\checkmark$												PSK
		$\checkmark$													MPSK
			$\checkmark$												FDM
				$\checkmark$											TDM

A Constant Amplitude

M Number states and Channels

$g(F(t))$  Constant Amplitude Pulse Train

$M_i(t)$  i<sup>th</sup> Stochastic Process

$c_i(t)$  i<sup>th</sup> Modulation Carrier for AM

t Continuous Time

$nT$  n<sup>th</sup> Period

$\left[\frac{i-1}{M}\right]_T$   $\left[\frac{i-1}{M}\right]^{\text{th}}$  Period for i<sup>th</sup> channel i=1,2..M

$w_s$  Synchronizing Signal Carrier Frequency

$w_c$  Carrier Frequency

$\theta$  Discrete Varying Phase Angle states 0,  $t_1$

$$\theta_j = \frac{2\pi-1}{M}, j = 1, 2 \dots M$$

Note: DM attributes, see BPPCM.

The combination of filters may be used to provide complex modulations where the signals are specified separately with attendant filters and the resultant signals summed. This approach could be extended to encompass unfiltered as well as filtered signals such as additive noise signals. In addition, the user should have the option of specifying any waveform point by point, which will require larger amounts of data, but which will allow great accuracy of waveform representation.

As discussed in Section 5.1.2.4, intermodulation, cross-modulation and nonlinearities shall be treated as coupling or receptor effects.

## 6.0 RECEPTOR MODELS

Presently, the only IAP receptor modeling is accomplished at the system level within IEMCAP. There, recorded receptor input port average power levels that result in susceptibility are provided as data in computing susceptibility margins (Section 4.2). It can be seen that this type of specification will not be adequate to represent all types of receptors and receptor effects. For that reason future IAP codes will have to include models that accurately characterize other effects. For the purpose of discussing the models that should be included in an IAP, this section is divided into two subsections. The first will discuss the present IAP receptor models and the second will discuss additional models recommended for inclusion in an IAP.

### 6.1 Present IAP Receptor Models

Modeling of receptors in IEMCAP is limited to specification of the receptor susceptibility. The current IEMCAP receptor models are summarized in Table 6.1.1 and are detailed in [Paul, no date]. These susceptibility representations do not adequately model today's high-performance superheterodyne receivers, which have many nonlinear characteristics. It is felt, therefore, that the receptor models currently in IEMCAP will have only restricted utility in future IAPs.

### 6.2 Recommended Additional Models

#### 6.2.1 System Level Nonlinear Receptor Models

To utilize the vast storehouse of spectrum signature data on file at various installations requires that additional models describing a system's nonlinear behavior be developed. Towards that end, considerable effort has been devoted to the theory of functional expansions. These expansions are similar in nature to the power series expansion of a function, except that the constant coefficients of the power series are replaced by the nonlinear transfer functions, which may be complex. These functional expansions have been examined in [Spina, 1979].

Table 6.1-1. Summary of Present IAP Receptor Susceptibility Models

Required Frequency Range

RF Ports

Receiver Sensitivity or User Defined  
Response Curve.

Power Signal or Control Ports

Operating Level -20 dB

Non-Required Frequency Range

RF Ports

MIL-STD-461A  
MIL-STD-6181D

Power, Signal or Control Ports

MIL-STD-461A  
MIL-STD-6181D

Equipment Case

MIL-STD-461A  
MIL-STD-6171D

User Defined

and, due to the detailed nature of the examinations, will not be repeated here. These expansions have been proved to accurately represent many nonlinear receptor effects. The complex nature of the nonlinear transfer functions makes this approach unsuitable for a system level analysis, however, as the phase information required to perform these expansions is seldom available in such an analysis. By making the transfer functions real functions, however, most of the information concerning a system's nonlinearities may be retained while the expansion itself becomes compatible with a system level analysis. Utilizing this type of expansion will allow prediction of interference due to all of the nonlinear effects enumerated in Table 6.2-1, which are the major nonlinearities associated with state-of-the-art receptors. It is felt that the availability of these models, and the parameters needed to utilize them as well as their importance in predicting nonlinear interference effects makes their inclusion into an IAP highly desirable.

Table 6.2-1 Nonlinear Receptor Effects

- 1) Gain Compression/Expansion
- 2) Desensitization
- 3) Second, Third, Fifth and Seventh order, two signal intermodulation products
- 4) Cross-modulation
- 5) Spurious Responses

#### 6.2.2 Time Domain Receptor Models

The modeling of transient and threshold effects on a receiver is desirable with the increased use of digital equipment. The exact models to be utilized have yet to be determined, however, and time domain representations of receptors must be examined in greater detail prior to their inclusion in the IAP.

### 6.2.3 User Defined Susceptibility

It is felt that the user should be afforded greater latitude in specifying a receiver's susceptibility characteristics. This could be accomplished in two ways 1) the user may specify the susceptibility curve point by point in a manner similar to the SPECT option in IEMCAP, 2) the user may define a "Bode" plot, discussed earlier in conjunction with emitter models. The "Bode" plot would specify the receiver susceptibility over the entire tuning range using only break points on the response curve, and rolloffs or slopes to define the curve between break points.

These two additions, as options, would greatly enhance the utility and ease of use of the present IEMCAP susceptibility specification, and should be included in any future receptor models.

## 7.0 COUPLING MODELS

A "coupling model" is an analytical technique used to predict induced electromagnetic quantities. Section 7.1 contains a precise definition of coupling models. A distinction is made between "basic" analytical methods and those that are combinations or extensions of the basic models. This distinction (1) significantly reduces the number of analytical coupling methods that must be thoroughly investigated for use in an IAP and (2) emphasizes the importance of developing and understanding mechanisms for combining methods.

Section 7.2 contains a summary of the pertinent attributes of specific coupling models that are important to an IAP designer. A full discussion of these attributes is presented in Appendices A and B.

### 7.1 Basic and Combined Coupling Models

Coupling models are used to predict electromagnetic quantities (fields, receptor input currents, etc.) that result from electromagnetic quantities (fields, emitter output currents, etc.). There are a great many such models that are of importance for an IAP. A thorough study of each would be unduly time-consuming; however fundamental models can be identified from which, through variation and/or combination, all important coupling models can be developed. A study of this reduced set and combining techniques is adequate for assessing the entire set.

A coupling problem (after idealization as described in Section 3.3.2), defined by its physical composition (media, etc.) and sources (frequencies, etc.), generally can be solved using any of a number of analytical models. Each model is capable, in theory, of solving the (idealized) problem almost exactly; however due to approximations in implementation, solution accuracies among models may differ. This is caused by differences in the formulation of the combined models, even though the same basic coupling models are employed. An example is shown in Figure 7.1-1(a).

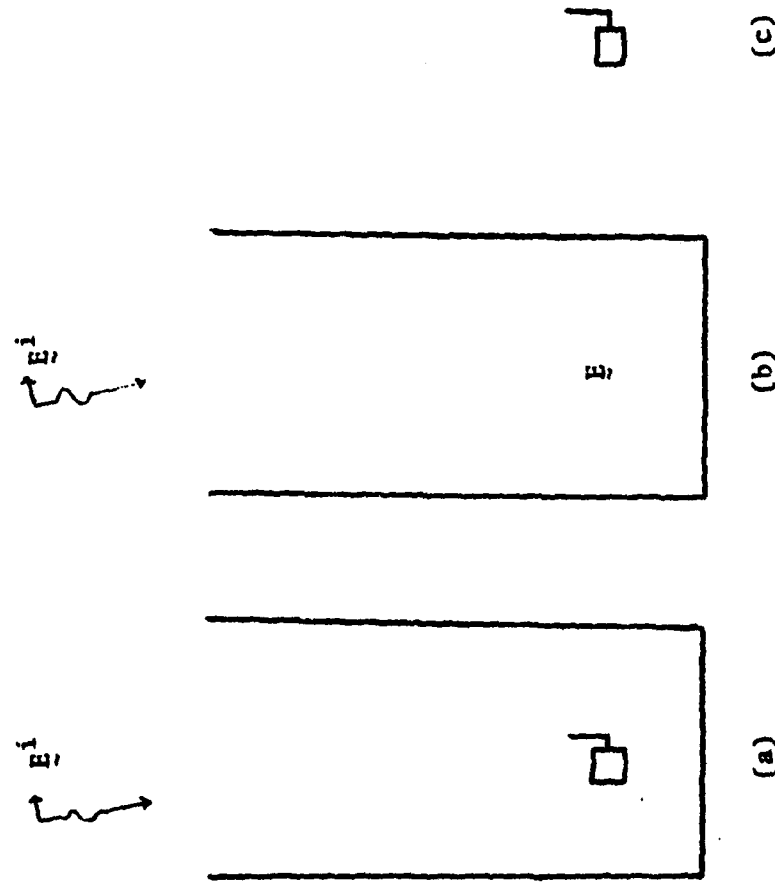


**Figure 7.1-1.** Field-to-wire coupling problem.  
The wire is attached to a small equipment box  
within an open-ended cylindrical conducting  
enclosure.

An electrically thin, open-ended, conducting cylindrical enclosure contains a small, conducting equipment box with an exposed wire. A given time-harmonic impressed field  $E^i$ , excites this system. A prediction of the current induced on the exposed wire is desired. Applicable coupling models can be constructed in a number of ways; e.g., a body of revolution (BOR) moment method (B-7), Table 7.2-1 can be used to determine the field,  $\tilde{E}$ , in the vicinity of the small equipment with the cavity empty (Figure 7.1-1(b)). Then, if it is assumed that the scattering current induced on the cylinder walls is not appreciably changed by the presence of the small equipment so that the equipment can be considered in free space and excited by an impressed field,  $E$  (Figure 7.2-1(c)), the application of a combined surface-patch/thin-wire moment method (C-1), (C-2), or (C-3), Table 7.2-2 can yield the induced current on the equipment wire. This overall coupling model (Model A) is a combination of three basic coupling models X, Y, and Z where

X = BOR moment method

Y = surface-patch moment method

Z = thin-wire moment method.

The electrical thinness of the cylinder, however, results in a numerical computation of  $\tilde{E}$  highly susceptible to errors due to normal approximations in moment method modeling [Schuman, Nov. 1978].

A second coupling model (Model B), that does not suffer from this drawback, can be constructed from the same three basic coupling models. Using an equivalence theorem [Schuman, Nov. 1978], X is now applied twice, first to a radiation problem and then to a scattering problem, in arriving at  $\tilde{E}$ . The problem represented in Figure 7.1-1(b), in which  $\tilde{E}$  is to be determined given  $E^i$ , is depicted again in Figure 7.1-2(a).

The fields in 7.1-2(a) are equal to the superposition of the fields shown in Figure 7.1-2(b) and (c). The aperture is covered with a perfectly conducting shorting plate in (b). Model X (scattering application) is applied, yielding the surface current,  $\tilde{J}$ , on the shorting plate. The original source field,  $\tilde{E}^i$ , and the shorting plate are removed and the aperture is excited with  $\tilde{J}$  (c). Model X (radiation application) is applied again, yielding,  $\tilde{E}$ . Theoretically, the cavity fields in Figures 7.1-1(b) (Model A) and 7.1-2(c) (Model B) are identical; however, accuracy considerations arising from moment method approximations favor the Model B application. This example demonstrates that careful choice of available models or combinations of such models increases the class of problems that can be solved within given constraints, e.g., accuracy. No "new" models need be developed.

There are two types of combining mechanisms: "explicit" and "implicit." Explicit combining refers generally to the cascading of models; i.e., the normal output of one model becomes the normal input to a second (or the same, if used repeatedly) model. For example, an antenna gain model might supply the field in the vicinity of an exposed wire. A moment method model might then use this field to determine the induced wire current. A second example is the repeated use of a moment method BOR model (Model X) to arrive at  $\tilde{E}$  in Figure 7.1-2(a). Here, as previously discussed, an equivalence theorem is introduced that reformulates the problem such that Model X is applied initially as a scattering problem resulting in  $\tilde{J}$  (Figure 7.1-2(b)) and then as a radiation problem, using  $\tilde{J}$  as an input, resulting in  $\tilde{E}$  (Figure 7.1-2(c)).

Implicit combining, on the other hand, refers to a more intricate association between models. For example, a thin-wire moment method (first model) might employ a geometrical theory of diffraction technique (second model) in its computation of the generalized impedance matrix elements for a wire such that diffraction from the edges of a nearby finite ground plane are

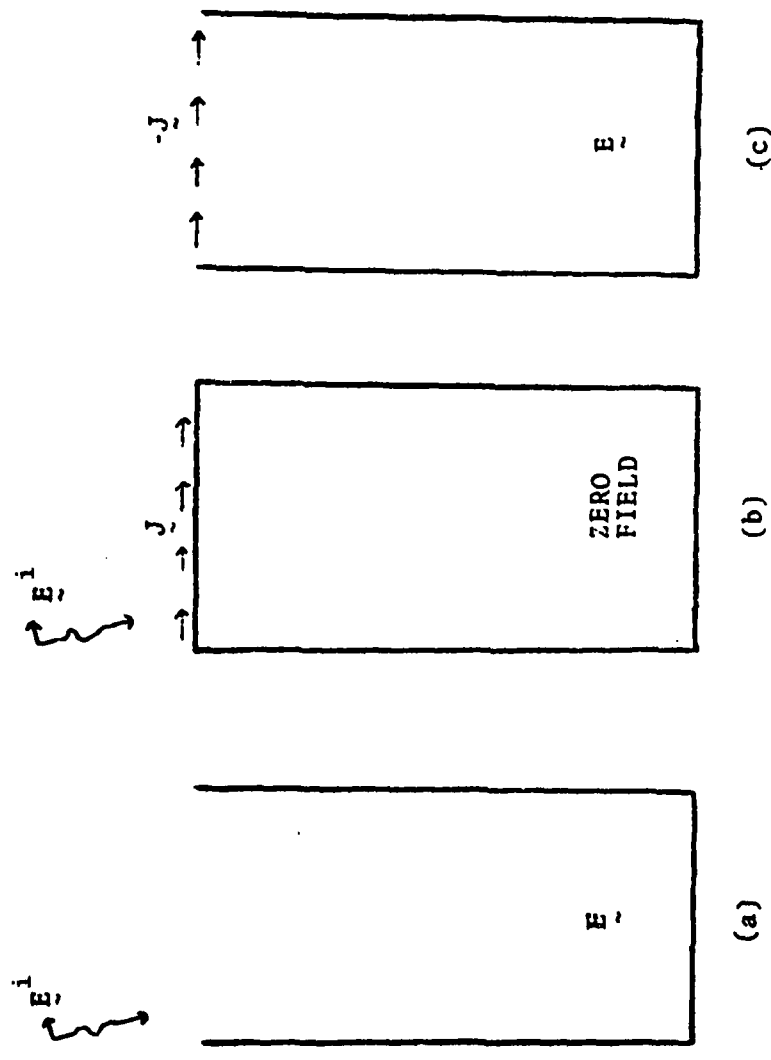


Figure 7.1-2. An alternative means for determining  $E$  of Figure 7.1-1(b).

accounted for (Table 7.2-2). Another example of implicit combining is the use of Models Y and Z in solving the problem of Figure 7.1-1. A thin-wire moment method (Z) is combined with a surface-patch moment method (Y) in a rather complicated fashion when one considers the interaction between surface patches and wire segments (C-1), (C-2), and (C-3), Table 7.2-2. In particular, the junctions between wires and surfaces may require special treatment.

The complexity inherent in many model combinations (especially implicit), suggests that they might better be considered as basic coupling models in themselves. With regard to building an IAP, the tradeoff is between duplication of computer code and sophistication of combining techniques. For model assessment purposes, however, it is efficient to minimize the number of model combinations that are considered basic coupling models, since the attributes of combinations usually can be inferred from those of the component models. A set of basic coupling models is described in Section 7.2. These are summarized in convenient tables together with selected combined models.

Mechanisms for combining available basic coupling models are essential for obtaining models that can solve problems within specified accuracies and efficiencies. A mechanism has been developed [Schuman, Aug. 1978] for accurately combining methods for the general aperture coupling problem. Optimum methods for the "exterior" and "interior" regions can be chosen. This technique is based on a formulation developed by Harrington and Mautz [Harrington, Nov. 1976] whereby two "generalized aperture admittance" matrices are defined, -- one for the interior region and one for the exterior region. The matrices are computed independently of the complexities in opposing regions and can be determined using different models. A simple matrix equation employing these matrices then can be solved for equivalent sources that excite either region.

The Unimoment method introduced by Mei [Mei, Nov. 1974] is similar to the Harrington-Mautz aperture formulation with regard to combining optimum methods. The radiation or scattering from a bounded, complex inhomogeneous region is analyzed by differentiating between an inhomogeneous "interior" region and a homogeneous "exterior" region. The Unimoment method alleviates difficulties by decoupling the exterior problem from the interior boundary value problem. The coupling model UM-BOR-FD ((C-4), Table 7.2-2 and Appendix B) is a Unimoment method applied to bodies of revolution.

The range of problems amenable to available models can be extended significantly by use of duality, reciprocity, equivalence theorems, etc. Babinet's principle and duality, for example, justifies the use of a conducting scatterer moment method to solve an aperture-in-an-infinite-ground-plane problem [Adams, June 1973]. A scattering model thus is "adapted" to an aperture problem. In Table 3.4-3, where models are grouped according to application, well-known concepts such as reciprocity and Babinet's principle are assumed. The need for developing and applying these concepts and combining techniques has been noted by Miller and Poggio [Miller, June 1976]:

"Future computer developments alone are unlikely to make it possible to sustain or match recent advances in EM computational techniques...Hybrid techniques which combine analysis, computation and/or experimentation appear to be increasingly promising...In most computer modeling work done to date, the greatest share of the effort has probably been devoted to numerical analysis and computational questions, with the formulation remaining relatively simple and unsophisticated. As we attempt to solve more demanding problems, we are finding that increased attention is likely to be needed in the formulation area, and innovative ideas in particular will be necessary if computer limitations are to be overcome."

## 7.2

Summary

Coupling models of current or potential use in an IAP (Tables 3.4-1 and 3.4-2) are summarized in Tables 7.2-1 (basic coupling models) and 7.2-2 (combined coupling models), where characteristics deemed important to an IAP are concisely presented. The tables allow the relative utility of each model to be rapidly assessed by an IAP designer. The tables provide a convenient guide to selecting models for an IAP and directing areas of future research; however, only a highlighting of each model with respect to a characteristic (attribute) can be presented in the tables. A greater understanding often may be required prior to final selection of a model to fulfill a specified IAP task. Appendices A (basic coupling models) and B (combined coupling models) contain additional model data that should prove useful for this understanding.

The attribute types considered in Tables 7.2-1 and 7.2-2 are described below.

1. Media denotes the physical characteristics of a coupling problem; e.g. "conducting wires" applies to radiation or scattering from stick models of aircraft, "conducting surfaces" to radiation and scattering from aircraft fuselages or wings, "inhomogeneous media" to insulated transmission lines, etc. A major distinction between coupling models is in the physical nature of applicable problems.

2. Electrical Size generally refers to the maximum permitted characteristic dimensions of physical bodies (aircraft fuselages and appendages, antennas, transmission lines, etc.) within the coupling environment. Unless otherwise stated, this attribute is given in free-space wavelengths, square wavelengths, or cubic wavelengths corresponding to the largest significant frequency component of the source waveform.

3. Source Type refers to the excitation; e.g., lumped circuit voltage or current sources, and incident field. Models for which only a voltage source is indicated usually can handle a current source,  $I$ , in an indirect manner. The model is invoked to determine the input impedance,  $Z$ , and then applied with the equivalent voltage source,  $V = ZI$ . Usually, in moment method computer codes such as AMP or GEMACS (model TW-FD), incident fields are restricted to plane waves, spherical waves, etc. This is only for data input convenience.

An arbitrary incident field can be considered if the user is willing to input its magnitude and phase at many points throughout the scatterer. Source code changes to permit this option generally are minor (a few lines or so).

4. Source Parameter refers to the set of excitation waveform parameters that are permissible model inputs; e.g., the magnitude and phase of a time harmonic emission.

5. Response Type characterizes the model output; e.g., port voltage, wire current, surface current, and radiated field.

6. Response Parameter refers to the set of model output waveform parameters; e.g., the magnitude and phase of a time harmonic response, the input impedance, or the "coupling." The latter may be referring to a transfer impedance, voltage transfer function, etc.

7. Accuracy is defined as the ratio of the model output to the actual problem solution, especially if satisfactory experimental results are available. Otherwise, the accuracy may reflect a comparison with exact theoretical solutions of idealized problems (Section 3.3.2). Accuracy is highly problem dependent; therefore, the resulting numbers are at best rough indicators.

8. Detail of Input Data indicates the most extensive input data type required by the model. In moment method problems, for example, this usually is the geometry description of scattering or radiating structures.

9. CPU Time indicates the run time in seconds relative to a Honeywell 6000 series system for typical computer codes if available. Run times of typical examples are given for some models. For others, the CPU time is related to model traits such as maximum characteristic dimensions of the coupling media. These dimensions, usually denoted L, A, or V, are defined within the same table column, usually with respect to the attribute "Electrical Size." Generally, only the major factor in CPU time consumption is considered. This, for example, is the matrix solution for large moment method problems. Any potential CPU time reduction due to special case symmetries for a particular model is not accounted for in these tables.

The model descriptions in Appendices A and B, together with cited references, provide the justification for many of the CPU time relations indicated; e.g., the appropriate relation for UM-BOR-FD (C-4) is derived in Section B.1.2. In all instances, the CPU time relations, or typical attribute values, were determined assuming the corresponding accuracy attribute values. In many instances, when dealing with a medium other than free space, such as with VC-FD (B-12) or UM-BOR-FD, the CPU time is given as a function of the medium's relative permittivity,  $\epsilon_r$ , and permeability,  $\mu_r$ , as well as dimensions L, A, or V. This is because the latter are assumed to be in units of free-space wavelengths, square wave-lengths, or cubic wavelengths, respectively.  $\lambda = \lambda_m \sqrt{\mu_r \epsilon_r}$ , where  $\lambda$  is the free-space wavelength and  $\lambda_m$  is the wavelength in the material medium.

All of the moment method model CPU time relations are for matrix computation only. These relations are based on that given in Section A.1.1.1.6. In most cases, the number of expansion functions (equations) was determined assuming approximately 10 expansion functions per wavelength (in the medium) per dimension. The use of Banded Matrix Iteration efficiency factor g [Balestri, April 1977] in reducing this CPU time as regards TW-FD also is discussed in Section A.1.1.1.6. The reduction in CPU time due to

body of revolution (BOR) modeling - - BOR-FD, etc. - - is discussed in Section A.1.1.3. The CPU time relations for surface patch moment method models (e.g., SPE-FD) that employ "triangular patch" expansion functions were determined assuming approximately 50 percent more expansion functions than needed for corresponding rectangular patch models for comparable accuracy (Section A.1.1.2).

If CPU times or relations were originally obtained in terms of a CDC system, they were converted to those for the Honeywell 6000 by multiplying by approximately 25 if(CDC 7600) and by approximately 10 if(CDC 6600).

10. Memory indicates the computer storage needs in number of real words. (A complex number is two real words.) As with CPU time, for some models, actual main memory usage is given for typical examples. For others, the main memory requirement is related to model traits such as largest characteristic dimensions (electrical size) of the coupling media. Generally, only the limiting factor is considered in these relations; e.g., matrix size for moment method models. Many of the comments pertaining to the derivations of the CPU time attribute values or relations also apply to the derivations of main memory attribute values or relations.

11. Availability indicates the status of the model. If a computer code is available, then a reference is provided. A number of codes are available for some models; however only typical ones, generally those most familiar to the authors, are referenced. This does not imply that others are not equally good.

12. Experience refers to the approximate level of expertise required to properly apply the model in its current state of development. An "engineer" refers to a user with the usual basic electrical engineering education. An "experienced engineer" is one with additional experience in electromagnetics.

Small, superscripted numbers in Tables 7.2-1 and 7.2-2 reference notes in Table 7.2-3.

TABLE 7.2-1  
BASIC COUPLING MODELS

Model Attribute	(B-1) TW-FD Thin Wire - Frequency Domain	(B-2) TW-FD Thin Wire - Frequency Domain	(B-3) TW-FD Thin Wire - Frequency Domain
Media	Loaded wires (stick models); overall structure is narrow in at least one dimension; linear	Loaded wires (stick models); overall structure has no dominant dimension; linear	Loaded surfaces (wire gridding); linear
Electrical Size (Wavelengths)	Total conductor length = L	Total conductor length = L	Surface area = A
Source Type	Voltage sources, incident field	Voltage sources, incident field	Voltage sources, incident field
Source Parameter	Magnitude and phase	Magnitude and phase	Magnitude and phase
Response Type	Current, near or far field	Current, near or far field	Current, near or far field
Response Parameter	Impedance, coupling, magnitude and phase	Impedance, coupling, magnitude and phase	Impedance, coupling, magnitude and phase
Accuracy (Ratio of Approximate to Exact)	$\pm 3$ dB in current, $\pm 1$ dB in field	$\pm 3$ dB in current, $\pm 1$ dB in field	$\pm 3$ dB in field, poor current accuracy
Detail of Input Data	Segmentation of Wires <sup>1</sup>	Segmentation of Wires <sup>1</sup>	Segmentation of Wires <sup>1</sup>
CPU Time (s) Relative to Honeywell 6000	$0.02L^3$ if $L > \approx 30$	$0.01L^3$ if $L > \approx 30$	$80A^3$ if $L > \approx 4$
Memory (Computer Words)	$200L^2$	$200L^2$	$5 \times 10^4 A^2$
Availability	GEMACS <sup>2</sup> (BMI efficiency $\approx 5$ )	GEMACS <sup>2</sup> AMP <sup>3</sup> NEC <sup>4</sup>	GEMACS <sup>2</sup> (BMI efficiency $\approx 5$ )
Experience Level	Experienced Engineer	Engineer	Experienced Engineer
Reference	Sec. A.1.1.1	Sec. A.1.1.1	Sec. A.1.1.1

See Table 7.2-3 for explanations of superscripted (small numbers) notations;  
e.g., GEMACS<sup>2</sup>

TABLE 7.2-1 (Continued)  
BASIC COUPLING MODELS

Attribute \ Model	(B-4) TW-FD Thin Wire - Frequency Domain	(B-5) SPH-FD Surface Patch (H-Field) Frequency Domain	(B-6) SPE-FD Surface Patch (E-Field) Frequency Domain
Media	Loaded surfaces (wire gridding); linear	Closed conducting surfaces; no edges; no loads	General conducting surfaces with loads; linear
Electrical Size (Wavelengths)	Surface area = A	Surface area = A	Surface area = A
Source Type	Voltage sources, incident field	Voltage sources, <sup>5</sup> incident field	Voltage sources, incident field
Source Parameter	Magnitude and phase	Magnitude and phase	Magnitude and phase
Response Type	Current, near or far field	Current, near or far field	Current, near or far field
Response Parameter	Impedance, coupling, magnitude and phase	Magnitude and phase	Magnitude and phase
Accuracy (Ratio of Approximate to Exact)	±3 dB in field, poor current accuracy	±3 dB in field, good current accuracy	±2 dB in current, excellent field accuracy
Detail of Input Data	Segmentation of wires <sup>1</sup>	Segmentation of surfaces <sup>1</sup>	Segmentation of surfaces <sup>1</sup>
CPU Time (s) Relative to Honeywell 6000	400 A <sup>3</sup> if A>≈4	12 A <sup>3</sup> if A>≈2 <sup>6</sup>	10 A <sup>3</sup> if A large
Memory (Computer Words)	5 × 10 <sup>4</sup> A <sup>2</sup>	5 × 10 <sup>3</sup> A <sup>2</sup>	4 × 10 <sup>3</sup> A <sup>2</sup>
Availability	GEMACS <sup>2</sup> AMP <sup>3</sup> NEC <sup>4</sup>	AMP <sup>3</sup> NEC <sup>4</sup> GEMACS <sup>6</sup>	Univ of. Mississippi <sup>7</sup>
Experience Level	Engineer	Engineer	Engineer
Reference	Sec. A.1.1.1	Sec. A.1.1.2	Sec. A.1.1.2

See Table 7.2-3 for explanations of superscripted (small numbers) notations;  
e.g., GEMACS<sup>2</sup>

TABLE 7.2-1 (Continued)  
BASIC COUPLING MODELS

Model Attribute	(B-7) BOR-FD Body of Revolution- Frequency Domain	(B-8) FE-BOR-FD Finite Element - Body of Revolution- Frequency Domain	(B-9) ESC-BOR-FD Equivalent Surface Current - Body of Revolution - Frequency Domain
Media	Rotationally symmetric, otherwise general conducting surface with loads; linear	For radiation and scattering problems see unimoment method "combined" coupling model UM-BOR-FD. Otherwise, this model applies only to finite region problems such as the cavity region of closed conducting shells.	Rotationally symmetric lossy homogeneous material body; linear <sup>12</sup>
Electrical Size (Wavelengths)	Largest latitude diameter = D; generating curve length = L		Largest latitude diameter = D; generating curve length = L (free space wavelengths)
Source Type	Voltage sources, incident field		Incident field
Source Parameter	Magnitude and phase		Magnitude and phase
Response Type	Current, near or far field		Near or far field
Response Parameter	Magnitude and phase		Magnitude and phase
Accuracy (Ratio of Approximate to Exact)	±3 dB in field ±1 dB in current		±3 dB in field
Detail of Input Data	Segmentation of generating curve		Segmentation of generating curve <sup>1</sup>
CPU Time (s) Relative to Honeywell 6000	2.5DL <sup>3</sup> if D>~4		20DL <sup>3</sup> if D>~4
Memory (Computer Words)	800L <sup>2</sup>		3.2 x 10 <sup>3</sup> L <sup>2</sup>
Availability	Syracuse Univ. <sup>8</sup> Univ. of Mississippi <sup>9</sup>		Univ. of Mississippi <sup>9</sup> Syracuse Univ. <sup>13</sup>
Experience Level	Engineer		Engineer
Reference	Sec. A.1.1.3	Sec. A.1.1.5	Sec. A.1.1.5

TABLE 7.2-1 (Continued)  
BASIC COUPLING MODELS

Model Attribute	(B-10) ESC-BOR-FD Equivalent Surface Current - Body of Revolution - Frequency Domain	(B-11) ESC-SP-FD Equivalent Surface Current - Surface Patch - Frequency Domain	'B-12) VC-FD Volume Current - Frequency Domain
Media	Rotationally sym- metric lossy in- homogeneous mater- ial <sup>13</sup> body; linear	General lossy homo- geneous material <sup>12</sup> bodies; linear	General lossy in- homogeneous mater- ial <sup>12</sup> bodies; linear
Electrical Size (Wavelengths)	Largest latitude diameter = D; aver- age generating curve length = L (free space wavelengths)	Surface area = A (free space square wavelengths)	Volume = V (free space cubic wavelengths)
Source Type	Incident field	Incident field	Incident field
Source Parameter	Magnitude and phase	Magnitude and phase	Magnitude and phase
Response Type	Near or far field	Near or far field	Near or far field
Response Parameter	Magnitude and phase	Magnitude and Phase	Magnitude and Phase
Accuracy (Ratio of Approximate to exact)	±3 dB in field	Not yet determined	±3 dB in field
Detail of Input Data	Segmentation of M generating curves	Segmentation of structure surface <sup>1</sup>	Cellular descrip- tion of structure including electri- cal properties
CPU Time (s) Relative to Honeywell 6000	$20D(ML)^3 \alpha^{3/2} 10$ ( $\alpha = \text{avg}  \epsilon_r^u $ )	$100A^3$ (A large)	$2 \times 10^7 \alpha^{9/2} V^3 11$ ( $\alpha = \text{avg}  \epsilon_r^u $ )
Memory (Computer Words)	$4 \times 10^3 (ML)^2 \alpha$	$2 \times 10^4 A^2$	$72 \times 10^6 \alpha^3 V^2 11$
Availability	Univ. of Mississippi <sup>14</sup>	Univ. of Mississippi <sup>7</sup>	Ohio State Univ. <sup>15</sup>
Experience Level	Experienced Engineer	Engineer	Engineer
Reference	Sec. A.1.1.5	Sec. A.1.1.4	Sec. A.1.1.6

TABLE 7.2-1 (Continued)  
BASIC COUPLING MODELS

Model Attribute	(B-13) SEM	(B-14) FE-TD	(B-15) TW-TD
Media	Singularity Expansion Method Linear	Finite Difference - Time Domain Completely general - nonlinear; inhomogeneous; etc.	Thin Wire - Time Domain Loaded wires; loads may be nonlinear
Electrical Size (Wavelengths)	A few wavelengths at highest complex freq of interest	Enclosed spherical volume = V	Total conductor length at highest significant source frequency = L
Source Type	Voltage sources, incident field	Incident field	Voltage sources, incident field
Source Parameter	Time waveform, LaPlace transform	Magnitude and phase (time harmonic)	Time waveform
Response Type	Currents, near or far fields	Currents, near fields	Currents, near or far fields
Response Parameter	Time waveform	Magnitude and phase (time harmonic)	Time waveform
Accuracy (Ratio of Approximate to Exact)	±3 dB in current	±2 dB in current	±2 dB in current
Detail of Input Data	Segmentation of wires, surfaces, etc.	Cellular description of structure including electrical properties	Segmentation of wires
CPU Time (s) Relative to Honeywell 6000	Increases with increasing early time accuracy	$15N_T V$ ( $N_T$ = no. of time steps) $^{16}$	$0.1 N_T L^2$ ( $N_T$ = no. of time steps) $^{16}$
Memory (Computer Words)	$2N^2$ (N=order of matrix at highest significant frequency in excitation)	$2.4 \times 10^4 V$	$40L^2$
Availability	Codes for specific conducting bodies only <sup>17</sup>	ITTRI <sup>18</sup>	Lawrence Livermore Laboratory <sup>19</sup>
Experience Level	Experienced Engineer	Engineer	Engineer
Reference	Sec. A.2.1.1	Sec. A.2.1.2	Sec. A.2.1.3

TABLE 7.2-1 (Continued)  
BASIC COUPLING MODELS

Attribute \ Model	(B-16) SPE-TD	(B-17) SPH-TD	(B-18) TML-DP-FD
Attribute	Surface Patch (E-Field) - Time Domain	Surface Patch (H-Field) - Time Domain	Transmission Line - Distributed Parameter - Frequency Domain
Media	General conducting surfaces with loads; loads may be non-linear	Closed conducting surfaces; no edges; no loads	Parallel, lossless wires; homogeneous, lossless, linear media <sup>27</sup>
Electrical Size (Wavelengths)	Surface area at highest significant source freq = A	Surface area at highest significant source freq = A	Wire separation<< $\lambda$ ; wire radii<< $\lambda$
Source Type	Voltage sources, incident field	Incident field	Voltage and current sources
Source Parameter	Time waveform	Time waveform	Magnitude and phase
Response Type	Currents, near or far fields	Currents, near or far fields	Voltages and currents
Response Parameter	Time waveform	Time waveform	Magnitude and phase
Accuracy (Ratio of Approximate to Exact)	$\pm 2$ dB in current	$\pm 2$ dB in current	$\pm 1$ dB (wire length $L \leq 0.1\lambda$ ) $6$ dB ( $L > 0.1\lambda$ ) <sup>22</sup>
Detail of Input Data	Segmentation of surfaces	Segmentation of surfaces	Cross-sectional wire placement
CPU Time (s) Relative to Honeywell 6000	$\alpha N_T A^2$ ( $N_T$ = no. of time steps) <sup>16</sup>	$12N_T A^2$ ( $N_T$ = no. of time steps) <sup>16</sup>	20 wires (ribbon plus ref), 10 freq $\rightarrow 5$ <sup>23</sup>
Memory (Computer Words)	$\approx 46A^{3/2}$	$46A^{3/2}$	20 wires (ribbon plus ref), 10 freq $\rightarrow 12,800$ <sup>23,24</sup>
Availability	Limited applicability and user-ability codes available <sup>20</sup>	Limited applicability and user-ability codes available <sup>20,21</sup>	XTALK <sup>25</sup>
Experience Level	Engineer	Engineer	Engineer
Reference	Sec. A.2.1.3	Sec. A.2.1.3	Sec. A.1.3.4

TABLE 7.2-1 (Continued)  
BASIC COUPLING MODELS

Attribute \ Model	(B-19) TML-DP-FD Transmission Line- Distributed Parameter - Frequency Domain	(B-20) TML-DP-FD Transmission Line- Distributed Parameter - Frequency Domain	(B-21) TML-DP-FD Transmission Line- Distributed Parameter - Frequency Domain
Media	Parallel, imperfectly conducting wires; homogeneous lossless, linear media <sup>27</sup>	Parallel, lossless wires; inhomogeneous, lossless, linear media <sup>27</sup>	Parallel, imperfectly conducting wires; inhomogeneous, lossless linear media <sup>27</sup>
Electrical Size (Wavelengths)	Wire separation << $\lambda$ ; wire radii << $\lambda$	Wire separation << $\lambda$ ; wire radii << $\lambda$	Wire separation << $\lambda$ ; wire radii << $\lambda$
Source Type	Voltage and current sources	Voltage and current sources	Voltages and current sources
Source Parameter	Magnitude and phase	Magnitude and phase	Magnitude and phase
Response Type	Voltages and currents	Voltages and currents	Voltages and currents
Response Parameter	Magnitude and phase	Magnitude and phase	Magnitude and phase
Accuracy (Ratio of Approximate to Exact)	$\pm 1$ dB (wire length $L \leq 0.1\lambda$ ) $\pm 6$ dB ( $L > 0.1\lambda$ ) <sup>22</sup>	$\pm 1$ dB (wire length $L \leq 0.1\lambda$ ) $\pm 6$ dB ( $L > 0.1\lambda$ ) <sup>22</sup>	$\pm 1$ dB (wire length $L \leq 0.1\lambda$ ) $\pm 6$ dB ( $L > 0.1\lambda$ ) <sup>22</sup>
Detail of Input Data	Cross-sectional wire placement	Cross-sectional wire placement	Cross-sectional wire placement
CPU Time (s) Relative to Honeywell 6000	20 wires (ribbon plus ref), 10 freq $\rightarrow$ 100 <sup>23</sup>	20 wires (ribbon plus ref), 10 freq $\rightarrow$ 25 <sup>23</sup>	20 wires (ribbon plus ref), 10 freq $\rightarrow$ 100 <sup>23</sup>
Memory (Computer Words)	20 wires (ribbon plus ref), 10 freq $\rightarrow$ 30,300 <sup>23,24</sup>	20 wires (ribbon plus ref, 10 freq $\rightarrow$ 14,300 <sup>23,24</sup>	20 wires (ribbon plus ref, 10 freq $\rightarrow$ 29,300 <sup>23,24</sup>
Availability	XTALK2 <sup>25</sup>	FLATPAK <sup>25</sup>	FLATPAK2 <sup>25</sup>
Experience Level	Engineer	Engineer	Engineer
Reference	Sec. A.1.3.4.	Sec. A.1.3.4.	Sec. A.1.3.4.

TABLE 7.2-1 (Continued)

## BASIC COUPLING MODELS

Model Attribute	(B-22) TML-LC-FD Transmission Line- Lumped Circuit - Frequency Domain	(B-23) TML-FC-FD Transmission Line- Lumped Circuit Weak Coupling - Frequency Domain	(B-24) TML-DP-FW-FD Transmission Line- Distributed Parameter Field-to-Wire - Frequency Domain
Media	Parallel, lossless wires; homogeneous lossless, linear media <sup>27</sup>	Parallel, lossless wires, lossy ground return <sup>27</sup>	Parallel, lossless wires; homogeneous lossless, linear media <sup>27</sup>
Electrical Size (Wavelengths)	Wire length $L > \lambda/10$ ; Wire separation $>> 4$ radii and $\ll \lambda$ ; Wire radii $\ll \lambda$	Wire length $L < 0.1\lambda$ <sup>28,29</sup>	Wire separation $> 5$ wire radii; transmission line diameter $\ll \lambda$
Source Type	Voltage and current sources	Voltage and current sources	Voltage and current sources, incident field.
Source Parameter	Magnitude and phase	Magnitude and phase	Magnitude and phase
Response Type	Voltages and currents	Voltages and currents	Voltages and currents
Response Parameter	Magnitude and phase	Magnitude and phase	Magnitude and phase
Accuracy (Ratio of Approximate to Exact)	$\pm 3$ dB ( $L < 0.1\lambda$ ); $\pm 10$ dB ( $\lambda/10 < L <$ $0.25\lambda$ )	$\pm 10$ dB ( $L < 0.1\lambda$ ) <sup>30</sup>	$\pm 1$ dB (wire length $L < 0.2\lambda$ )
Detail of Input Data	Cross-sectional wire placement	Wire separations	Cross-sectional wire placement
CPU Time (s) Relative to Honeywell 6000	Three wires $\rightarrow 0.005$	Three conductors $\rightarrow 10^{-3}$	Two wires, 105 frequencies $\rightarrow 3$
Memory (Computer Words)	Fixed in size	1,500	2 wires $\rightarrow 8,200$ <sup>24</sup>
Availability	STRAP <sup>26</sup> IVEMCAP <sup>26</sup>	IEMCAP (WTWTFR) <sup>31</sup>	Wire <sup>32</sup>
Experience Level	Engineer	Engineer	Engineer
Reference	Sec. A.1.3.5	Sec. A.1.3.6.	Sec. A.1.3.4.

TABLE 7.2-1 (Continued)

## BASIC COUPLING MODELS

Model Attribute	(B-25) TML-WC-FW-FD	(B-26) TML-DP-TD	(B-27) FST
	Transmission Line- Lumped Circuit Weak Coupling - Field-to-Wire - Frequency Domain	Transmission Line- Distributed Parameter - Time Domain	Free Space Transmission
Media	Parallel, lossless wires; homogeneous lossless, linear media <sup>27</sup>	Parallel, lossless wires; inhomogeneous cross-section	Free space
Electrical Size (Wavelengths)	Wire separation > 5 wire radii; transmission line diameter $\ll \lambda$ ; wire length $L < 0.2\lambda$ .	Wire separation $<0.2\lambda$ ( $\lambda$ = wave- length at highest significant frequency)	Arbitrary
Source Type	Voltage and current sources, incident field	Voltage and current sources, incident field	Antenna input
Source Parameter	Magnitude and phase	Magnitude and phase	Average power
Response Type	Voltages and currents	Voltages and currents	Antenna output
Response Parameter	Magnitude and phase	Magnitude and phase	Average power
Accuracy (Ratio of Approximate to Exact)	$\pm 10$ dB ( $L < 0.2\lambda$ )	$\pm 3$ dB for low- frequency waveforms	$\pm 2$ dB <sup>44</sup>
Detail of Input Data	Cross-sectional wire placement	Cross-sectional wire placement	Transmitter and receiver antenna locations and gains
CPU Time (s) Relative to Honeywell 6000	Two wires $\rightarrow 10^{-3}$	20 wires, 10 frequencies $\rightarrow \sim 100$	<1
Memory (Computer Words)	1,000	24	30
Availability	IEMCAP Field- to-wire <sup>31</sup>	40	IEMCAP <sup>43</sup>
Experience Level	Engineer	Engineer	Engineer
Reference	Sec. A.1.3.6	Sec. A.2.2.	Sec. A.1.2.1

TABLE 7.2-1 (Continued)  
BASIC COUPLING MODELS

Attribute \ Model	(B-28) GO	(B-29) GTD	(B-30) PTD
Media	Linear, homogeneous; conducting surfaces	Linear; homogeneous; conducting bodies with edges	Linear; homogeneous conducting bodies with edges
Electrical Size (Wavelengths)	Each surface dimension > several $\lambda$	Each surface dimension and edge length > several $\lambda$	Each surface dimension and edge length > several $\lambda$
Source Type	Field from sources located $> \lambda/4$ from curved surfaces	Field from sources located $> \lambda/4$ from curved surfaces and edges	Incident field
Source Parameter	Magnitude and phase	Magnitude and phase	Magnitude and phase
Response Type	Near and far fields	Fields located $>$ several $\lambda$ from edges	Near and far fields; scattering currents
Response Parameter	Magnitude and phase	Magnitude and phase	Magnitude and phase
Accuracy (Ratio of Approximate to Exact)	$\pm 2$ dB	$\pm 2$ dB	$\pm 2$ dB
Detail of Input Data	Curvatures and orientations of surfaces	Curvatures and orientations of surfaces and edges	Curvatures and orientations of surfaces and edges
CPU Time (s) Relative to Honeywell 6000	Few seconds typical for flat surface scatterers <sup>41</sup>	Few seconds typical for flat surface scatterers <sup>41</sup>	-
Memory (Computer Words)	50K (typical) <sup>41</sup>	50K (typical) <sup>41</sup>	-
Availability	Flat rectangular plates and cylinders Ohio State Univ. <sup>41</sup> connected plates: Univ. of Denmark	Flat rectangular plates and cylinders Ohio State Univ. <sup>41</sup> connected plates: Univ. of Denmark	User oriented code of general applicability not now available
Experience Level	Engineer	Engineer	Engineer
Reference	Sec. A.1.2.2	Sec. A.1.2.3.	Sec. A.1.2.4.

TABLE 7.2-2  
COMBINED COUPLING MODELS

Model Attribute	(C-1) TW-FD/SPH-FD Thin Wire, Surface Patch ( $H$ -Field) - Frequency Domain	(C-2) TW-FD/SPE-FD Thin Wire, Surface Patch ( $E$ -Field) - Frequency Domain	(C-3) TW-FD/SPE-FD Thin Wire, Surface Patch ( $E$ -Field) - Frequency Domain
Media	Loaded wires attached to closed surfaces (all conductors); linear	Loaded wires attached to plates (rectangular sub-domains) with loads; linear	Loaded wires attached to arbitrary conducting surfaces with loads; linear
Electrical Size (Wavelengths)	Total wire length= $L$ ; surface area= $A$ , $A_c$ for open (wire grid), closed surfaces, respectively	Total wire length= $L$ , surface area= $A$	Total wire length= $L$ ; surface area= $A$
Source Type	Voltage sources, incident field	Voltage sources, incident field	Voltage sources, incident field
Source Parameter	Magnitude and phase	Magnitude and phase	Magnitude and phase
Response Type	Currents, near or far field	Currents, near or far field	Currents, near or far field
Response Parameter	Impedance, coupling, magnitude and phase	Impedance, coupling, magnitude and phase	Impedance, coupling, magnitude and phase
Accuracy (Ratio of Approximate to Exact)	$\pm 3$ dB in field, good current accuracy on wires and <u>closed</u> surface only	$\pm 2$ dB in current, excellent field accuracy	Not yet determined
Detail of Input Data	Segmentation of wires of surfaces <sup>1</sup>	Segmentation of wires and surfaces <sup>1</sup>	Segmentation of wires and surfaces <sup>1</sup>
CPU Time (s) Relative to Honeywell 6000	$0.1 (L + 16A_0 + 5A_c)^3$ ( $L, A_0$ , or $A_c$ large) <sup>4</sup>	$0.1 (L + 4A)^3$ ( $L$ or $A$ large)	$0.1 (L + 5A)^3$ ( $L$ or $A$ large)
Memory (Computer Words)	$200 (L + 16A_0 + 5A_c)^2$	$200 (L + 4A)^2$	$200 (L + 5A)^2$
Availability	AMP <sup>3</sup> GEMACS <sup>6</sup>	Ohio State University <sup>3E</sup>	Soon - University of Mississippi <sup>7</sup>
Experience Level	Engineer	Engineer	Engineer
Reference	Sec. B.1.1	Sec. B.1.1	Sec. B.1.1

AD-A103 899

ATLANTIC RESEARCH CORP ALEXANDRIA VA  
INTRASYSTEM ANALYSIS PROGRAM (IAP) STRUCTURAL DESIGN STUDY (U)  
JUN 81 W G DUFF, L D THOMPSON, H K SCHUMAN F30602-77-C-0150  
UNCLASSIFIED ARC-53-6111 RADC-TR-81-133 NL

F/G 20/3

2 - 3  
26-21000

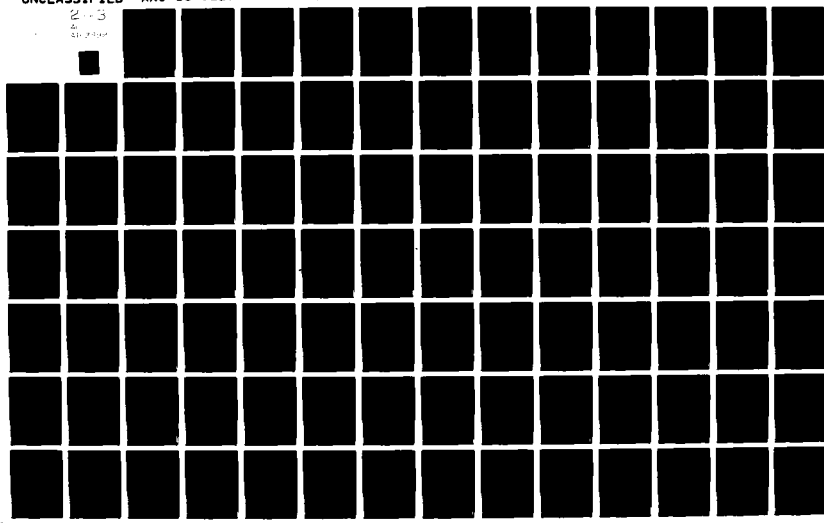


TABLE 7.2-2 (Continued)  
COMBINED COUPLING MODELS

Model Attribute	(C-4) UM-BOR-FD Unimoment Method, Body of Revolution Frequency Domain	(C-5) TW-FD/BOR-FD Thin Wire, Body of Revolution - Frequency Domain
Media	Rationally symmetric lossy in-homogeneous material bodies and conductors; linear	Conducting rotationally symmetric surface with attached bent, loaded wires; linear
Electrical Size (Wavelengths)	Diameter of enclosing sphere = D (free-space wavelengths)	Total wire length=L, largest BOR surface latitude=D, BOR generating curve = L'
Source Type	Voltage sources, incident field	Voltage sources, incident field
Source Parameter	Magnitude and phase	Magnitude and phase
Response Type	Currents, near or far field	Currents, near or far field
Response Parameter	Magnitude and phase	Impedance, coupling, magnitude and phase
Accuracy (Ratio of Approximate to Exact)	$\pm 5$ dB in field, good current accuracy	$\pm 3$ dB in field
Detail of Input Data	Complex (relative) $\epsilon_r$ and $\mu_r$ at mesh points within a $\phi = \text{constant}$ cross section of enclosing sphere	Segmentation of wires and generating curve
CPU Time(s) Relative to Honeywell 6000	$D^4 (2.1\alpha^2 + 1.75\alpha^{3/2})$ ( $\alpha = \text{avg. value of }  \epsilon_r \mu_r $ )	$7.5(DL')^3 + 0.1L^3$ 33
Memory (Computer Words)	$5000D^2 \times \text{average value of }  \epsilon_r \mu_r $	$200 (13DL' + 13DL'L + L^2)$
Availability	University of California	McDonnell Douglas
Experience Level	Engineer	Engineer
Reference	Sec. B.1.2	Sec. B.1.1

TABLE 7.2-2 (Continued)  
COMBINED COUPLING MODELS

Attribute \ Model	(C-6) BOR-FD/ESC-BOR-FD  Body of Revolution Equivalent Surface Current - Frequency Domain	(C-7) TW-FD/VC-FD  Thin Wire-Volume Currents - Frequency Domain
Media	Rotationally symmetric lossy in-homogeneous material <sup>12</sup> and partially conducting body; linear	General lossy inhomogeneous material bodies <sup>12</sup> plus loaded wires; linear
Electrical Size (Wavelengths)	Largest latitude diameter = D; conductor generating curve length=L; L' for material BOR (free-space wavelengths) generating curve	Total length of wires = L; volume of material = V (free-space cubic wavelengths)
Source Type	Voltage sources, incident field	Voltage sources, incident field
Source Parameter	Magnitude and phase	Magnitude and phase
Response Type	Currents, near or far field	Currents, near or far field
Response Parameter	Magnitude and phase	Magnitude and phase
Accuracy (Ratio of Approximate to Exact)	±3 dB in field	±3 dB in current
Detail of Input Data	Segmentation of M generating curves	Cellular description of bodies including electrical properties, segmentation of wires <sup>1</sup>
CPU Time (s) Relative to Honeywell 6000	$2.5D(L+2MaL')^3$ 10 (a = avg. $ \epsilon_{rur} $ )	$0.1(600a^{3/2}V + L)^2$ (a = avg. $ \epsilon_{rur} $ )
Memory (Computer Words)	$800D(L+2MaL')^2$	$200(600a^{3/2}V + L)^2$
Availability	Special application code for missile plume analysis - University of Mississippi <sup>14</sup>	Ohio State University <sup>15</sup>
Experience Level	Experienced Engineer	Engineer
Reference	Sec. B.1.2	Sec. B.1.2

TABLE 7.2-2 (Continued)  
COMBINED COUPLING MODELS

Attribute	(C-8) TW-TD/SPH-TD Thin Wire - Surface Patch (H-Field) - Time Domain	(C-9) SPE-TD/SPH-TD Surface Patch E-Field and H-Field -Time Domain
Media	Loaded wires attached to closed surfaces (all conductors); loads may be nonlinear	Open surfaces attached to closed surfaces; open surfaces may have nonlinear loads
Electrical Size (Wavelengths)	At highest significant source freq. total wire length = L and closed surface area = A	At highest significant source freq. total surface area = A
Source Type	Voltage sources, incident field	Voltage sources, incident field
Source Parameter	Time waveform	Time waveform
Response Type	Currents, near or far field	Currents, near or far field
Response Parameter	Time waveform	Time waveform
Accuracy (Ratio of Approximate to Exact)	$\pm 2$ dB in current	$\pm 2$ dB in current
Detail of Input Data	Segmentation of wires and surfaces	Segmentation of surfaces
CPU Time (s) Relative to Honeywell 6000	$0.2N_T(L + 6A)^2$ ( $N_T$ = No. of time steps) <sup>16</sup>	Proportional to $N_T A$ ( $N_T$ = No. of time steps) <sup>16</sup>
Memory (Computer Words)	$40L^2$ if $L \gg A$ ; $46A^{3/2}$ if $A \gg L$	$\approx 46A^{3/2}$
Availability	Limited applicability and user-bility codes available-Sperry <sup>37</sup>	Limited applicability and user-bility codes available-Sperry <sup>38</sup>
Experience Level	Engineer	Engineer
Reference	Sec. B.3	Sec. B.3

TABLE 7.2-2 (Continued)  
COMBINED COUPLING MODELS

Attribute \ Model	(C-10) TDA  Time Domain Augmentation	(C-11) TML-FD/N  Transmission Line- Network - Frequency Domain	(C-12) TML-WC-FD/S  Transmission Line- Weak Coupling - Summation Frequency Domain
Media	Loaded conduct- ing surfaces and wires	Lossless homogen- eous, parallel wire bundles branching between networks	Parallel, lossless wires, lossy ground return for branches between networks
Electrical Size (Wavelengths)	Unlimited	Wire separation $\ll \lambda$	Wire separation $\ll \lambda$ , branch lengths $< 0.1\lambda$
Source Type	Voltage sources, incident field	Voltage and current sources, incident field	Voltage sources
Source Parameter	Time waveform	Magnitude and phase	Magnitude and phase
Response Type	Currents, near or far field	Voltages and currents	Voltages
Response Parameter	Time waveform	Magnitude and phase	Magnitude and phase
Accuracy (Ratio of Approximate to Exact)	$\pm 2$ dB in current	$\pm 3$ dB	$\pm 10$ dB
Detail of Input Data	Segmentation of wires and surfaces; singu- larity functions de- rived from physical optics, GTD, etc.	Locations of junctions, cross- sectional wire placement	Number of wires, branch lengths
CPU Time (s) Relative to Honeywell 6000	Reasonable	Proportional to TML-DP-FD time	$10^{-3}$ sec
Memory (Computer Words)	Reasonable	Square of total number of wires in all branches	Total number of wires in all branches
Availability	No user-oriented code available. For aircraft/ missile, see Sperry <sup>20</sup>	LU Tech <sup>39</sup>	IEMCAP (WTWTFR) <sup>31</sup>
Experience Level	Experienced Engineer	Engineer	Engineer
Reference	Sec. B.3	Sec. B.4	Sec. B.4

TABLE 7.2-2 (Continued)  
COMBINED COUPLING MODELS

Attribute \ Model	(C-13) GO/GTD Geometrical Optics Geometrical Theory of Diffraction	(C-14) GTD/MOM Ray Methods, Moment Methods
Media	Linear; homogeneous; conducting bodies with edges	Loaded wires and complex, not large, surfaces in presence of large conduct- ing bodies with edges; linear; homogeneous
Electrical Size (Wavelengths)	Each surface dimen- sion and edge length $>\lambda$	Arbitrary
Source Type	Field from sources lo- cated $>\lambda/4$ from edges or curved surfaces	Voltage sources; incident field
Source Parameter	Magnitude and phase	Magnitude and phase
Response Type	Fields located $>$ several $\lambda$ from edges	Near and far fields; currents
Response Parameter	Magnitude and phase	Impedance, coupling; magnitude and phase
Accuracy (Ratio of Approximate to Exact)	$\pm 2$ dB	$\pm 2$ dB
Detail of Input Data	Curvatures and orientations of surfaces and edges	Segmentation of loaded wires and complex, not large, surfaces
CPU Time (s) Relative to Honeywell 6000	Few seconds typical for flat plate scatterer <sup>41</sup>	Dominated by moment method matrix solution if antenna is complex <sup>45</sup>
Memory (Computer Words)	50K (typical) <sup>41</sup>	Dominated by appropriate moment method if antenna is complex <sup>46</sup>
Availability	Flat rectangular plates and cylinder: Ohio State Univ. <sup>41</sup> ; connected plates: Univ. of Denmark <sup>42</sup>	User oriented code of general applicability not now available
Experience Level	Engineer	-
Reference	Sec. B.2.1	Sec. B.2.2

Table 7.2-3. Notes for Tables 7.2-1 and 7.2-2.

1. Facilitating geometry generation routines are assumed included in computer codes of model.
2. [Balestri, April 1977]
3. [AMP, July 1972]
4. [Burke, July 1977]
5. Via reciprocity
6. GEMACS will include the model in 1 year if not already
7. [Rao, April 1979]
8. [Mautz, May 1977] [Harrington, July 1968]
9. [Glisson, June 1978]
10. This number can be reduced significantly for M>2 if sparse matrix techniques are used.
11. These numbers reduce considerably if media is dielectric or ferrite only.
12. "Material bodies" refers to those of arbitrary permittivity, permeability, and conductivity.
13. [Mautz, Nov. 1977]
14. [Wilton, April 1979]
15. [Newman, July 1978]
16. Number of time steps is typically 600.
17. For example [Tesche, January 1973] [Marin, March 1974]
18. [Taflove, June 1978]
19. [Landt, May 1974]
20. [Bennett, Sept. 1977]
21. [Bevensee, 1976]
22. Also limited by accuracy of physical measurements which can be critical in region of nulls.
23. Double precision used in this example.
24. Memory requirement =  $AN^2 + BN + C$  where N = number of wires and A, B, and C are constants.
25. [Paul, July 1977]
26. [Paul, April 1976 (pg. 70)]
27. Wire terminals may be loaded.
28. All terminal impedances must be of comparable magnitude.
29. Large difference in terminal impedance magnitudes produces unreliable results.
30. Accuracy pertains only to two wires plus reference and terminal impedances of same magnitude.
31. [Paul, no date]
32. [Paul, Feb. 1978 (Vol. VI of RADC-TR-76-1010)]
33. Only matrix inversions and solution time considered; CPU time could be considerably increased due to necessary matrix multiplications.
34. [Morgan, March 1979]
35. [Schaeffer, June 1979]
36. [Newman, Nov. 1978]
27. [Bennett, June 1970]
38. [Bennett, July 1974]
39. [Baum, Nov. 1978]
40. [Marx, July 1973]
41. [Marhefka, March 1978]
42. [Bach, Sept. 1975]
43. [Paul, no date]

Table 7.2-3 (Continued)

44. This accuracy assumes antennas are polarization matched and environment is relatively scatterer clean.
45. The CPU time for the appropriate moment method (TW-FD, SPH-FD, TW-FD/SPH-FD, etc.) applies here if the antenna is complex or large since the number of unknowns (basic functions) N is then large and matrix solution (proportional to  $N^3$ ) is then significantly greater than matrix computation (proportional to  $N^2$ ). This is a consequence of the time required for computing GO and GTD rays being contained in matrix computation and not matrix solution. On the other hand, for smaller N, say less than 1000, the time required for computing the rays may add significantly to the overall time, especially if many diffracting and reflecting edges and surfaces need be considered.
46. The appropriate moment method model may be TW-FD, SPH-FD, TW-FD/SPH-FD, etc.

It is important to realize that attribute values for a given model are related; e.g., the  $\pm 3$  dB accuracy for SPH-FD((B-5), Table 7.2-1) corresponds to the CPU time of  $12(A)^3$ , where A is the surface area of the scatterer in square wavelengths. Some models therefore are presented via a number of columns, each one referring to a different combination of attribute values; e.g., the thin wire frequency domain model, TW-FD, occupies columns (B-1),(B-2),(B-3), and (B-4) in Table 7.2-1. These four columns reflect different media (thin bodies via stick models or surfaces via wire gridding) and different CPU times (banded matrix iteration (GEMACS) timing or straight matrix solution timing). Obviously, not all combinations of attribute values can be presented here; however, those that are listed are likely to illuminate the capabilities and drawbacks of a model with regard to usage by an IAP designer.

All of the models considered are of fairly general applicability. For the most part, they are based on 3-dimensional methods only. Except for bodies of revolution (BORs), methods applicable only to media with special symmetries are excluded. The exception for BORs is because of the prevalence of available BOR models, the existence of many important scatterers and radiators that may be approximated by BORs, and the significant increase in frequency at which such bodies can be analyzed.

Models based on bodies of translation (finite cylinders of arbitrary cross section) have been investigated recently [Medgyesi-Mitschang, May 1978]. They appear promising, although still in the development stage, and are not included in the tables.

Network analysis models have been excluded from this summary. Linear network analysis codes in frequency and time domains based on Kirchoff's circuit laws are readily available. A description of the frequency domain IAP code NCAP, applicable also to mildly nonlinear networks, is available [Spina, 1979]. Network models applicable to general, rather than restricted, circuit types that apply at higher frequencies where circuits begin to exhibit distributed effects as well as radiation are not

available. In particular, circuits designed for audio frequency operation exhibit significant parasitic effects at radio frequencies; these parasitic effects are difficult to model in a general nature [Whalen, Nov. 1979].

Many other combined coupling models, as well as additional basic coupling models, may belong in these tables. The particular combinations of basic coupling models chosen for Table 7.2-2, however, already have been developed and coded or are of particular interest to an IAP designer.

## Appendix A

### Basic Coupling Models

The basic coupling models summarized in Table 7.2-1 are discussed here. Those models considered as combinations of basic coupling models and summarized in Table 7.2-2 are discussed in Appendix B.

#### A.1      Frequency Domain

Frequency domain models encompass those methods and associated computer codes that either solve an electromagnetic problem at a specified time-harmonic frequency (usually  $e^{j2\pi ft}$  temporal variation assumed) or solve a quasi-static problem ( $f \rightarrow 0$ ) or an asymptotic-with-frequency problem ( $f \rightarrow \infty$ ). Of course, through Fourier transform, frequency domain models can often be used to solve many time domain problems and vice versa.

##### A.1.1    Low to Medium Frequency Radiation and Scattering

Many of those models considered applicable to radiation or scattering from bodies having largest extent not exceeding a few wavelengths are based on the method of moments [Harrington, 1968]. Many pertinent moment method aspects will be detailed here only in conjunction with the thin wire model TW-FD in Section A.1.1.1 and simply referenced back wherever appropriate while discussing other models. For example, once the moment method matrix equation is defined then the procedure for determining current or related parameters such as scattered or radiated field, impedance, and "coupling" generally proceeds along the same lines for all moment method models. Therefore, methods for solving matrix equations and also general equations relating these solutions to desired electromagnetic parameters are described in depth only with regard to TW-FD.

The models discussed here are generally grouped in accordance with applicable classes of structures. Thus there are separate subsections devoted to thin wire models, conducting surface models and material body (e.g., dielectric radomes, composite wings, etc.) models. In addition, material body models that are based on volume current formulations appear in separate subsections from those based on equivalent surface current formulations. Also conducting surface and material body models applicable to bodies of revolution (BORs) (rotationally symmetric structures) have their own subsections. This is because of the prevalence of BOR models in use and currently under development. Many streamlined structures such as missiles and aircraft fuselages can be approximated as BORs. Also BOR models greatly extend the size and complexity of a problem that can be solved within present day computer constraints.

Another specialized model employs a moment method conducting surface technique applicable only to bodies of translation (BOTs). A BOT surface may be constructed by translating an arbitrary curve lying in the x,y plane a finite distance along the z axis. Such a surface might well approximate certain aircraft wings and fuselages. Also a thin, straight wire is, of course, a BOT. However, an examination of the theory indicates that BOT sinusoidal "modes" do not decouple the moment method generalized impedance matrix as do BOR sinusoidal modes. Thus it is not clear whether a BOT model offers advantages over, for example, a surface patch code (SPH-FD or SPE-FD in Section A.1.1.2) if the latter makes full use of BOT symmetry. An investigation of the advantages, if any, of a moment method subsectional expansion (TW-FD) applied to a thin straight wire (TW-FD) versus a sinusoidal expansion similar to King's three-term theory [King, 1968] applied to the same wire may offer a clue here since a thin wire is a degenerate BOT. (However, one should be aware that King's expansion functions are not strictly BOT sinusoidal modes but related functions that

provide more rapid convergence.) Whereas matrix inversion may be faster for the BOT model because the number of required modes may be fewer than the number of corresponding patches from end to end in the axial direction for the surface patch model, the BOT model may require far greater matrix fill time. The BOT model is not discussed further here, however, work is currently progressing in developing a BOT model [Medgyesi-Mitschang, 1978] and results of this should be closely watched.

#### A.1.1.1 Thin Wires (TW-FD)

One principal feature of moment methods for solving EM fields problems is the ease with which a single computer code can be written which is applicable to a wide class of structural configurations and excitations. For example, over the past decade a number of codes have been written each of which is applicable to both radiation and scattering from arbitrarily oriented collections of bent conducting wires with either lumped or distributed loads. The scattering problem is usually plane-wave excited, the latter being of arbitrary polarization and incidence. However, more complex exciting fields, such as those arising from near field sources, can be readily included in these codes. The trade-off is simply ease in data input specification vs. generality. The radiation problem is usually specified simply by a voltage source at any location on the wire model. Current sources can also be specified. However, the latter would be handled by first computing an input impedance and then multiplying it with the specified current to arrive at an equivalent voltage excitation [Harrington, 1968 (Chapter 6)].

Moment method codes applicable to conducting surfaces and even inhomogeneous material bodies have also been developed. However, these have not received until recently the attention that thin-wire codes have. Thus they will not receive as extensive an overview as the thin-wire codes in this report. But they are certainly important and will be dealt with sufficiently in later

sections. Many of the pertinent aspects to moment method modeling such as the concept of subsectional expansion functions, weighting functions, etc. will be dealt with in connection with wire modeling and simply referenced back in the sections dealing with surface and volume modeling.

In this section the moment method basic coupling model termed thin wire-frequency domain (TW-FD) is described. Generally the wires should, at least for scattering applications, have diameters not exceeding  $0.2\lambda$  in order to be considered "thin" [Miller, June 1973 (pg. 53)].

#### A.1.1.1.1 Applications of TW-FD

There are many structures to which the thin wire-frequency domain model can be applied. Examples include stick model representations of aircraft (Figure A.1.1-1) and wire-gridded models of surfaces such as equipment boxes (Figure A.1.1-2) and aircraft fuselages or wings [Lin, September 1972]. With wire gridding, discussed in Section A.1.1.1.5, the user is given the task of choosing reasonable wire radii and grid size so that the wire grid model is "equivalent" to the surface structure. This often difficult decision is, of course, absent in surface formulations. However, as previously mentioned, wire grid modeling has been used more extensively than, for example, surface patch modeling because the former is more easily applied to rather general surfaces especially if open surfaces are involved. It should be kept in mind though that the more accurate surface methods are beginning to experience wide use.

As with many (but not all) moment method conducting body codes, lumped impedance loads can be handled by TW-FD. The loads may be placed essentially anywhere along the wires and may represent the input or output impedances of entire linear circuits. Also distributed loads such as with wires of finite conductivity can be handled by TW-FD.

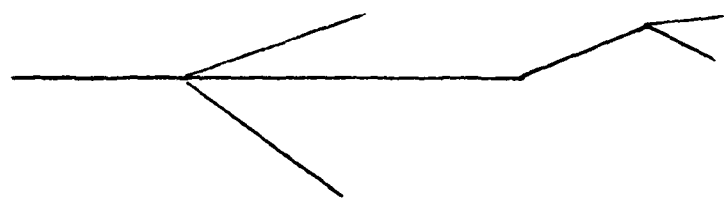


Figure A.1.1-1. Stick Model Representation of an Aircraft.

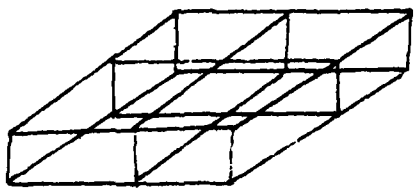


Figure A.1.1-2. Wire Grid Model of an Equipment Box.

Since TW-FD is a frequency domain method it basically applies only to linear media. However, the Volterra Series concept, as developed by RADC [Spina, 1979] with regard to circuit analysis, has been extended to permit treating radiation and scattering from wires with weakly non-linear loads via frequency domain analyses [Sarkar, March 1976; Sarkar, May 1978]. A "weak" non-linearity is identified by a current-voltage relationship that is expressible in only the first few terms of a power series expansion.

Aperture coupling problems can also be solved with this model. For example an entire cavity enclosure except, of course, for the aperture can be wire-gridded [Piatkowski, June 1975] or Babinet's Principle can be applied. In the latter case a complementary scattering problem is formed by removing the conducting screen or cavity walls and wire gridding the aperture. After appropriately modifying the excitation the resulting scattered fields are directly related to the aperture coupled fields [Adams, June 1973].

The effects of an imperfect, flat, homogeneous ground on wire antennas or scatterers have been included in TW-FD approximately via the plane-wave reflection coefficient method [AMP, July 1972; Sarkar, July 1976]. If greater accuracy is desired, as is necessarily the case if some wires are within a small fraction of a wavelength to the ground, then, Sommerfeld's formulation must be used [AMP, July 1972 (Engineering Manual); Sarkar, December 1975]. Sommerfeld's formulation requires considerably more cpu time than does the reflection coefficient method and so should be avoided if possible. An arbitrarily-bent-wire code using Sommerfeld's formulation is not, to our knowledge, presently available.\*

\* However, the NEC code [Burke, July 1977] sponsored by the Naval Ocean Systems Center will soon (if not already) be available, which stores a grid of Sommerfeld solutions for grid points in computing the ground effect for arbitrarily oriented wires. This method has been demonstrated to successfully apply to wires less than  $0.01\lambda$  above a typical earth ground. The generation of a grid requires 15 sec. of CDC 7600 cpu time [Burke, March 1979].

If the imperfect ground is not adequately modeled as infinite and flat but can be considered as adjacent, finite-extent flat layers of differing heights ("cliff" problem) then this too can be approximately modeled via the reflection coefficient method [AMP, July 1972].

An overview of the moment method as applied to the time-harmonic (frequency domain) analysis of radiation from a collection of bent conducting wires follows. Much of this is adopted from a previous RADC report [Perini, May 1978]. The straightforward extensions to loaded wires and to scattering are also briefly considered. Expressions for radiated and scattered fields and also input impedance are given.

#### A.1.1.1.2 Thin-Wire Antenna Theory

The most popular formulations for solving thin-wire antenna problems are of the  $\mathbf{E}$ -field type. The wire surface current  $\mathbf{J}$  is sought such that the  $\mathbf{E}$ -field it radiates satisfies the condition

$$E|_{\tan} = \begin{cases} 0 & \text{on perfectly conducting surface of wire} \\ & \text{applied field at location of excitation} \\ & \text{(gap) on wire.} \end{cases} \quad (\text{A.1.1-1})$$

where  $|_{\tan}$  signifies "component tangential to wire surface". Two simplifications are usually invoked prior to implementing these formulations. First, the thin-wire approximation is made. With reference to Figure A.1.1-3 this approximation assumes (a) there is no circumferentially directed component of  $\mathbf{J}$ , (b)  $\mathbf{J}$  is replaced by a filament of current  $I$  located along the wire axis  $C'$ , (c) equation (A.1.1-1) applies only to a path  $C$  parallel to the wire axis and offset a wire radius  $a$  from the axis rather than the entire wire surface, and (d) Equation (A.1.1-1) is applied only to the axial component of  $\mathbf{E}$ . Points along  $C'$  are defined by the length variable  $\ell'$  and those along  $C$  by  $\ell$ .

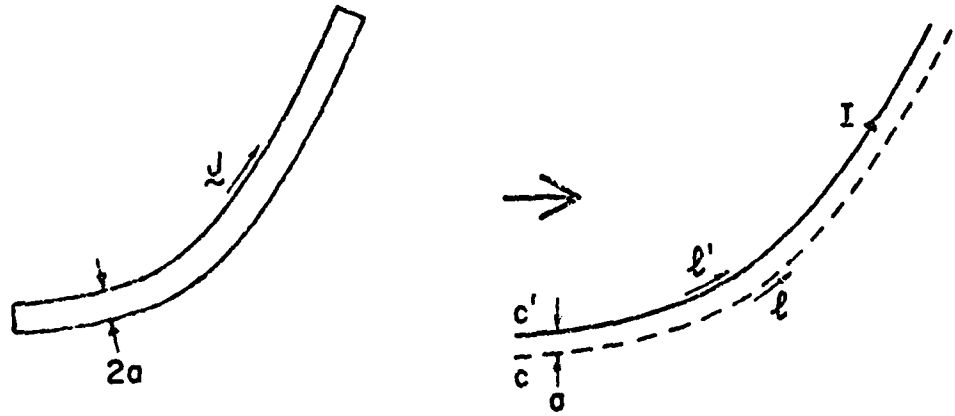


Figure A.1.1-3. Arbitrary Wire and Thin Wire Approximation.

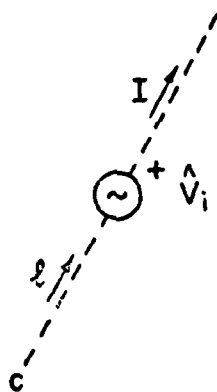


Figure A.1.1-4. Choice of Positive Reference for Voltage Excitation.

The second simplification often used is that the  $i$ th applied field is specified as a finite voltage  $\hat{V}_i$  over a small gap  $\Delta_i$  (delta gap excitation). Thus (A.1.1-1) becomes

$$L(I, \ell) = \sum_i \hat{V}_i \delta(\ell - \ell_i) \quad (\text{A.1.1-2})$$

where

$$L(I, \ell) = -\hat{E} \cdot \hat{\ell} \quad (\text{A.1.1-3})$$

$\delta(\ell - \ell_i)$  is the Dirac delta function, the  $\ell_i$  are the locations of applied voltage excitations  $\hat{V}_i$  referenced as shown in Figure A.1.1-4 and  $\hat{\ell}$  denotes a unit vector at  $\ell$  oriented parallel to C.

Most frequency domain, moment method, thin-wire computer codes are based on one of two forms for the operator L.

#### A. Potential Integrodifferential Equation

Here L has the form [Harrington, 1968 (Chapter 4)]

$$L(I, \ell) = j\omega\mu \int_{C'} \hat{\ell} \cdot \hat{\ell}' I(\ell') G(\ell, \ell') d\ell' - \frac{1}{j\omega\epsilon} \frac{d}{d\ell} \int_{C'} \frac{dI(\ell')}{d\ell'} G(\ell, \ell') d\ell' \quad (\text{A.1.1-4})$$

where

$$G(\ell, \ell') = \frac{e^{-jkR}}{4\pi R} \quad (\text{A.1.1-5})$$

and R is the distance between a "source" point at  $\ell'$  ( $\hat{\ell}'$  is the corresponding unit vector) on the wire axis  $C'$  and a "field" point at  $\ell$  on the wire surface path C. The remaining variables have their usual meanings.

#### B. Pocklington's Equation

Here L has the form [Miller 1974]

$$L(I, \ell) = \frac{1}{j\omega\epsilon} \int_{C'} I(\ell') \left( \frac{\partial}{\partial \ell} \frac{\partial}{\partial \ell'} - k^2 \hat{\ell} \cdot \hat{\ell}' \right) G(\ell, \ell') d\ell' \quad (\text{A.1.1-6})$$

where G is given by (A.1.1-5) and  $k^2 = \omega^2 \mu \epsilon$ .

A major difference between these two formulations is that (A.1.1-4) involves derivatives of the unknown current  $I$  and (A.1.1-6) involves derivatives of the Green's function  $G$ . For a finite wire radius (A.1.1-4) and (A.1.1-6) can be derived from one another. Thus exact solutions, if they exist, are independent of the formulation used to obtain them. However, when approximate solutions are sought, as via the moment method, the particular formulation used may have a significant effect on convergence, computational ease, etc.

#### A.1.1.1.3 Method of Moments

The method of moments (or moment method) is a unifying concept for reducing a linear, inhomogeneous integrodifferential equation such as (A.1.1-2) to a set of simultaneous, linear, algebraic equations. In matrix form the latter become

$$[Z]\vec{I} = \vec{V} \quad (\text{A.1.1-7})$$

where  $[Z]$  is a known square matrix and  $\vec{V}$  and  $\vec{I}$  are known and unknown column vectors respectively. An in-depth treatment of the moment method is given by Harrington [Harrington, 1968]. Once suitable  $[Z]$  and  $\vec{V}$  are known (A.1.1-7) can be solved for  $\vec{I}$ . The elements of  $\vec{I}$  are the coefficients in an expansion of the current that satisfies the original equation. Only  $\vec{V}$  contains information on the sources of the original equation. Thus  $[Z]$  need be computed only once to solve a problem for a fixed geometry and frequency but where the source distribution varies.

Equation (A.1.1-7) is of a form often appearing in network theory as relating voltages and currents of an N-port network. Thus  $[Z]$  is often referred to as the "generalized impedance" matrix and  $\vec{I}$  and  $\vec{V}$  the "generalized current" and "generalized voltage" column matrices, respectively.

The process of reducing (A.1.1-2) to (A.1.1-7) begins with the selection of a set of  $N$  independent functions  $\{f_n\}$  defined on  $C'$  with which to expand  $I$ . Thus

$$I(\ell') = \sum_{n=1}^N I_n f_n(\ell') \quad (\text{A.1.1-8})$$

where the coefficients  $I_n$  are unknown. A set of  $N$  independent testing functions  $\{g_m\}$  defined on  $C$  are then chosen. Finally a suitable symmetric product [Harrington, 1968] usually of the form

$$\langle \phi_1, \phi_2 \rangle = \int_C \phi_1(\ell) \phi_2(\ell) d\ell \quad (A.1.1-9)$$

is chosen and the symmetric product of each side of (A.1.1-2) is taken after multiplication of both sides with each  $g_m$ . The resulting N equations in N unknowns (the  $I_n$ ) are expressed in matrix form by (A.1.1-7) where the nth element of  $\vec{I}$  is  $I_n$ , the mth element of  $\vec{V}$  is

$$V_m = \sum_i \hat{V}_i g_m(\ell_i) \quad (A.1.1-10)$$

and the m,nth element of  $[Z]$  is

$$Z_{mn} = \int_C g_m(\ell) L(f_n, \ell) d\ell \quad (A.1.1-11)$$

The "expansion" or "basis" functions  $f_n$ , with which  $I$  is expanded, must be independent. Also the  $f_n$  should be chosen to well approximate a basis for the domain of  $L$ . One expects that  $f_n$  individually exhibiting characteristics of  $I$  will result in fewer  $f_n$  and consequently less effort in solving (A.1.1-7). Thus the  $f_n$  are usually chosen to force  $I$  to satisfy current continuity at each point along  $C'$ . This implies that the  $f_n$  should be continuous along a wire excluding a junction point formed by three or more wires and that  $f_n = 0$  at a wire end. Also at a multi-wire junction the  $f_n$  from each of the wires are often distributed such that the total junction current satisfies continuity.

Occasionally the  $f_n$  are not within the domain of  $L$ . For example pulse functions (constant over a small region of  $C'$  and zero elsewhere) are not within the domain of  $L$  as given by (A.1.1-4). However, such simple basis functions can still be used if  $L$  is "approximated", for example, with a finite-difference evaluation of the derivatives. The computer code WRSMOM [Warren, 1974] discussed later, is based on pulse expansion functions with a finite-difference approximation to  $L$ .

Further discussions concerning "approximate operators" and other techniques such as "extended domains", etc. are given in [Harrington, 1968].

The  $f_n$  are generally composed of one of two function types -- entire functions or subsectional functions. Subsectional functions are each defined other than zero only over a small region of  $C'$ . An example is the pulse functions discussed above. Entire functions are not so constrained. Examples of entire function bases are Maclaurin Series polynomials, Fourier trigonometric functions and Legendre polynomials. These three bases are comprised of independent functions. In addition, the latter two are comprised of functions orthogonal with respect to (A.1.1-9). However, neither basis necessarily orthogonalizes  $L$  (i.e.,  $\langle \phi_1, L\phi_2 \rangle = 0$  if  $\phi_1 \neq \phi_2$ ) a condition which would result in a diagonal  $[Z]$ . A set of functions which does diagonalize  $[Z]$  would, of course, form an excellent basis but, for arbitrary geometries such a set of functions is costly to compute. (The class of rotationally symmetric bodies is an exception in that basis functions with sinusoidal circumferential variation are known to "block" orthogonalize  $L$ . Models for analyzing these "bodies of revolution" have been developed and are discussed later.)

Experience indicates that entire function expansions tend to converge faster than subsectional function expansions [Thiele, 1973]. However, the latter tend to result in "better conditioned"  $[Z]$  matrices in that the ratio of diagonal to off-diagonal  $[Z]$  elements has generally greater magnitude. A procedure for solving (A.1.1-7) when  $[Z]$  is better conditioned is generally less sensitive to round-off errors.

The computation of  $[Z]$  for an entire function expansion is usually considerably more involved than for a subsectional function expansion. Thus for complex wire geometry problems

a subsectional function expansion is more inviting than an entire function expansion. Hence, the vast majority of available moment method computer codes for modeling arbitrary collections of bent wires is based on subsectional function expansions. Three examples of subsectional functions are shown in Figure A.1.1-5. The  $f_n$  in Figure A.1.1-5(a) are pulses defined by

$$f_n(\ell') = \begin{cases} 1 & \ell_n - \Delta_n^- / 2 < \ell' < \ell_n + \Delta_n^+ / 2 \\ 0 & \text{Otherwise} \end{cases} \quad (\text{A.1.1-12})$$

where  $\Delta_n^-$  is the pulse width defined in the figure. The  $f_n$  in Figure A.1.1-5(b) are overlapping triangles given by

$$f_n(\ell') = \begin{cases} (\ell' - \ell_{n-1}) / \Delta_n^- & \ell_{n-1} \leq \ell' \leq \ell_n \\ (\ell_{n+1} - \ell') / \Delta_n^+ & \ell_n \leq \ell' \leq \ell_{n+1} \\ 0 & \text{Otherwise} \end{cases}$$

(A.1.1-13)

where  $\Delta_n^-$  and  $\Delta_n^+$  are defined in the figure. The  $f_n$  in Figure A.1.1-5(c) are overlapping sinusoids given by

$$f_n(\ell') = \begin{cases} \sin k(\ell' - \ell_{n-1}) / \sin k\Delta_n^- & \ell_{n-1} \leq \ell' \leq \ell_n \\ \sin k(\ell_{n+1} - \ell') / \sin k\Delta_n^+ & \ell_n \leq \ell' \leq \ell_{n+1} \\ 0 & \text{Otherwise} \end{cases}$$

where  $\Delta_n^+$  and  $\Delta_n^-$  are defined in the figure and  $k = 2\pi/\lambda$ . (A.1.1-14)

A fourth expansion function in popular use is the "sine-plus-cosine-plus-constant" function. The nth expansion function here is a linear combination of sine, cosine, and constant functions extending only over the nth segment of width  $\Delta_n$ . The relative weights of these three functions are determined

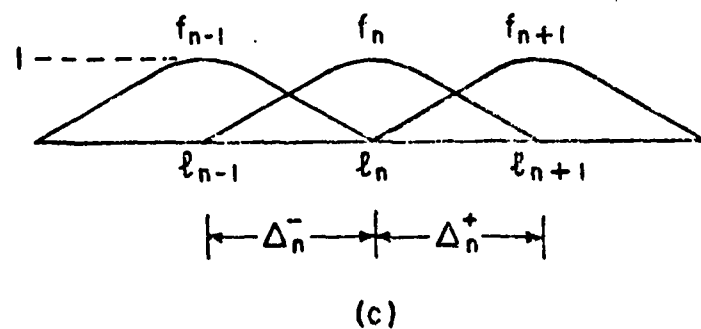
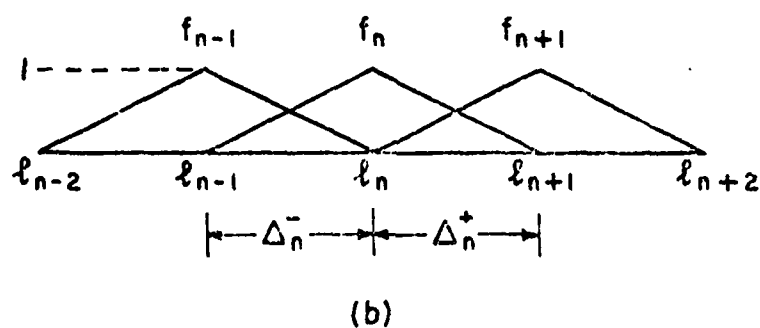
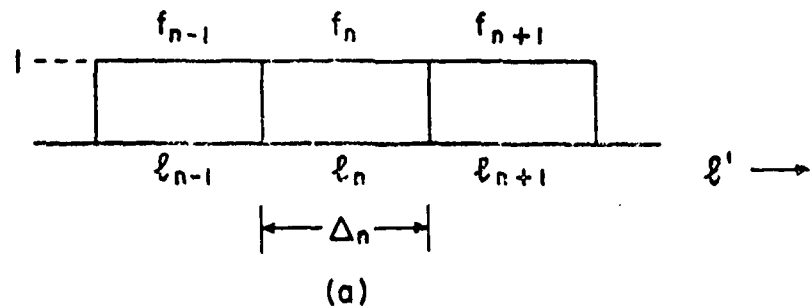


**Figure A.1.1-5.** Subsectional Functions: (a) Pulse (Piece-wise Constant), (b) Triangular (Piece-wise Linear), and (c) Piece-wise Sinusoidal.

by requiring that if the  $n$ th expansion function was extended to the mid-points of the adjacent segments ( $n-1$  and  $n+1$ ) then the current (linear combination of these expansion functions) would be continuous at these midpoints. Note, however, that continuity at the intersections between segments is not guaranteed. The widely used AMP [AMP, July 1972] and GEMACS [Balestri, April 1977] codes use this expansion function type.

Geometry description and [Z] computation in a computer program applicable to arbitrary configurations of bent wires is facilitated usually by approximating the paths  $C'$  (and  $C$ ) with straight line segments. A typical segmentation is shown in Figure A.1.1-6. For pulse expansion functions the segments usually coincide with the  $\Delta_n^-$  of Figure A.1.1-5(a). For triangle and piece-wise sinusoid expansion functions the segments generally coincide with the  $\Delta_n^-$  (and  $\Delta_n^+$ ).

As previously mentioned, it is desirable to incorporate within the  $f_n$  known constraints on  $I$ . Continuity of  $I$  is one such constraint. The pulse functions of Figure A.1.1-5(a) do not enforce continuity of  $I$ . However, they are generally used in conjunction with approximate operators that afford additional smoothing. The triangle and sinusoid (piece-wise) functions of Figure A.1.1-5(b,c), on the other hand, do enforce continuity of current at each point along  $C'$ . These two bases also maintain continuity of current at multiple-wire junctions if a simple rule is followed in modeling the wires. To illustrate, consider the 3-wire junction shown in Figure A.1.1-7. The modeling begins by choosing any one of the wires as terminated at the junction (Figure A.1.1-7(b)). Then the remaining wires are added in succession such that each overlaps any previously placed wire (Figure A.1.1-7(c,d)). This overlapping is accomplished by aligning the junction point with the peak of the end triangle (or sinusoid) function on the wire being added. The

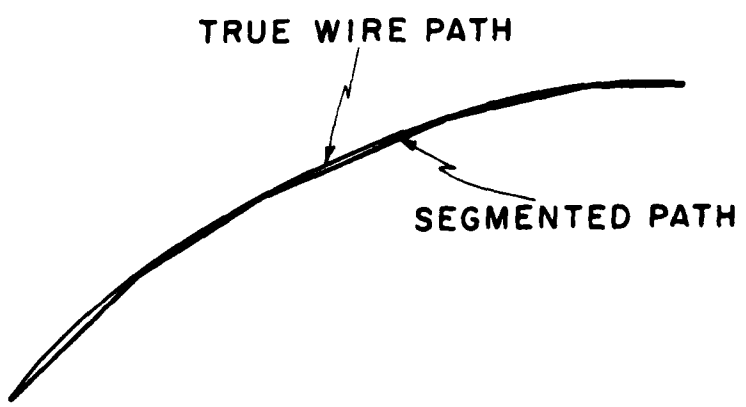


Figure A.1.1-6. Segmentation of a Wire.

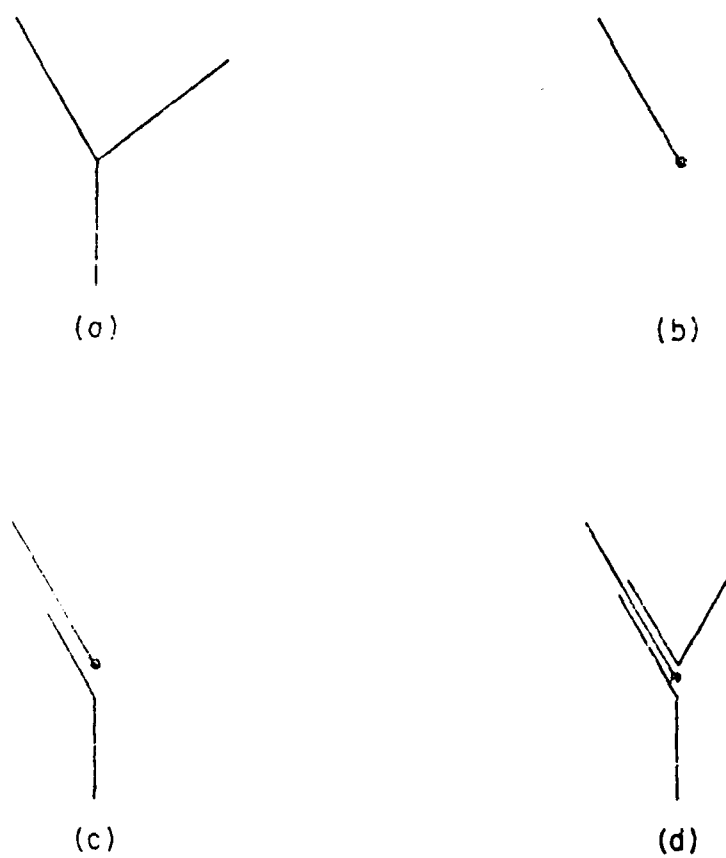


Figure A.1.1-7. (a) A 3-wire Junction. (b) One Wire chosen Terminated at Junction. (c) Addition of a Second Wire by Overlapping First Wire. (d) Addition of a Third Wire also by Overlapping First Wire.

justification for this method is given in [Chao, September 1970]. It is also presented in terms of "independent loop currents" in [Richmond, (no date)].

The set of testing functions  $\{g_m\}$  must also be independent. Other restrictions on the  $\{g_m\}$  are not obvious from their explicit use as indicated by (A.1.1-10) and (A.1.1-11). However, one notes that the moment method is equivalent to the Rayleigh-Ritz procedure if the  $g_m$  are in the domain of  $L^a$  the adjoint operator of  $L$  [Harrington, 1968] defined by

$$\langle \phi_1, L\phi_2 \rangle = \langle L^a \phi_1, \phi_2 \rangle$$

This equivalence is noteworthy since the Rayleigh-Ritz procedure achieves an approximate solution to a variational expression for a scalar quantity  $\rho$  of interest (impedance, far-field, etc.), i.e., small errors in  $I$  when used to compute a variational expression for  $\rho$  result in proportionately less error in  $\rho$ . For the "symmetric" inner product defined by (A.1.1-9) the operators of (A.1.1-4) and (A.1.1-6) are self-adjoint, i.e.,  $L^a = L$ . Thus it is desirable to choose the  $g_m$  from the domain of  $L$ .

Two types of  $\{g_m\}$  are often found in existing moment method computer codes. One type sets  $\{g_m\} = \{f_n\}$ . This is often called Galerkin's method. One advantage of Galerkin's method is that  $[Z]$  is then symmetric. This decreases the effort required for computing  $[Z]$  and for solving (A.1.1-7). It also saves computer storage since only the upper or lower triangle of  $[Z]$  is needed. A disadvantage is that the  $g_m$  may complicate the evaluation of (A.1.1-11). Examples of codes based on Galerkin's method are the Syracuse [Kuo, November 1972] and Ohio State [Richmond, (no date)] codes (subsectional triangles and subsectional sinusoids respectively). The Syracuse code only approximates a Galerkin solution, however, and so the resulting  $[Z]$  is not quite symmetric.

The other frequently chosen  $\{g_m\}$  is the set of impulses positioned at the centers of the  $\{f_n\}$ . This choice of  $\{g_m\}$  reduces the integral computation in (A.1.1-11) to a trivial operation. The choice of impulse functions for testing is occasionally called collocation. Of course, these  $\{g_m\}$  are not within the domain of  $L$ . However, they are often used in conjunction with a finite-difference approximation to  $L$  which, as discussed earlier, provides a compensating smoothing effect. In fact, it has been shown that a finite-difference approximation to Pocklington's equation is closely akin to testing with triangles or sinusoids (Wilton, January 1976). The computer code WRSMOM (Warren, March 1974) uses impulse testing.

Equation (A.1.1-10) takes a different form when  $\{g_m\}$  is an impulse function. In this case the  $i$ th antenna excitation is generally treated as a specified voltage  $\hat{V}_i$  over a small but finite gap. The gap size is equal to the segment width  $\Delta_{n_i}$  of the  $n_i$ th pulse expansion (basis) function occurring at the  $i$ th excited port. Then (A.1.1-2) becomes

$$L(I, \ell') = \sum_i \hat{V}_i \frac{1}{\Delta_{n_i}} \quad (A.1.1-15)$$

The testing functions are weighted impulses of the form

$$g_m = \delta(\ell - \ell_m) \Delta_m \quad (A.1.1-16)$$

Thus under impulse testing and pulse expansion (A.1.1-10) and (A.1.1-11) are replaced by

$$v_m = \begin{cases} \hat{V}_i & \text{if the } i\text{th excitation occurs} \\ & \text{at } m\text{th expansion function } (m=n_i) \\ 0 & \text{Otherwise} \end{cases} \quad (A.1.1-17)$$

$$z_{mn} = L(f_n, \ell_m) \Delta_m \quad (A.1.1-18)$$

#### Extension to Loaded or Lossy Wires

If the wire surface is lossy or if lumped impedance loads are located along the wire as in Figure A.1.1-8 then  $\vec{V}$  in (A.1.1-7) is replaced by

$$\vec{V} = \vec{V}^i - [Z_L] \vec{I}$$

and (A.1.1-7) becomes

$$([Z] + [Z_L]) \vec{I} = \vec{V}^i \quad (\text{A.1.1-19})$$

In (A.1.1-19) the  $m$ th element of  $\vec{V}^i$  is  $V_m$  of (A.1.1-10) and the  $mn$ th element of the  $N \times N$  matrix  $[Z_L]$  is in general the mutual impedance (complex number) relating  $I_n$  to the voltage across the load at the  $m$ th port. In most applications, except e.g., with antenna transmit or receive arrays, only self-impedances occur and  $[Z_L]$  is then adequately approximated by a diagonal matrix.

#### Extension to Scatterers

If the wire structure is a scatterer then  $\vec{V}^i$  in (A.1.1-19) arises from the incident field  $\vec{E}^i$  (field in the absence of the scatterer). The  $m$ th element of  $\vec{V}^i$  is then

$$V_m^i = \int_C g_m(\ell) (\vec{E}^i \cdot \hat{\ell}) d\ell \quad (\text{A.1.1-20})$$

#### Solution for Current and Other Parameters

Once the wire current  $I$  is determined by solving either (A.1.1-7) or (A.1.1-19) then it is a simple matter to obtain other parameters such as input impedance, radiated field, power gain, and scattered field.\* These parameters are readily determined from  $\vec{I}$  with the formulas derived in [Harrington, 1968 (Sections 4-4 and 4-5)] and are given below.

\* Another parameter "coupling" is not precisely defined in general but is usually easily calculable from these other parameters and  $I$ .

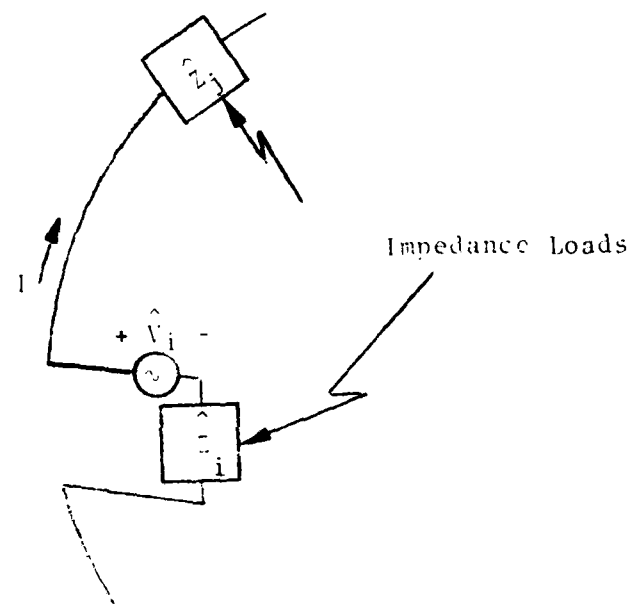


Figure A.1.1-8. Wire Antenna with Linear Loads.

The input impedance (ohms) at the  $i$ th excited port of a wire antenna is simply  $Z_i = \frac{\hat{V}_i}{I_{n_i}}$  where  $\hat{V}_i$  and  $\hat{Z}_i$  are the  $n$ th port source Thevenin equivalent circuit as indicated in Figure A.1.1-8 and  $I_{n_i}$  is the element of  $\vec{I}$  corresponding to the  $i$ th excited port ( $n=n_i$  at the  $i$ th excited port).

The  $\hat{t}$  directed component of radiated  $E$ -field (volts/meter) at any point  $r$  is given through reciprocity in terms of a "test" dipole  $\vec{I}_{\ell}^r = I_{\ell}^r \hat{t}$  located at  $r$ . The result is

$$E \cdot \hat{t} = \frac{1}{I_{\ell}^r} \tilde{V}^r \vec{I} \quad (\text{A.1.1-21})$$

where the  $n$ th element of the row vector  $\tilde{V}^r$  is

$$\tilde{V}_n^r = \int_C f_n(\ell') E^r \cdot \ell' d\ell' \quad (\text{A.1.1-22})$$

The  $\hat{t}$ -polarized power gain is then simply

$$g = \frac{4\pi r^2 |E \cdot \hat{t}|^2}{P_{in}} \quad (\text{A.1.1-23})$$

where  $\eta$  is the free-space wave impedance and  $P_{in}$  is the total power (Watts) given by

$$P_{in} = \sum_i |I_{n_i}|^2 \operatorname{Re}\{Z_i\} \quad (\text{A.1.1-24})$$

In (A.1.1-24) the summation is over all excited ports and  $\operatorname{Re}\{Z_i\}$  indicates "real part of  $Z_i$ ".

In scattering, the scattered field is also given by (A.1.1-21) but with  $\vec{I}$  now determined from (A.1.1-7) or (A.1.1-19) with the elements of  $\tilde{V}^i$  given by (A.1.1-20).

For large problems,  $N > 200$ , the cpu time in solving a problem by the moment method is generally limited by the time

required to solve (A.1.1-7) (or its equivalent such as (A.1.1-19)) once  $[Z]$  and  $\vec{V}^i$  are determined. Gauss - Jordan matrix inversion is one popular method. However, if the entire matrix inverse is not needed, as is often the case, then the preferred method is Gauss - Doolittle [Ralston, 1965] which is also called L-U decomposition. The latter is about three times faster than the solution by matrix inversion for large N. In Gauss-Doolittle lower  $[L]$  and upper  $[U]$  triangular matrices are determined such that

$$[Z] = [L] [U] \quad (A.1.1-25)$$

This decomposition is performed only once for all excitations. Then for each excitation vector  $\vec{V}^i$  the equations

$$\begin{aligned} [L]\vec{F} &= \vec{V} \\ [U]\vec{I} &= \vec{F} \end{aligned} \quad (A.1.1-26)$$

are solved by Gaussian Elimination to arrive at  $\vec{I}$ .

The GEMACS code [Balestri, April 1977] offers further reduction in the cpu time needed to solve (A.1.1-7). A banded matrix iterative (BMI) technique is incorporated which, for certain problem types, provides accurate approximations to the solution to (A.1.1-7) at significant cpu time savings over Gauss-Doolittle. The BMI method works best for bodies with at most two dimensions significantly larger than the third and for a subsectional basis. For example the BMI method does not appear to offer significant cpu time savings when incorporated in body of revolution (BOR) models [Balestri, April 1977 (pg. 71)]. Although each expansion function in a moment method BOR formulation is of subsectional extent along a constant longitudinal coordinate path, it is of full circular extent along a constant meridinal coordinate path (sinusoid). Large BOR modal matrix (Section A.1.1.3) BMI "bandwidths" result, eliminating the advantages of BMI.

#### A.1.1.1.4 General Accuracy Considerations

General accuracy considerations with regard to TW-FD follow.

1. If the wire current is not expected to vary rapidly then segment lengths of  $\Delta = \lambda/4$  are usually adequate. Otherwise  $\Delta < \lambda/10$  is necessary.

2. Straight-line segment modeling of curved wires is generally adequate.

3. As the wires become thicker azimuthal currents and asymmetric axial current modes may be significant. However, for wire diameters not much larger than  $.2\lambda$  this is not of concern unless scattering current distributions, very near fields, or aperture coupling (to regions within "wire" enclosures such as coaxial cable interiors) are of interest. In this regard it is noted that thin-wire models do not account for wire end cap effects.

4. The inaccuracy due to wire bends is localized quite near the bends as long as the included angles are not very acute. For distances greater than  $\sim 5$  wire radii from an "elbow" there is good agreement with experiment [Miller, June 1976]. This same effect applies to multiple wire junctions as long as the chosen expansion functions permit the most general representation of current within the constraint of continuity of current.

#### A.1.1.1.5 Wire-Grid Surface Modeling

The ease with which moment method thin wire models can be applied to arbitrary wire geometries has led to their use in solving radiation and scattering from solid conducting surfaces by approximating the latter with wire grids. The thin-wire equations are simpler in form than the  $E$ -field surface patch equations (surface patch models are discussed in a later section). However, the  $H$ -field surface patch  $[Z]$  matrices, although only applicable to closed conducting surfaces, are generally diagonally dominant whereas the thin-wire  $[Z]$  matrices are not.

Also about 16 times more mesh elements (wire grid "windows") are needed for wire gridding over surface patching in applications where the mesh cell width  $\Delta < \lambda/20$  [Jones, July 1974]. It is noted though that in problems with less stringent accuracy constraints or where far-field quantities are of interest then a  $\Delta \approx \lambda/4$  is adequate in areas where the current is not expected to vary rapidly.

In wire gridding the user must carefully choose the wire radius  $a$ . For scattering from a conducting disk, greater than 3 dB errors in current resulted when  $\frac{\Delta}{a}$  was varied beyond 250 [Castillo, February 1975]. Also for scattering from elongated structures better results appear achievable if the polarization is parallel to the major axis [Castillo, February 1975].

An extensive analysis of wire grid solutions to low-frequency scattering from aircraft has been performed [Lin, September 1972]. The Ohio State piecewise sinusoid code [Richmond, (No date)] discussed earlier was used. Far-field broadside scattering from a square plate of side  $\lambda$  was within ~2dB agreement with measurement for a wire-grid of 4 windows (15 overlapping sinusoids). The optimum wire radius  $a$  was found to be  $.005\lambda < a < .01\lambda$ , and the effect of varying tended to decrease as the number of segments increased. A choice of  $a = .005\lambda$  appeared good if  $\Delta = \lambda/4$ , and  $a = .01\lambda$  was favored for smaller  $\Delta$ . If  $a = .01\lambda$  and  $\Delta = .1\lambda$  then  $\frac{\Delta}{a}$  would equal 10. Approximately 6-dB agreement with scale model experiment was achieved for backscattering from a MIG-19 aircraft of length  $L = .826\lambda$  with approximately  $N = 18$  expansion functions. For  $L = 1.4\lambda$ ,  $N = 70$  gave good agreement. In all these cases the E-field was polarized parallel to the fuselage. Results for other aspect angles indicated a need for a finer grid. The authors suggested a segment to radius ratio of  $\Delta/a = 25$ . As a guide to wire gridding, the indication is that radiation pattern shape depends primarily on major geometrical dimensions such as wing span, fuselage length, etc.

Results with models based on pulse expansion functions and impulse weighting [Lin, September 1974] also indicated a preferable  $\Delta/a$  of 20 or 25 for wire gridding. Results of applying this thin-wire moment model to scattering from a square plate resulted in ~2 dB agreement with experiment for a physical wire-grid plate but only between 5 dB and 20 dB agreement for a solid plate. The plate was  $0.6\lambda$  on a side and  $\Delta=.15\lambda$  for the wire grid.

Comparisons of experimental scattering from solid ogives and mesh ogives indicated that although broadside results agreed to within ~3 dB for  $\Delta=0.2\lambda$ , on-axis results differed by more than 10 dB for  $\Delta=0.1\lambda$  [Frediani, May 1974].

For additional references (annotated) on wire gridding see [Buchanan, January 1977].

#### A.1.1.1.6 Computational Constraints

The cpu time in seconds consumed by a frequency domain moment method code for computing far fields from thin wires or surfaces is approximated by [Miller, June 1973] as

$$t = AN^2/M + BN^3/M^2 + CN^2N_I/M + DNN_IN_A/M \quad (\text{A.1.1-27})$$

where

$N$  = order of linear system (number of expansion functions)

$N_I$  = Number of incident fields or source configurations

$N_A$  = Number of observation points in far field

The number  $M$  indicates potential time savings arising from any

structural symmetries that might exist.  $M = \frac{2\pi}{\alpha} 2^m$  where  $m$  = number of reflection planes of symmetry and  $\alpha$  = minimum angle through which the structure must be rotated to reproduce itself. The constants A, B, C, and D are machine dependent. The A term is associated with "matrix fill", that is, the computation of  $[Z]$ . The B term is associated with the factoring (first step in

L-U decomposition) or inversion of [Z]. The C term is associated with the current computation. Finally the D term is associated with computing the far field.

The matrix fill time coefficients A for a number of wire codes are given below for a Honeywell 6000 [Perini, May 1978].

<u>Code</u>	<u>Matrix fill Time Coefficient(A)</u>
Pulse Expansion-Impulse Weighting (WRSMOM)	$9 \times 10^{-3}$
Sine + Cosine + Constant (AMP, GEMACS, NEC)	$1 \times 10^{-2}$
Piecewise Sinusoidal - Galerkin (Ohio State - OS)	$9 \times 10^{-3}$
Piecewise Linear - Galerkin (Syracuse - SYR)	$6 \times 10^{-3}$

The CDC 7600 matrix fill time coefficients are ~25 times smaller [Miller, June 1973]. As previously mentioned, without use of symmetry matrix fill usually dominates run time for N less than approximately 200 if L-U decomposition is used. For large N matrix solution generally dominates run time. Of course, the BMI technique can reduce matrix solution time as discussed shortly.

For a surface without symmetries and of average radius of curvature R the number of expansion functions N is proportional to  $R^2$ . Thus matrix fill time is proportional to  $R^4$ , and matrix solution time is proportional to  $R^6$ . Also matrix storage is approximately equal to  $N^2$  and thus proportional to  $R^4$ . The limitations of applying moment method models alone to electrically large problems is thus evident. Combined moment method/high-frequency models discussed in Appendix B as GTD/MOM overcome these limitations.

The effect of matrix round-off error on final numerical results for  $N \approx 250$  is roughly approximated empirically by [Miller, June 1973] by

$$E = e^{(11.5-sd)}$$

(A.1.1-28)

where  $E$  is a relative error,  $d$  is a structure dependent coefficient, and  $s$  is the number of mantissa bits in each matrix element word. The data used in arriving at (A.1.1-28) were input impedances of dipoles and LORAN transmitting antennas computed with increasing numbers of expansion functions up to  $N=240$ . The resulting value of  $d$  was  $d \approx 0.77$ . Hence, only  $\sim 1.0\%$  inaccuracy is suggested by (A.1.1-28) as attributed to round-off error for 21 bit mantissa computer words. It is noted that most large machines use words having mantissas in excess of 21 bits. Equation (A.1.1-28) appears to hold for  $N \geq 250$  and perhaps even for significantly larger  $N$ . However, it is noted that ill-conditioned matrices may be extremely more sensitive to round-off error.

An ill - conditioned matrix is difficult to accurately invert. The ill-conditioning could be due to either of two reasons: 1. The exact formulation that the finite dimensional matrix approximates has an operator that is nearly singular at the frequency of interest. Formulations for closed perfectly conducting surfaces that have non-singular operators at all frequencies are discussed in [Mautz, May 1977]. Usually a more involved operator than the  $\mathbf{E}$ -field operator alone is then called for. One notes, however, that the judicious inclusion of slightly dissipative ambient media or lumped or distributed loads may be sufficient to remove the singularities resulting from use of the  $\mathbf{E}$ -field operator alone. 2. The choice of basis and other approximations in developing the matrix operator may result in the matrix having extraneous small eigenvalues. A near zero eigenvalue indicates a nearly singular matrix. A primary defense against this hazard lies in its detection. In this regard one useful measure of matrix conditioning is the "matrix condition" number which can be defined as the ratio of maximum to minimum eigenvalues of the matrix: the greater this number the worse the conditioning. This and other definitions of matrix condition number are described in [Klein, Nov. 1973; Klein, May 1975]. Once an ill-conditioned matrix is detected the problem can perhaps be rerun at a slightly different frequency.

As previously mentioned, the banded matrix iteration BMI technique incorporated in GEMACS [Balestri, April 1977] has successfully demonstrated a significant shortening of cpu time in solving certain types of antenna and scatterer problems. The advantage of BMI over standard L-U decomposition, quantitatively defined as efficiency  $g$ , is lessened unless the antenna or scatterer has one or two dimensions considerably larger than the third. The efficiency  $g$  is the ratio of the L-U solution time to the BMI solution time for the same matrix equation. For long and thin objects and loose convergence ( $\sim 10\%$  or greater in the iterative procedure),  $g$  is approximately linearly related to the object's largest dimension. It is important to note, however, that for very large problems, e.g.,  $N=1000$ , peripheral storage will usually be required. In a CDC 7600 the upper limit for main memory storage corresponds to  $N \approx 500$  [Bevensee, February 1978]. In such cases I/O time may be significant.

The scattering from a  $4\lambda^2$  conducting plate was satisfactorily computed on a CDC 6600 using GEMACS with  $N=544$  unknowns. With a BMI efficiency of  $g \approx 6$  the matrix solution time (138 secs) was only 1/4 the matrix fill time (608 secs). Thus for problems amenable to BMI, with reasonable efficiencies, the cpu time is limited by matrix fill time for considerably larger  $N$  with BMI than if L-U decomposition or matrix inversion is used.

#### A.1.1.2 Conducting Surfaces (SPH-FD, SPE-FD)

Conducting surfaces occur in many coupling paths between emitters and receptors. Examples include aircraft fuselages and wings and satellite solar panels. Two formulations have been frequently used to solve conducting surface electromagnetic problems: the magnetic field integral equation MFIE and the electric field integral equation EFIE. Although the EFIE is directly applicable to a wider class of problems than is the MFIE (such as radiation\* as well as scattering, thin conducting sheets or shells, and thin dielectric or resistive shells) the MFIE is generally better behaved computationally. Both formulations are in terms of the surface electric current  $\tilde{J}$ . The MFIE constrains  $\tilde{J}$  to satisfy zero tangential  $\tilde{H}$ -field just inside the surface of the conductor. The EFIE constrains  $\tilde{J}$  to satisfy zero tangential  $\tilde{E}$  on the surface of the conductor.

---

\* The MFIE can solve radiation problems indirectly via reciprocity.

A third formulation, the "combined field formulation", is also in use [Mautz, Feb. 1977]. This formulation is a result of linearly combining the EFIE and MFIE. Thus, it also is an equation in unknown  $J$ . Although associated computation is greater than for either the EFIE or MFIE taken alone, the combined field formulation exhibits greater stability especially at internal resonance frequencies of closed conducting bodies where the EFIE and MFIE operators become singular. Also, the combined field formulation can be applied to thin conducting surfaces and wires where the MFIE alone is not applicable although the number of unknowns (in a moment method solution) is then twice that in the EFIE taken alone. However, if the coupling to regions within thin bodies such as aircraft wings or electrically thin fuselages is of interest, then the combined field formulation shows promise of providing more accurate solutions than does the EFIE [Wilton, April 1979]. The extent to which the combined field formulation should be incorporated in models for general use is presently unresolved. Increased computation of the combined field formulation over EFIE or MFIE alone may often be prohibitive and other methods of avoiding the internal resonance problem can perhaps be applied [Jones, July 1974]. An example is the Schenck method [Schenck, 1968] whereby the MFIE is applied in full and the EFIE at only a few interior region points. However, even this method is not "foolproof" and further research is indicated [Jones, July 1974]. It is possible, on the other hand, that the incorporation of reasonable values of dissipative loading may alleviate the problem [Harrington, Feb. 1979]. In fact real-world problems almost always involve lossy structures and the modeling of loss in a moment method technique for the EFIE at least, is relatively straightforward.

A number of computer codes based on a moment method solution to the MFIE or EFIE have been developed. Some of the characteristics of these are discussed below. Based on subsectorial expansion functions which extend over "patches", they are referred to as SPH-FD and SPE-FD models if applied to the MFIE or EFIE respectively. Surface models incorporating expansion functions more suited for bodies of revolution are covered in Section A.1.1.3.

The MFIE can be expressed as [Mautz, Feb. 1977]

$$\begin{aligned} \frac{\underline{J}(\underline{r})}{2} + \frac{1}{4\pi} \int_S \left( \frac{1+jk|\underline{r}-\underline{r}'|}{|\underline{r}-\underline{r}'|^3} \right) e^{-jk|\underline{r}-\underline{r}'|} \hat{n} \times [(\underline{r}-\underline{r}') \times \underline{J}(\underline{r}')] ds' \\ = \hat{n} \times \underline{H}^i(\underline{r}) \end{aligned} \quad (\text{A.1.1-29})$$

where  $\underline{r}$  and  $\underline{r}'$  are points on the conducting surface  $S$ , the integration is with respect to the  $\underline{r}'$  points,  $k$  is the propagation constant (usually  $2\pi$  divided by the wavelength  $\lambda$ ),  $\hat{n}$  is a unit vector outward normal to the surface at  $\underline{r}$ , and  $\underline{H}^i(\underline{r})$  is the  $\underline{H}$ -field at  $\underline{r}$  in the absence of the scatterer (impressed field).

The EFIE can be expressed as

$$-\underline{E}_{\tan}^s = \underline{E}_{\tan}^i + \underline{E}_{\tan}^t \quad (\text{A.1.1-30})$$

at  $\underline{r}$  on the surface of  $S$  where the subscript  $\tan$  denotes tangential components on  $S$ ,  $\underline{E}^i$  is the  $\underline{E}$ -field in the absence of the scatterer (impressed field),  $\underline{E}^t$  is the total  $\underline{E}$ -field, and  $\underline{E}^s$  is the scattered field due to  $\underline{J}$  and the surface charge density  $\sigma$ . The  $\underline{E}^s$ ,  $\underline{J}$ , and  $\sigma$  are related by

$$\underline{E}^s = -j\omega \underline{A}(\underline{J}) - \nabla \Phi(\underline{J})$$

where

$$A(\tilde{J}) = \mu \iint_S J(\tilde{r}') \frac{e^{-jk|\tilde{r}-\tilde{r}'|}}{4\pi|\tilde{r}-\tilde{r}'|} ds'$$

$$\Phi(\tilde{J}) = \frac{1}{\epsilon} \iint_S \sigma \frac{e^{-jk|\tilde{r}-\tilde{r}'|}}{4\pi|\tilde{r}-\tilde{r}'|} ds'$$

$$\sigma = -\frac{1}{j\omega} \lim_{\Delta S \rightarrow 0} \left( \frac{\int_C \tilde{J}(\tilde{r}) \cdot \hat{p} d\tilde{r}}{\Delta S} \right) = -\frac{1}{j\omega} \nabla_s \cdot \tilde{J}(\tilde{r})$$

where  $\hat{p}$  is the unit vector tangential to  $S$  and normal to the curve  $C$  which bounds the small portion  $\Delta S$  of  $S$ . Also  $\hat{p}$  points away from  $\Delta S$ . The operator " $\nabla_s$ " is the surface divergence on  $S$ . The field  $\tilde{E}^t$  is usually either zero for a perfect conductor, an excitation field for an antenna problem, or a known function of  $J$  for an "impedance sheet" problem [Harrington, July 1975]. The latter occur, for example, in dielectric radome analyses.

A moment method representation of either (A.1.1-29) or (A.1.1-30) results in  $N = 2N_p$  equations in  $N$  unknowns where  $N_p$  is the number of "patches" through which the surface is subdivided. Each patch corresponds to a two-dimensional surface current expansion function which explains the factor of 2.

As the patch size is made increasingly small the EFIE moment method matrix becomes ill-conditioned. On the other hand the  $J/2$  term in the MFIE results in a matrix that becomes more diagonally dominant. In addition the MFIE matrix terms are simpler to compute than are the EFIE terms. Thus, the MFIE has often been the preferred formulation for solving conducting surface problems. The application of moment methods to (A.1.1-29) results in the matrix equation

$$[B]\tilde{J} = \tilde{H} \quad (A.1.1-31)$$

where  $\vec{J}$  is the  $2N_p$  column vector of surface current expansion function coefficients,  $\vec{H}$  is the  $2N_p$  column vector of elements proportional to the surface tangential impressed  $\vec{H}$ -field, and  $[B]$  is the  $2N_p \times 2N_p$  moment method interaction matrix obtained from (A.1.1-29) in the usual fashion. The general theory behind the moment method was discussed in Section A.1.1.1.3 in addition to means for solving (A.1.1-31).

One of the first widely used surface patch computer codes based on the MFIE [Albertsen, Sept. 1973] employs quadrilateral shaped patches with two constant pulse-like current expansion functions (one for each polarization) for each patch and two impulses near the center of each patch for testing. This code has been incorporated in AMP [AMP, July 1972] and the more recent NEC code [Burke, July 1977]. Approximately 50 basic functions (25 patches) per square wavelength usually results in within 3 dB accuracy in field computation. This was determined from extensive application to satellite modeling. Further discussion of this code is left to Section B.1.1 since it usually appears as part of a combined model containing thin wire modeling(TW-FD/SPH-FD).

The MFIE, and thus SPH-FD, is applicable only to lossless, closed conducting scatterers. Scatterers with edges such as a missile with a non-conducting nose cone are not amenable to the MFIE. Radiation problems, however, can usually be solved indirectly by solving the reciprocal scattering problem.

On the other hand, the EFIE is, as previously mentioned, applicable to a much wider class of problems. Recently a number of moment method codes have been developed based on the EFIE. A major concern has been the choice of patch type. Since the integrations in the EFIE are not as simple as in the MFIE, more elaborate expansion functions need be considered. These are often difficult to use in conjunction with arbitrary quadrilateral patches. An EFIE rectangular patch code has been developed

[Newman, Nov. 1978]. The expansion function set is a surface extension of the thin wire piecewise sinusoid basis (Section A.1.1.1). The surface is divided into rectangular patches. On this subdivided surface are placed two orthogonal overlapping expansion function sets allowing a vector surface current to be represented satisfying continuity of current everywhere. In the direction of its polarization a single expansion function traverses two patches and is piecewise sinusoidal. In the orthogonal direction only one patch is traversed and the variation is cosinusoidal. This permits the expanded current along a surface edge to behave approximately as expected since the edge normal component vanishes and the tangential component rises to infinity with decreasing distance from the edge. For two adjacent rectangular patches as indicated in Figure A.1.1-9, the current expansion function extending over both patches is directed normal to the common edge ( $y$ -directed) and of the form

$$f = \hat{y} \frac{kP_1 \sin(y-y_1) \cos kx}{2 \sin(y_2-y_1) \sin k w} + \hat{y} \frac{kP_2 \sin(y_3-y) \cos kx}{2 \sin(y_3-y_2) \sin k w} \quad (\text{A.1.1-32})$$

where  $\hat{y}$  is the  $y$ -directed unit vector and  $P_1$  and  $P_2$  are unit pulse functions extending over  $y_1 < y < y_2$  and  $y_2 < y < y_3$  respectively. The use of sinusoidal variations permits computing the fields due to an expansion function in closed form [Richmond, May 1978]. This facilitates the Galerkin moment method impedance matrix  $[Z^s]$  computation where  $[Z^s]$  relates the column vector  $\vec{J}$  of  $N_s$  surface patch current coefficients to the generalized voltage column vector  $\vec{V}^s$  by

$$[Z^s] \vec{J} = \vec{V}^s \quad (\text{A.1.1-33})$$

In (A.1.1-33) each element of the  $N_s$  element column vector  $\vec{V}^s$  is the surface integral of the dot product of the impressed electric field  $E^i$  with an  $f$  of (A.1.1-32). The  $[Z^s]$  is  $N_s \times N_s$ . Note that  $N_s$  is not quite  $2N_p$  since edge patches are not "overlapped".

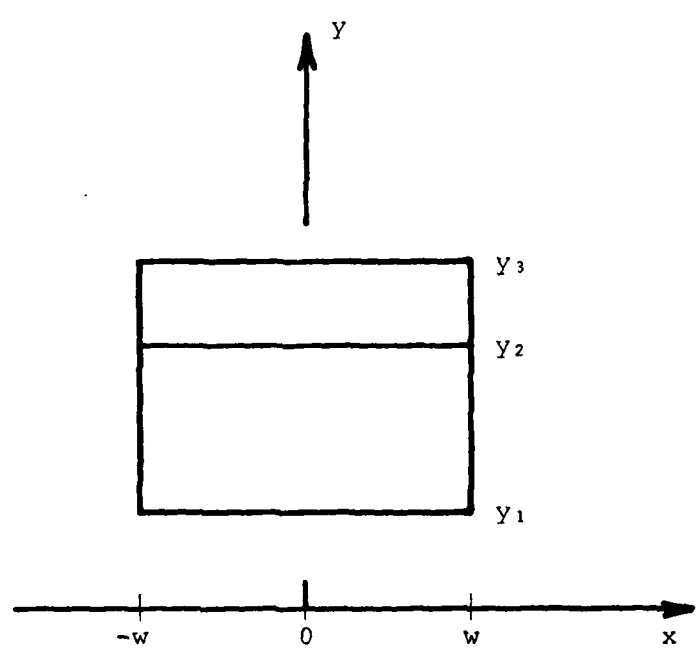


Figure A.1.1-9. Two Adjacent Rectangular Surface Patches.

Results [Newman, Nov. 1978] indicate that rectangular patches of  $\lambda/4$  side lengths are adequate for many problems. This translates to  $N \approx 32$  unknowns per square wavelength. Further discussion of this code appears in Section B.1.1.

The difficulty with rectangular patches is that they are not suited for many curved surfaces such as hemispheres. A convenient patch shape of general applicability is the triangle. Triangular patches are advantageous over general quadrilaterals for the following reasons [Glisson, June 1978]:

1. A minimum possible number of points is required to specify patch boundaries. Thus, data input is less.
2. Triangular patches are always planar whereas quadrilaterals may not be, and planar patches facilitate numerical computation.
3. Triangular patches conform more readily to rapidly changing surface boundaries or curvatures and facilitate sampling the unknown current more densely in critical regions.

A convenient, appropriate expansion function for triangular patches has recently been detailed [Glisson, June 1978]. The expansion functions are determined by assuming uniform surface charge per patch and continuity of current across each interface between patches. The patches need not be identical. Rao and Wilton have recently completed a user-oriented computer code based on this theory [Rao, April 1979] and results are forthcoming.

If a surface is subdivided into  $t$  triangular patches with  $e$  patch sides along the surface edge then the number of unknowns  $N$  is given by

$$N = \frac{3t - e}{2}$$

If a closed surface is subdivided into  $N_p$  quadrilaterals and a triangular patch representation is obtained by dividing each quadrilateral into two triangles then about a 50% larger matrix equation would result for the triangular case. (In the quadrilateral case there are  $2N_p$  unknowns; in the triangular case  $\frac{3}{2}(2N_p)$ .) This reasoning, although not necessarily justified, was used in assessing cpu time and computer memory for a triangular patch code from rectangular patch code results for the coupling model assessment table in Section 7. Thus,  $N \approx 48$  unknowns per square wavelength was assumed in assessing SPE-FD.

A triangular surface patch code is thus highly applicable to arbitrarily shaped conducting surface problems. The surfaces may have edges as in disks, rims as in right cylinders, apertures, or loads. Also, both radiation and scattering problems can be handled with equal ease. As indicated in Section A.1.1.1.6 the frequency cannot be too high, however, since the required matrix size grows rapidly with frequency.

#### A.1.1.3 Conducting Bodies of Revolution (BOR-FD)

Many problems in EMC involve structures which are, either exactly or approximately, rotationally symmetric. Such structures, called bodies of revolution BORs, are efficient to model because of their modal decoupling properties whereby a Fourier sine wave component (with respect to the rotational, or  $\phi$ , coordinate) of excitation (incident field, voltage, etc.) results in the same Fourier component of response (induced current, scattered field, etc.). In a moment method formulation, if expansion functions having sinusoidal  $\phi$  variation are chosen, this immediately leads to the reduction of one perhaps huge matrix to a number of relatively small matrices. Large matrices often result from problems with arbitrarily shaped bodies devoid of symmetries. The BOR formulation has been applied to many EMC related problems. Some of these are summarized in [Schuman, July 1976]. They include radiation and scattering from loaded BORs and coupling through apertures in BORs.

A BOR is shown in Figure A.1.1-10. The surface enclosing a BOR is traced by the rotation of an arbitrarily curved line in the  $x$ - $z$  plane about the  $z$ -axis. This line in the  $x$ - $z$  plane is called the "generating curve" of the BOR. Also, the "axis" of the BOR is in this case coincident with the  $z$ -axis.

Either  $H$ - or  $E$ -field formulations (A.1.1-29) or (A.1.1-30) respectively or a combined field formulation (previous section) can be applied. The set of expansion functions  $\tilde{F}_{nj}^t = f_j(t)e^{jn\phi}\hat{t}$  and  $\tilde{F}_{nj}^\phi = f_j(t)e^{jn\phi}\hat{\phi}$  ( $t$  and  $\phi$  are unit vectors) and the symmetric product

$$\langle \tilde{J}_1, \tilde{J}_2 \rangle = \iint_S \tilde{J}_1 \cdot \tilde{J}_2 ds = \int_{gc} \int_0^{2\pi} \tilde{J}_1 \cdot \tilde{J}_2 \rho d\phi dt \quad (\text{A.1.1-34})$$

are chosen. (The "gc" stands for BOR generating curve.) The  $f_j(t)$ , which express the  $t$  variation of the expansion functions, are usually selected in accordance with the method of subsections as discussed in Section A.1.1.1. In the Harrington-Mautz BOR model [Harrington, July 1969; Mautz, Feb. 1977] which is applied to the  $E$ -field formulation, they are triangles (overlapping) divided by the BOR radial coordinate  $\rho$ . This choice permits differentiation of the expansion functions and a non-zero value where the poles of the BOR meet the axis. The Fourier components  $e^{jn\phi}$  are chosen so that the above noted modal decoupling property of rotationally symmetric bodies applies. Thus for  $N$  triangles on the generating curve  $\tilde{J}$  is expanded as

$$\tilde{J} = \sum_{n=-\infty}^{\infty} \sum_{j=1}^N (I_{nj}^t f_j(t)e^{jn\phi}\hat{t} + I_{nj}^\phi f_j(t)e^{jn\phi}\hat{\phi}) \quad (\text{A.1.1-35})$$

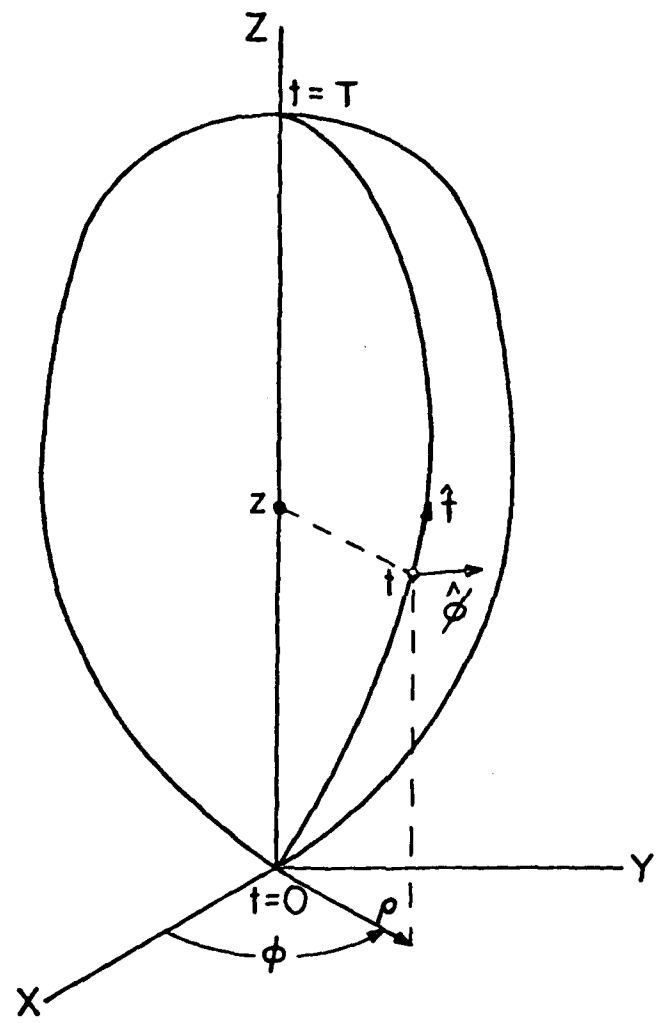


Figure A.1.1-10.  
Body of Revolution and Coordinate System.

where  $I_{nj}^t$  and  $I_{nj}^\phi$  are the unknown coefficients to be determined such that (A.1.1-30) is satisfied. The inner product of both sides of (A.1.1-30) is taken with respect to each of the weighting functions  $w_{ni}^t = f_i(t)e^{-jn\phi}\hat{t}$  and  $w_{ni}^\phi = f_i(t)e^{-jn\phi}\hat{\phi}$  resulting in the matrix equation

$$\vec{V}_n = [Z_n] \vec{I}_n \quad (\text{A.1.1-36})$$

for each  $n$ . Upon partitioning, (A.1.1-36) becomes

$$\begin{bmatrix} V_n^t \\ \vdots \\ V_n^\phi \end{bmatrix} = \begin{bmatrix} [Z_n^{tt}] & [Z_n^{t\phi}] \\ \vdots & \vdots \\ [Z_n^{\phi t}] & [Z_n^{\phi\phi}] \end{bmatrix} \begin{bmatrix} \vec{I}_n^t \\ \vdots \\ \vec{I}_n^\phi \end{bmatrix}$$

With  $a=t$  or  $\phi$  the  $i^{\text{th}}$  element of each  $\vec{V}_n^a$  and  $\vec{I}_n^a$   $N \times 1$  subvector is  $\langle w_{ni}^a, E^i \rangle$  and  $I_{ni}^a$  respectively. The  $i,j^{\text{th}}$  element of each  $N \times N [Z_n^{ab}]$  submatrix is  $\langle w_{ni}^a, L(F_{nj}^b) \rangle$  where  $ab=tt, \Delta t, t\phi, \phi\phi$ .

Each mode of  $J$  is determined independently from (A.1.1-35, 36) resulting in significant savings in computer processing time and memory. The solution to (A.1.1-36) can be expressed as

$$\vec{I}_n = [Y_n] \vec{V}_n \quad (\text{A.1.1-37})$$

where  $[Y_n] = [Z_n]^{-1}$  is the  $n^{\text{th}}$  mode generalized admittance matrix.

The  $n^{\text{th}}$  mode radiated, or scattered, field  $E_n$  can be determined from (A.1.1-37) by reciprocity. A current element  $I_1^r$  is located at the field point of interest,  $r$ , and oriented parallel to the polarization of interest. If  $\hat{V}_n^f$  is the  $n^{\text{th}}$  mode excitation vector due to  $I_1^r$  then

$$E_n \cdot I_1^r = \hat{V}_n^f [Y_n] \hat{V}_n \quad (\text{A.1.1-38})$$

Here  $\hat{V}_n^f$  is the transpose of  $\hat{V}_n^f$ ,  $\hat{V}_n^f = \begin{bmatrix} \hat{V}_n^t \\ \hat{V}_n^\phi \end{bmatrix}$ , the  $j^{\text{th}}$  element of  $\hat{V}_n^{fa}$  is  $\langle E_{nj}^a, E^r \rangle$  where  $a = t$  or  $\phi$ , and  $E^r$  is the field radiated by  $I_1^r$ . Both far and near fields [Bevensee, May 1974] can be determined from (A.1.1-38).

It is important to note that in the above development negative modes ( $n < 0$ ) as well as positive modes must be determined. However, the solution (A.1.1-37) for negative  $n$  is readily obtained from that for positive  $n$ , i.e., (A.1.1-36) need not be solved directly for negative  $n$  [Mautz, Feb. 1977].

The elements of  $[Z_n]$  are difficult to compute in comparison to computing the elements of  $[Z^S]$  of (A.1.1-33) in a surface patch formulation (previous section). The relative effort can be viewed as applying a basis transformation to  $[Z^S]$  resulting in a block diagonal matrix, each block being a  $[Z_n]$ . The basis transformation is from a surface patch expansion to the BOR modes of (A.1.1-35). As indicated in [AMP, July 1972] this transformation is proportional in cpu time to  $(2N_p)^2$  where  $N_p$  = number of surface patches. However, for reasonably large bodies this number is small compared to the  $(2N_p)^3$  term in the inversion time for  $[Z^S]$ . The inversion time for  $N_m$  non-negative BOR modes, on the other hand, is proportional to  $N_m(N)^3$  where  $N$  is, of course, considerably less than  $N_p$ .

The BOR modes required to solve a plane wave scattering problem is given by all integers  $N_n$  such that [Harrington, July 1969].

$$|n| < 1 + C_{\max} \quad (\text{A.1.1-39})$$

where  $C_{\max}$  is the largest circumference in wavelengths of the BOR. In some cases only one BOR mode is excited. For example, a plane wave axially incident on a BOR excites only the  $n = \pm 1$  modes ( $\sin\phi, \cos\phi$  azimuthal variation). Also, a uniformly excited  $360^\circ$  circumferential aperture excites only the  $n = 0$  mode (constant  $\phi$  variation). Furthermore, the  $n = 0$  mode permits additional savings in computer time since there are no cross polarization fields resulting from  $t$ -directed or  $\phi$ -directed components of current. Hence, for the  $n = 0$  mode  $[Z_n]$  reduces to

$$\begin{bmatrix} [z_n^{tt}] & 0 \\ 0 & [z_n^{\phi\phi}] \end{bmatrix}$$

where  $[z_n^{tt}]$  depends only on the  $t$ -directed current and  $z_n^{\phi\phi}$  depends only on the  $\phi$ -directed current.

Another E-field/BOR code based on a pulse expansion, for the  $t$ -variation has been developed with significant success especially with regard to handling troublesome aperture or surface edges [Glisson, June 1978]. Both "triangles" and "pulse" methods were successfully applied to the combined field formulation (Section A.1.1.2) thus avoiding "internal resonance" problems [Mautz, Feb. 1977; Glisson, June 1978].

A.1.1.4 Material Bodies - Surface Current Formulations  
(ESC-SP-FD)

Rarely in present EMC "coupling path" models are material body electromagnetic scatterers (fiberglass radomes, missile plumes, etc.) approximated as other than either perfectly conducting or completely transparent. This is a consequence of the quite loose accuracy requirements (10 dB or greater error) often necessitated by other complexities of the associated problems. However, improved modeling techniques and computer capabilities are expected to permit increasingly tighter accuracies in the future. This will eventually lead to greater emphasis on material body modeling. Thus the current status of such modeling is reviewed in this and the following two sections.

The scattering from a homogeneous material body (arbitrary  $\epsilon$ ,  $\mu$ , and  $\sigma$ ) can be analyzed by replacing the body with equivalent electric  $J$  and magnetic  $M$  surface currents along its surface  $S$ . These surface currents are postulated to excite  $E$  and  $H$  fields according to operators similar to those in (A.1.1-29) and (A.1.1-30). The boundary conditions of continuous tangential components of  $E$  and  $H$  across  $S$  result in four equations in unknowns  $J$  and  $M$ . These equations can be combined many different ways to limit the number of equations to the number of unknowns [Mautz, Nov. 1977]. One combination gives

$$\hat{n} \times (\underline{E}_e^- + \alpha \underline{E}_d^+) = \hat{n} \times \underline{E}^i \quad (A.1.1-40a)$$

$$\hat{n} \times (\underline{H}_e^- + \beta \underline{H}_d^+) = \hat{n} \times \underline{H}^i \quad (A.1.1-40b)$$

where  $\hat{n}$  is the outward normal unit vector on  $S$ ,  $\underline{E}_d^-(\underline{H}_d^-)$  is the electric (magnetic) field just inside  $S$  due to  $J$  and  $M$  radiating in the internal medium throughout all space, and  $\underline{E}_e^+(\underline{H}_e^+)$  is the electric (magnetic) field just outside  $S$  due to  $J$  and  $M$  radiating in the external medium (generally free space) throughout all space. The complex constants  $\alpha$  and  $\beta$  are arbitrary. However, it can be shown that solutions are unique if  $\alpha\beta^*$  is real and positive (\* indicates conjugate) [Mautz, Nov. 1977]. Two widely used choices for  $\alpha$  and  $\beta$  have been  $\alpha=\beta=1$  and  $\alpha = \frac{\epsilon_d}{\epsilon_e}$ ,  $\beta = -\frac{\mu_d}{\mu_e}$  where subscript d(e) indicates the internal (external) medium.

The second choice of  $\alpha$  and  $\beta$  results in what is commonly referred to as Muller's equation [Mautz, Nov. 1977].

Application of a moment method surface patch technique to (A.1.1-40) (model ESC-SP-FD) results in  $4N_p$  equations in  $4N_p$  unknowns where  $N_p$  = number of patches. The quadruple factor is due to two types of current,  $J$  and  $M$ , each having two polarizations. For scattering problems, where the sources are constrained to the external medium, the required number of expansion functions is probably largely dependent on the external medium wavelength. However, the usually smaller internal medium wavelength is expected to require significant effort in computing the matrix elements due to a rapidly varying  $e^{jkr}/r$  Green's function [Wilton, April 1979]. A triangular patch ESC-SP-FD is currently being considered for development [Wilton, April 1979]. Because of the present availability of a combined field surface patch moment method code as discussed in Section A.1.1.2 (the necessary operators are thus already coded) this development should not take long.

#### A.1.1.5 Material Bodies of Revolution (ESC-BOR-FD, FE-BOR-FD)

The moment method body of revolution formulation discussed in Section A.1.1.3 has been applied to rotationally symmetric homogeneous material bodies as formulated via equivalent surface electric  $J$  and magnetic  $M$  currents (A.1.1-40) [Mautz, Nov. 1977; Glisson, June 1978]. This model, ESC-BOR-FD, has been successfully applied to a number of dielectric scatterer problems on the order of a few wavelengths in circumference with better than 3 dB accuracy in scattered field [Glisson, June 1978]. For each BOR mode (see Section A.1.1.3) about 20 expansion functions (10 for each polarization) per external medium wavelength (usually free space) per current type ( $J$  or  $M$ ) is suggested.

Inhomogeneous BOR scattering can be analyzed through an extension of the equivalent surface current method. Here the BOR is approximated by layers of homogeneous material resulting in "stepped" inhomogeneities. Equivalent surface currents reside

between each layer, and a moment method formulation enables these currents to be determined. The overall generalized matrix relating these currents grows rapidly with number of layers. However, this matrix is block tri-diagonal and if only the external scattered fields are of interest, the corresponding equations can be solved relatively efficiently [Pogorzelski, Oct. 1976]. A computer code is now available with a corresponding report available soon [Wilton, April 1979]. Two principal difficulties with this method are (a) the surfaces, and, hence, their descriptive input data, may need changing if the media constitutive parameters change, and (b) if these parameters are highly nonuniform many surfaces may be needed resulting in exorbitant cpu time and computer memory needs. The models VC-FD (Section A.1.1.6) and FE-TD (Section A.2.1.2) do not suffer these drawbacks. Neither does the FE-BOR-FD model discussed below.

A frequency domain finite difference solution to Maxwell's equations also treats inhomogeneous bodies. The  $\tilde{E}$  and  $\tilde{H}$  fields themselves are the unknowns rather than equivalent surface currents (above) or volume density currents (Section A.1.1.6). A matrix equation results by writing six equations at each of a series of points distributed in three dimensions forming a "mesh". The matrix is sparse and the method is good for problems involving bounded regions, e.g., cavities, waveguide, etc. Difficulty arises for external radiation and scattering problems since the boundary condition at infinity must be approximated at the edges of a finite mesh. This results in an unknown error in addition to an erroneous "reflection" [Jones, July 1974]. However, in conjunction with "external" methods the finite difference technique proves useful. A resulting "combined" technique is the unimoment method or UM-BOR-FD of Section B.1.2. Thus, in preparation for describing UM-BOR-FD, which is limited to rotationally symmetric bodies, the finite-element BOR model FE-BOR-FD is summarized below. The details are given in [Morgan, May 1977]. One purpose for limiting the method to BORs is that a convenient potential formulation is then apparent. Potential formulations offer numerical advantages by usually having fewer coupled unknowns and a higher order of continuity than the original EM fields.

The FE-BOR-FD model uses the "coupled azimuthal potential" method [Morgan, May 1977]. In this method two coupled azimuthal potentials, having a one-to-one relationship with the azimuthal components of the BOR modal electric and magnetic fields, represent the fields in generally inhomogeneous isotropic rotationally symmetric media where electrical properties  $\epsilon(r)$  and  $\mu(r)$  are constant functions of the azimuthal BOR coordinates. (Note that a conductivity  $\sigma(r)$  can be included by subtracting  $\sigma/(2\pi f \text{freq.})$  from the imaginary part of complex  $\epsilon$ .)

Fields are expanded in terms of BOR modal fields  $e_n, h_m$  as

$$E(R, Z, \phi) = \sum_{n=-\infty}^{\infty} e_n(R, Z) e^{jn\phi}$$

$$\frac{c_0}{\rho} H(R, Z, \phi) = \sum_{n=-\infty}^{\infty} h_n(R, Z) e^{jn\phi}$$

where  $c_0$  = free space wave impedance, a normalized cylindrical coordinate system is assumed -  $(R, Z, \phi) = (k_0 r, k_0 z, \phi)$ , and  $k_0$  = free space wave number ( $2\pi/\lambda$ ).

Two modal scalar potential functions  $\psi_1(R, Z, n)$  and  $\psi_2(R, Z, n)$  satisfy the coupled second-order linear partial differential equations

$$\nabla \cdot [f_n(R \epsilon_r \nabla \psi_1 + n \hat{x} \times \nabla \psi_2)] + \epsilon_r \psi_1 / R = 0 \quad (\text{A.1.1-41a})$$

$$\nabla \cdot [f_n(R \mu_r \nabla \psi_2 - n \hat{x} \times \nabla \psi_1)] + \mu_r \psi_2 / R = 0 \quad (\text{A.1.1-41b})$$

and specified surface boundary conditions where  $\epsilon_r = \epsilon_r(R, Z)$ ,  $\mu_r = \mu_r(R, Z)$  are the relative constitutive parameters, " is the 2-dimensional gradient defined by

$$\nabla = \hat{R} \frac{\partial}{\partial R} + \hat{Z} \frac{\partial}{\partial Z}$$

and

$$f_n = f_n(R, Z) = \left[ \mu_r(R, Z) \epsilon_r(R, Z) R^2 - n^2 \right]^{-1}$$

The functions  $\psi_1$  and  $\psi_2$  give rise to the modal field components  $e_n$ ,  $h_n$  via

$$\hat{\phi} \times e_n = j f_n (n \hat{\phi} \times \nabla \psi_1 - R u_r \nabla \psi_2)$$

$$\hat{\phi} \cdot e_n = \psi_1 / R$$

$$\hat{\phi} \times h_n = j f_n (n \hat{\phi} \times \nabla \psi_2 + R \epsilon_r \nabla \psi_1)$$

$$\hat{\phi} \cdot h_n = \psi_2 / R$$

If standard spherical coordinates are preferred then the above equations can be trivially changed by using the substitutions  $R = k_o r \sin \theta$ ,  $Z = k_o r \cos \theta$ , and  $\nabla = [(1/k_o)r(\partial/\partial r) + \hat{\theta} (\frac{1}{r})(\partial/\partial \theta)]$ .

Note that since  $\psi_1$  and  $\psi_2$  are proportional to  $\phi$ -components of  $e_n$  and  $h_n$  they are continuous everywhere including dielectric and magnetic interfaces. This property is very desirable in numerical computations since no supplemental boundary conditions need then be included in an algorithm.

The solution to (A.1.1-41) can be obtained by either a finite difference method or, as is preferred, a variational formulation in conjunction with a finite element method. The finite difference method involves a rectangular mesh whereas the finite element is a triangular one. The solution (stationary point) to the variational formulation

$$F = \int f_n [\nabla \psi_1 \cdot (R \epsilon_r \nabla \psi_1 + n \hat{\phi} \times \nabla \psi_2) + \nabla \psi_2 \cdot (R u_r \nabla \psi_2 - n \hat{\phi} \times \nabla \psi_1)] - (\epsilon_r \psi_1^2 + \mu_r \psi_2^2) / R dR dz$$

where the integration is over the BOR longitudinal cross section, is obtained by a Rayleigh-Ritz procedure which is equivalently a Galerkin moment method solution to (A.1.1-41).

This method cannot presently effectively treat thin, perfectly conducting structures imbedded in the material media. However, an effort to alleviate this is currently being investigated [Tesche, March 1979].

#### A.1.1.6 Material Bodies - Volume Current Formulation (VC-FD)

The volume current formulation analyzes the scattering from inhomogeneous dielectric (including finitely conducting) and/or magnetic lossy scatterers by replacement with equivalent free-space electric  $\tilde{J}$  and/or magnetic  $\tilde{M}$  current densities [Harrington, 1968 (Secs. 5-5, 6, 7)]. These current densities can be determined from a moment method solution of

$$\tilde{J} = j\omega\Delta\epsilon (\tilde{E}_\infty^i + \tilde{E}_\infty^s) \quad (A.1.1-42)$$

$$\tilde{M} = j\omega\Delta\mu (\tilde{H}_\infty^i + \tilde{H}_\infty^s) \quad (A.1.1-43)$$

where

$$\Delta\epsilon = \frac{\sigma}{j\omega} + \epsilon - \epsilon_0$$

$$\Delta\mu = \mu - \mu_0$$

$\tilde{E}_\infty^i$  = impressed (body absent) electric field

$\tilde{H}_\infty^i$  = impressed (body absent) magnetic field

$\epsilon, \mu, \sigma$  = material permittivity, permeability, and conductivity

$\epsilon_0, \mu_0$  = free space permittivity and permeability

$$\omega = 2\pi \times \text{freq.}$$

and  $\tilde{E}_\infty^s$  and  $\tilde{H}_\infty^s$  are the free-space radiated fields from  $\tilde{J}$  and  $\tilde{M}$ .

Note that  $\tilde{E}_\infty^s$  and  $\tilde{H}_\infty^s$  are each functions of both  $\tilde{J}$  and  $\tilde{M}$ . A moment method procedure for solving (A.1.1-42, 43) constitutes a VC-FD model.

The moment method solution to (A.1.1-42,43) discussed below is obtained by subdividing the body into electrically small cells. To each cell is associated six constant expansion functions arising from the generally three polarizations for both  $\hat{J}$  and  $\hat{M}$ . A point-matching specification (impulse testing) is then applied in standard moment method fashion resulting in a matrix equation in  $6N_c$  unknowns where  $N_c$  is the number of cells. Hence, the order of the generalized matrix rapidly increases with frequency. In addition, since high dielectric and/or permeable media generally result in correspondingly small wavelengths, the density of cells may need to be considerably larger than is dictated by free-space wavelengths above.

It is not presently clear which cell size (side length =  $d$ ) is adequate. If the wavelength in the body  $\lambda_b$  is approximately the free-space wavelength  $\lambda_0$ , then  $d \approx 0.2\lambda_0$  should be adequate for most scattering problems to within  $\sim 3$  dB accuracy. However, if  $\lambda_b \ll \lambda_0$  then perhaps  $d \approx 0.2\lambda_b$  is necessary. The latter constraint, of course, presents far greater limitations on body sizes that can be handled by VC-FD.

A VC-FD model has been developed with rectangular volumes (parallelepipeds) for cells and point-match testing [Newman, July 1978]. Applications of this model are discussed as the combined model TW-FD/VC-FD in Section B.1.2. Although restricted to relatively small bodies VC-FD appears particularly suited for highly complex, non-uniform ones. Thus, VC-FD can, under certain conditions, provide a viable alternative to the equivalent surface formulation ESC-BOR-FD, the latter requiring many layers of different homogeneous materials in order to approximate a highly nonuniform body (Section A.1.1.5).

If the body is only dielectric (and/or conductive) or permeable but not both then only a  $\hat{J}$  or  $\hat{M}$  need be determined. Larger such bodies can then be handled by VC-FD.

### A.1.2      High Frequency

The high frequency methods described in this section apply principally to electromagnetic scattering from conducting bodies with extents greater than a few wavelengths. These methods are of increasing importance especially since systems operating at increasingly higher frequencies are becoming more prevalent. Although computer power is also increasing dramatically, with associated increase in the number of problems amenable to moment methods, it is not nearly rapid enough to obviate the need for these high frequency techniques in the distant future. For example, it is highly improbable that wire gridding (Section A.1.1.1.5) or surface patching (Section A.1.1.2) an entire B-52 bomber at a frequency of 1 GHz will be feasible for many years to come.

The basic high frequency techniques, considered here as basic coupling models, are free space transmission (FST), geometrical optics (GO), geometrical theory of diffraction (GTD), and physical theory of diffraction (PTD). Generally, the basis to many of these methods are highly accurate solutions to canonical problems such as the two-dimensional plane wave scattering from an infinite wedge or cylinder. Simple approximations to these solutions are then obtained which are generally valid at sufficiently high frequencies. These solutions are then modified and combined to form methods that are postulated to apply to more complex problems such as predicting the field radiated by an omnidirectional antenna placed on a satellite. Thus, one often does not know for certain whether a high frequency method actually solves a given problem. This is in contrast to the moment method low and medium frequency techniques discussed in previous sections. Prior to applying a moment method technique an actual problem is usually replaced with one similar but simpler. For example, a missile may be modeled as

a body of revolution by discarding fins and other asymmetries. The simpler problem is then analyzed reliably in that an approximate solution to Maxwell's equations is usually assured. With high frequency methods, on the other hand, pertinent edges and surfaces are analyzed as isolated problems and the concept of representing EM fields as rays (Section A.1.2.2.1) is usually employed to effect interaction between them. The choice of important rays is based largely on qualitative reasoning and experience. Thus there is no assurance that a ray theory solution to a given problem of complicated geometry is accurate unless, of course, there is experimental or other independent validation. In fact a ray in itself at best only approximates a solution to Maxwell's field equations; the higher the frequency the better the approximation.

#### A.1.2.1 Free Space Transmission (FST)

Free space transmission (FST) is one of the simplest high frequency models because it involves the transmission of an electromagnetic wave between two points in free space with no intervening structure to scatter the wave. It is presently an IEMCAP transmission model [Paul, no date]. It applies quite well for source and receptor separated by a distance large compared to a wavelength. No account is taken of reflection or diffraction phenomena. However, with a scatterer present FST often provides the incident field from which reflected and/or diffracted fields can be obtained.

##### A.1.2.1.1 Basic Theory

The power density  $P$  at a distance  $D$  from an isotropic source radiating a total power  $W_T$  is

$$P = \frac{W_T}{4\pi D^2} \quad (\text{A.1.2-1})$$

The power  $W_R$  received by an antenna at this point is related to its effective aperture  $A_R$  by

$$A_R = \frac{W_R}{P} \quad (A.1.2-2)$$

In addition, if the emitter has a gain  $G_T$  (relative to an isotropic point source) then

$$\frac{W_R}{W_T} = \frac{G_T A_R}{4\pi D^2} \quad (A.1.2-3a)$$

Also the gain  $G_R$  of the receiver antenna is related to  $A_R$  by

$$G_R = \frac{4\pi}{\lambda^2} A_R \quad (A.1.2-3b)$$

Together (A.1.2-1,2,3) yield the well known Friis free space transmission formula

$$\frac{W_R}{W_T} = G_T G_R \left( \frac{\lambda}{4\pi D} \right)^2 \quad (A.1.2-4)$$

In dB this becomes the transmission factor

$$TFS = G_T(dB) + G_R(dB) + 20 \log_{10} \frac{\lambda}{4\pi D} \quad (A.1.2-5)$$

#### A.1.2.2 Geometrical Optics (GO)

Geometrical optics (GO) provides a high frequency approximation to the total field excited in the presence of an electrically wide conducting surface. Both incident and reflected fields are obtained as well as refracted fields if the surface is not perfectly conducting. Also, the surface need not be flat. However, only smooth variations from a plane are assumed in GO such as naturally occurs with aircraft wing surfaces, fuselages and other structures designed for streamlined shape. The presence of sharp bends or edges requires other models such as the geometrical theory of diffraction GTD discussed later. Only applications to conducting surfaces will be considered here since (a) most current EMC problems can be modeled adequately with perfectly conducting surfaces (see Section A.1.1.4) and (b) most available computer codes employing GO, that are applicable to problems involving bodies of relatively general shape, assume perfect conductors [Marhefka, March 1978; Bach, September 1975].

As will become clear below, in GO the field in the shadow of the conducting scatterer (wing, for example) is assumed zero. Thus, the GO field exhibits erroneous discontinuities along shadow and reflection "optical" boundaries in space. In the vicinity of these boundaries GO solutions are significantly in error. Other models based on, for example, GTD are then needed to improve the solutions. In fact, GO is of no use for predicting transmission to receptors in shadow regions since the shadow region fields are composed entirely of diffracted fields.

A second concern in applying GO is that the GO field, defined in terms of rays, erroneously becomes infinite at certain points or surfaces in space. These regions, called caustics, occur wherever rays converge. Thus, they impose a limitation on all ray theories. This includes GTD as well as GO.

Other potential models such as those based on the physical theory of diffraction PTD or the spectral theory of diffraction STD avoid this difficulty. However, these latter methods (Section A.1.2.4) are presently not sufficiently developed for implementation as models of general applicability for use in EMC analysis.

The principal practical limitation with applying GO to surfaces of general curvature is the problem of locating surface reflection points. For arbitrarily curved surfaces this entails a time consuming search routine, in accordance with Fermat's Principle, that minimizes the path between source and field points under the constraint that one path point (reflection point) lies on the surface.

#### A.1.2.2.1 Basic Theory

The basic theory of geometric optics (GO) will be treated in a fair amount of detail as an example of a high frequency calculation involving ray fields. It is felt that GO illustrates all the basic techniques involved in any ray calculation (including GTD) but yet is simple enough to understand rather easily. The theory will be illustrated by applying GO to scattering from a finite planar conducting screen. There will be no wave transmitted through the screen in this case, but formulas for such transmission are derived similarly for a lossy (non-perfectly conducting) screen.

The GO field is composed of incident  $\tilde{E}^i$  and reflected  $\tilde{E}^r$  fields as indicated in Figure A.1.2-1. A source at  $\tilde{r}_0$  radiates  $\tilde{E}^i$ . This field is assumed to approximately behave as a ray, i.e.,

$$\tilde{E}^i(\tilde{r}) = \tilde{e}^i(\tilde{r}) e^{-jks^i(\tilde{r})} \quad (A.1.2-6)$$

where  $\tilde{e}^i(\tilde{r})$  contains the magnitude and polarization of the ray at  $\tilde{r}$  and  $ks^i(\tilde{r})$  its "phase" at  $\tilde{r}$ . The problem then is to determine

the total field  $\tilde{E}^t$  produced by the source when the screen S is present. According to GO part of the incident field is blocked by S and casts a shadow behind it. The screen S divides the space into a lit region and a shadow region. The boundary between the shadow and lit regions of the incident ray field is called the shadow boundary. This is illustrated in Figure A.1.2-1a. In addition to the incident field GO also requires the existence of a reflected field  $\tilde{E}^r$  of the form

$$\tilde{E}^r(\tilde{r}) = \tilde{e}^r(\tilde{r}) e^{-jks^r(\tilde{r})} \quad (\text{A.1.2-7})$$

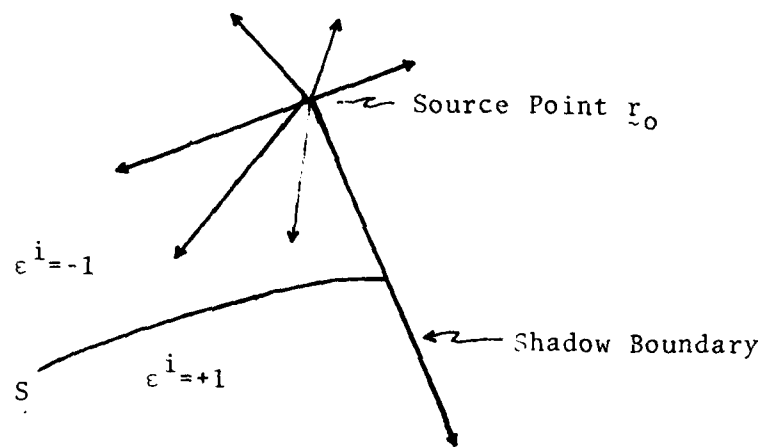
which is also a ray with similarly defined variables. The screen S also divides the space into a lit region and a shadow region for the reflected field. The boundary between these two regions is the reflection boundary. This is illustrated in Figure A.1.2-1b. The total field is then given by

$$\tilde{E}^t = \tilde{E}^i + \tilde{E}^r \quad (\text{A.1.2-8})$$

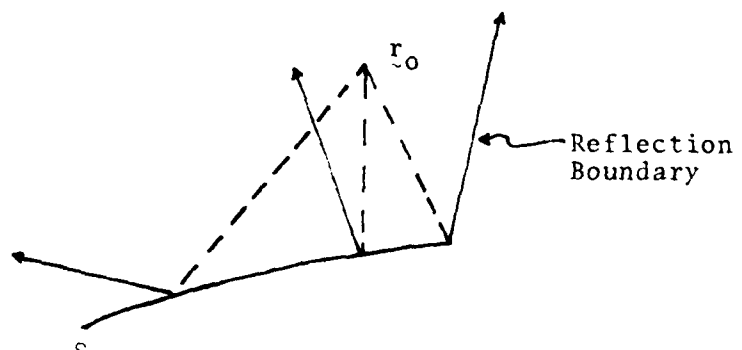
and is called the geometrical optics field. In using (A.1.2-8) due attention must be given to the regions of space where  $\tilde{E}^i$  and  $\tilde{E}^r$  are meaningful. For example, these fields are zero in their respective shadow regions. To introduce this fact into (A.1.2-8) two special functions, called shadow indicator functions, are defined for the incident and reflected fields. For the incident field, the shadow indicator function is  $\epsilon^i(\tilde{r})$  which is defined by

$$\epsilon^i(\tilde{r}) = \begin{cases} +1, & \text{if } \tilde{r} \text{ is in the shadow region} \\ & \text{of the incident field} \\ -1, & \text{if } \tilde{r} \text{ is in the lit region} \\ & \text{of the incident field} \end{cases} \quad (\text{A.1.2-9})$$

Then, in the presence of S, the incident field  $\tilde{E}^i$  is modified to become  $U(-\epsilon^i) \tilde{E}^i(\tilde{r})$  where  $U(x)$  is the unit step function



(a) Incident Field



(b) Reflected Field

Figure A.1.2-1. Illuminated and Shadow Regions of the Incident and Reflected Fields from a Point Source.

$$U(x) = \begin{cases} +1, & x > 0 \\ 0, & x < 0 \end{cases} \quad (\text{A.1.2-10})$$

The shadow indicator function for the reflected field is defined analogously. The geometrical optics field then becomes

$$\tilde{E}^t(\tilde{r}) = U(-\varepsilon^i)\tilde{E}^i(\tilde{r}) + U(-\varepsilon^r)\tilde{E}^r(\tilde{r}) \quad (\text{A.1.2-11})$$

Given a ray at any point in space, the path it travels can be readily determined by a method called ray tracing [Lee, March 1975; James, 1976; Lee, May 1978, Deschamps, September 1972]. If the medium is homogeneous the path is a straight line. The amplitude and phase of the ray at any point along its path is also provided by ray tracing methods as long as the curvatures of each dimension of the two-dimensional waveform for the ray at one point along its path is known. Examples of typical "curvatures" are zero for each dimension for plane waves; circular in one dimension and zero for the other for cylindrical waves; and circular in both dimensions for spherical waves. The principal difficulty with GO is in choosing the correct rays at the outset. In homogeneous media the "direct" ray is easily determined as that  $\tilde{E}^i$  which travels the straight line path between emitter and field point (typically a receptor location). However, choice of reflected ray is generally not so simple since the point of reflection on S must be determined. This can be accomplished by finding that point on S at which the angle of incidence  $\theta^i$  between the normal to S (directed toward source region) and the incident ray is equal to the angle of reflection  $\theta^r$  between this normal and the reflected ray (Snell's Law). For practical applications, however, it is easier to determine the reflection point by invoking Fermat's Principle which states that, for homogeneous media, the combined incident ray/reflected ray path is a minimum. For conducting scatterers of other than simply defined shape, i.e., not plates, cylinders, ellipsoids, etc., a search procedure must be employed

to find this minimum path. If many different source and field points are of interest this could result in costly computer run time. Also between an emitter and a field point a number of scatterers could reside requiring consideration of many "multiple" reflections for each trial path. (A reflected ray for one surface becomes an incident ray for a second surface, etc.) Perhaps this is why the only available GO codes of wide applicability apply only to modeling scatterers via simple shapes such as flat plates and cylinders [Marhefka, March 1978].

Another complication in applying GO to arbitrarily curved scattering surfaces deals with determining the wave front curvature of the reflected rays. The curvature of a wave front determines the attenuation or amplification of the corresponding ray. For example if  $\rho_1^i$  and  $\rho_2^i$  are the principal radii of curvature [James, 1976; Lee, October 1977] of the incident ray then the incident ray at a distance  $s_o^i$  from a local origin along the ray is given by

$$E^i(s_o^i) = \left[ \frac{\rho_1^i + s_o^i}{(\rho_1^i + s_o^i)(\rho_2^i + s_o^i)} \right]^{1/2} E^i(o) e^{-jks_o^i} \quad (A.1.2-12)$$

The radii of curvature for the reflected ray depends on both the curvature of the incident ray at the point of reflection on S and also the curvature of S at this point. For smooth surfaces this relationship is known [James, 1976, page 108].

In conclusion, GO can account for incident, reflected (and refracted) rays in the lit region of a scatterer but not diffracted rays in either the lit or the shadow region. More sophisticated methods such as GTD (next section) are needed to treat these cases. It should be noted, however, that for sufficiently high frequencies the geometrical optics field may require no correction i.e., the scattering process is completely dominated by the geometrical optics term. The total field is

then well approximated by the incident plus reflected (plus refracted) fields in the lit region and zero (or refracted) fields in the shadow region.

#### A.1.2.3 Geometrical Theory of Diffraction (GTD)

The geometrical theory of diffraction (GTD) is a procedure for including the effects of waves diffracted from edges or around curved surfaces in an electromagnetic scattering or radiation problem. Together with the geometrical optics field obtained from the GO model, GTD usually produces a more accurate total field for the problem under consideration than with GO alone. The combined GO/GTD model is discussed in Section B.2.1.

The theory of GTD has been successfully applied to a wide variety of high-frequency radiation and scattering problems. Of particular interest is the excellent agreement obtained between GTD analysis and scale model experiment regarding radiation patterns of aircraft antennas mounted on a KC-135 [Burnside, May 1975] and both a Boeing 737 and the space shuttle orbiter [Balanis, July 1976]. Reference to other GTD results, with particular emphasis on shipboard applications can be found in [Ryan, August 1975].

##### A.1.2.3.1 Basic Theory

The general diffraction case for GTD is handled in a manner similar to geometric optics. Again because of the high frequency, the diffraction process is a local one involving rays. The appropriate rays and points of diffraction are chosen according to a modified form of Fermat's Principle which states that a diffracted ray traveling from point  $P$  to point  $Q$  traverses the minimum path length subject to the constraint that one path point lies on the diffracting edge. In the case of a smooth surface and a homogeneous medium, the point on the diffracting edge is replaced by a geodesic path segment (shortest path constrained to lie on the surface). The canonical problem for edge diffraction

is two-dimensional plane wave scattering from an infinite wedge. The canonical problem for smooth convex surface diffraction is two-dimensional plane wave scattering from an infinite cylinder. These problems form the basis for obtaining diffraction coefficients from which result the magnitudes and phases of diffracted rays relative to the amplitudes and phases of rays incident on the scatterer.

The original GTD formulas [Keller, February 1962] for edge diffracted rays are in significant error near reflection and shadow boundaries (optical boundaries as defined in Sections A.1.2.2 and A.1.2.2.1). Subsequent theories improved upon these formulas by either adjusting them to provide continuity of total field across the optical boundaries [Kouyoumjian, November 1974] or adjusting both the GO formulas as well as GTD formulas to assure this continuity [Lee, 1977 ("Uniform Asymptotic Theory...")]. The former method, termed the "Uniform Theory of Diffraction" by its developers Kouyoumjian and Pathak, will be considered here as representative of the GTD model especially since this method forms the basis of a highly versatile computer code currently available [Marhefka, March 1978].

The elements in the basic theory of the GTD model involve diffraction from the edge of a conducting "wedge" with perhaps non-flat surfaces. Also the wedge edge need not be straight. If the ray  $E^i(p_0)$  incident on the edge at point  $p_0$  is assumed polarized parallel to the plane formed by the edge and the incident ray path (electric polarization) then the diffracted ray at  $r$ , which is added to the GO rays in arriving at a better approximation to the total field by accounting for edges, is given by [James, 1976]

$$E^d(r) = D^e E^i(p_0) \left( \frac{\rho^d}{s^d (\rho^d + s^d)} \right)^{1/2} e^{-jks^d} \quad (A.1.2-13)$$

where  $s^d$  is the distance between  $P_0$  and  $r$ ,  $\rho^d$  is the principal radius of curvature of the diffracted ray in the plane formed by the diffracted ray and the edge, and  $D^e$  is the electric polarization edge diffraction coefficient.

The edge diffraction coefficient  $D^e$  is a simple function of  $s^d$ ,  $\rho^d$ , the angular directions of the incident ray with respect to the point of diffraction  $P_0$  on the edge, the radii of curvature of the incident and reflected rays at  $P_0$ , the curvature of the edge at  $P_0$ , the angle of the wedge containing the edge at which diffraction is occurring, and the Fresnel integral. In addition  $\rho^d$  depends on the curvature of the edge at  $P_0$ . The Fresnel integral does not have an exact closed form solution. However, it is well tabulated, and accurate approximating polynomial expansions exist for the full range of its argument [Boersma, 1960]. Furthermore, a quite simple asymptotic approximation of the Fresnel Integral is available and often employed [Keller, February 1962; James, 1976]. However, this approximation is not accurate in the vicinity of the shadow and reflection boundaries. In fact along these boundaries this approximation is infinite.

An expression similar to (A.1.2-13) exists for diffracted rays arising from incident rays polarized normal to the plane formed by the incident ray path and the edge (magnetic polarization). An arbitrary ray can be decomposed into electrically and magnetically polarized rays.

The GTD diffraction coefficients associated with edges and surfaces of complicated shapes may be costly to determine. Considerable computer time may be required if many diffracted rays need be computed and if the curvatures of the edges and surfaces can only be described numerically. As with GO, arbitrarily curved edges and surfaces may require many trial computations until the ray which minimizes path length is found (Fermat's Principle).

The GTD model for analyzing diffraction around smooth convex curved surfaces such as aircraft fuselages is developed in a manner similar to the edge diffraction development [James, 1976; Kouyoumjian, 1975; Keller, February 1962]. As previously mentioned, the canonical problem is plane wave diffraction around a circular cylinder. The scattering process, as with any convex surface, involves a region of deep illumination, a region of deep shadow, and a transition region. The deeply illuminated regions involve the incident and reflected ray fields obtainable from GO. The fields which exist in the deep shadow region are referred to as creeping rays. These rays are launched from points of incidence on the cylinder and propagate around the cylinder on geodesic paths shedding rays tangentially as they travel. The geodesic path is the shortest path on the surface between the points at which the incident ray impinges on the surface and the diffracted ray leaves the surface. Analysis here proceeds in a manner similar to that with edge diffraction. The principal difficulty with applying surface diffraction to general surfaces is in determining the geodesic path over which the creeping waves travel. If the surface shape is not simple such as cylindrical, conical, etc., and can only be described numerically then a time-consuming trial and error process is required.

#### A.1.2.4 Physical Theory of Diffraction

The Physical Theory of Diffraction (PTD) [Ufimtsev, September 1971] is another method for taking edge effects (wing tips, etc.) into account in analyzing the coupling between emitters and receptors. It thus extends the applicability of GO as does GTD. The principal difference between PTD and GTD is that in the former additional surface currents are determined which radiate the corrections to the physical optics field. The physical optics (PO) field is obtained by computing the radiation from surface currents that are taken to be twice the tangential component of incident magnetic field on the illuminated portion of the scatterer and zero on the shadow portion. Thus PTD (and PO)

employ wave theory, rather than ray theory, to compute the total fields. This avoids the difficulties caused by caustics and optical boundaries discussed earlier in connection with GO and GTD.

The principal difficulty with PTD is in obtaining the surface current corrections to the PO currents. There are no general expressions for these currents and approximations have been obtained only for special cases. General purpose computer codes do not appear to be presently available. However, the above stated advantage of PTD over GTD makes future PTD codes worth considering or perhaps even developing. Related theories that may prove promising in developing general computer codes are the Spectral Theory of Diffraction [Mittra, 1976], and the Method of Equivalent Currents [Knott, November 1974; Clemmow, July 1956].

#### A.1.3      Transmission Line

Transmission lines are prevalent in modern day systems and subsystems. They appear as coaxial cables, twin-wire cables, strip-line, etc. and as bundles of such lines. They are designed to conduct electromagnetic energy at wavelengths considerably larger than the cross section of the transmission line. Under this assumption there is considerable simplification in their mathematical modeling since a distributed lumped circuit viewpoint then applies. Thus models for transmission lines at frequencies that do not violate this assumption are considered in subsequent sections as a distinct class of models. Such models are governed by the lowest order, or "transmission line," mode of propagation. At higher frequencies, other, higher order, modes of propagation may be significant. However, since little research has appeared to date concerning higher order modes [Paul, 1979], they are not discussed further here. The following discussion of transmission line modeling is primarily from a twin-wire viewpoint. However, coaxial cable, stripline, etc. analyses result in similar expressions.

#### A.1.3.1 Transmission Line Equations

The basic transmission line (TML) can be represented by two bare parallel straight wires in free space. The basic TML equations are derived assuming the wire separation and wire radii are small relative to a wavelength, and the media the wires pass through is homogeneous along the length of the wires. Under these assumptions the wave propagation is predominantly transverse electromagnetic (TEM) with a planar wave front traveling along the lines.

The absence of longitudinal field components insures that the definition of voltage is unique and any flow of current in the dielectric around the conductors is only in the transverse plane. The transmission line equations are then

$$\frac{dI}{dx} = -(j\omega C + G)V \quad (\text{A.1.3-1a})$$

$$\frac{dV}{dx} = -(R + j\omega L)I \quad (\text{A.1.3-1b})$$

where  $I$  and  $V$  are the TML current and voltage respectively,  $x$  is the axial coordinate of the TML,  $R$  and  $L$  are the TML series resistance and inductance, respectively, per unit length,  $G$  and  $C$  are the TML shunt conductance and capacitance, respectively, per unit length, and  $\omega$  = the radian frequency ( $2\pi f$ ). The TEM assumption permits calculating  $R$ ,  $L$ ,  $G$ , and  $C$  under static conditions (zero frequency).

#### A.1.3.2 State Vector Representation of TML Equations

The TML equations can be computerized in the form of a state transition matrix. If the voltage and current are known at a point along the TML, then via the state transition matrix the voltage and current can be calculated at any other point along the TML. The state transition matrix equation representing the relationship between the values of the currents and voltages at different points along the line is given by [Paul, April 1976]

$$\begin{bmatrix} I_{x+x'} \\ V_{x+x'} \end{bmatrix} = \phi(x') \begin{bmatrix} I_x \\ V_x \end{bmatrix} \quad (\text{A.1.3-2})$$

where

$$\phi(x') = \begin{bmatrix} \cosh(x'\gamma) & -(Y/\gamma)\sinh(x'\gamma) \\ -(\gamma/Y)\sinh(x'\gamma) & \cosh(x'\gamma) \end{bmatrix}$$

$$\gamma = YZ, \quad Y = G+j\omega C, \quad \text{and} \quad Z = R+j\omega L.$$

Thus, if the voltage and current are known at point  $x$ , then the voltage and current at any distance  $x'$  further along the line are determined from (A.1.3-2).

#### A.1.3.3 Multi-Conductor Transmission Lines

The transition matrix for an  $N$  wire (plus ground return) multi-conductor TML can be obtained by replacing  $I$  and  $V$  in (A.1.3-1) with column vectors of  $2N$  elements. For the general multi-conductor TML case the matrix  $[YZ]$  becomes

$$[YZ] = ([G]+j\omega[C])([R_c]+j\omega[L_c]) + ([G]+j\omega[C])(j\omega[L]) \quad (\text{A.1.3-3})$$

The conductance  $[G]$ , capacitance  $[C]$ , inductance  $[L]$ , conductor resistance  $[R_c]$  and conductor internal inductance  $[L_c]$  are now  $2Nx2N$  matrices representing all self and mutual terms. For perfect conductors in a lossless homogeneous medium (A.1.3-3) becomes

$$[YZ] = -\omega^2 [C] ([L_c] + [L])$$

Equation (A.1.3-2) can then be generalized to square matrices and column vectors of order 2N. The diagonalization of the corresponding transition matrix is often of interest in analyzing as well as computing coupling between lines [Paul, August 1973].

#### A.1.3.4 Cross Coupling Within Transmission Line Bundles (TML-DP-FD, TML-DP-FW-FD)

Of major EMC interest regarding TML analysis is the prediction of coupling between transmission lines. In Figure A.1.3-1 a two-wire TML bundle plus ground is indicated. Shown also are termination Thevenin equivalent networks. The relationship between the voltages and currents at some point x in terms of termination voltages and currents is given by [Paul, Feb. 1978 (Vol. EMC-20); Paul, April 1976]

$$\begin{bmatrix} I_g(x) \\ I_r(x) \\ V_g(x) \\ V_r(x) \end{bmatrix} = \Phi(x) \begin{bmatrix} I_{go} \\ I_{ro} \\ V_{go} \\ V_{ro} \end{bmatrix} \quad (A.1.3-4)$$

where  $\Phi(x)$  is the counterpart to that in (A.1.3-2).

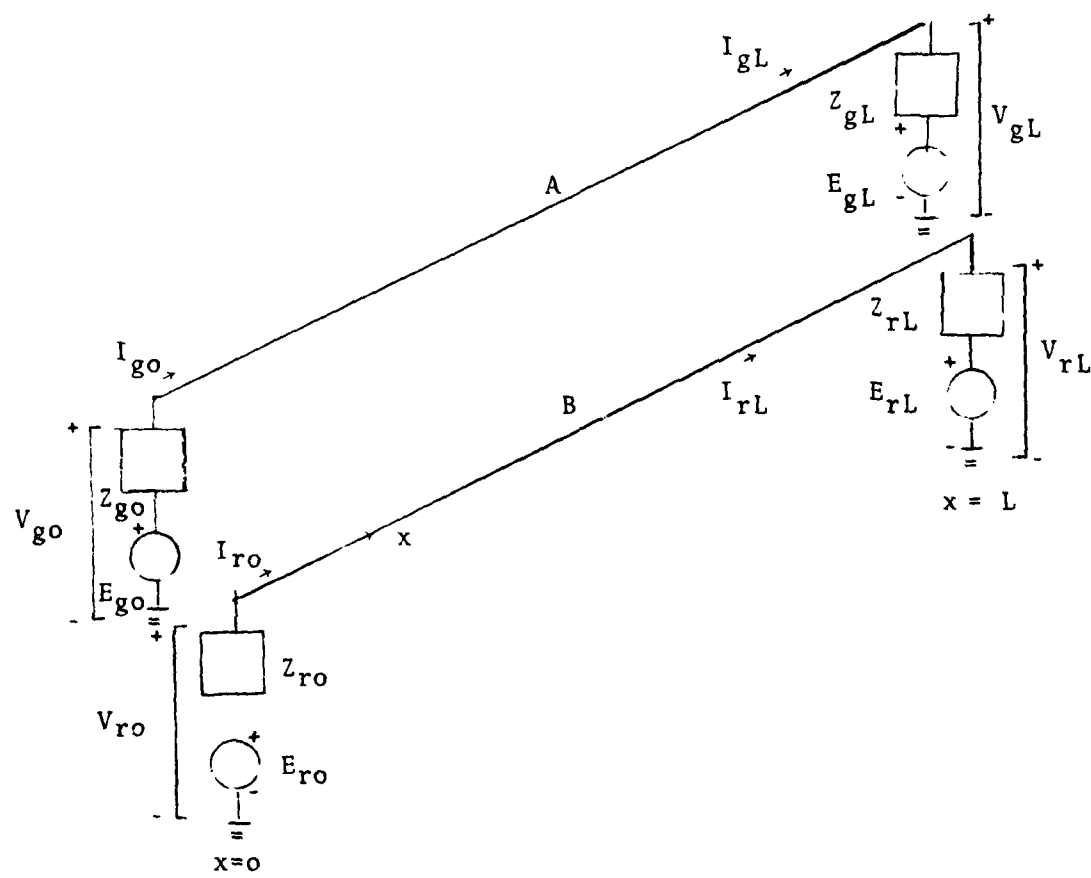


Figure A.1.3-1. Three Conductor TML with Terminations.

When  $x=L$  (A.1.3-4) relates terminal voltages and currents. There is usually only one source connected to a wire. The other Thevenin voltage sources can be set to zero to represent "receptors". It is sometimes useful to rewrite (A.1.3-4) in terms of currents, and Thevenin sources and impedances, i.e., no line voltages [Paul, Feb. 1978 (Vol. EMC-20); Liu, Dec. 1976; Tesche, no date].

If an incident field is present, there will be an additional component of current and voltage induced on the receptor line. This additional component of current can be represented as distributed sources. The effect of the distributed sources at the TML terminations is found by integrating the transition matrix times the induced currents and voltages over the length of the lines [Paul, Feb. 1978 (Vol. EMC-20); Paul, Nov. 1976; Lee, May 1978; Tesche, Sept. 1978; Smith, 1977].

#### A.1.3.5 Lumped Circuit TML (TML-LC-FD)

In the lumped circuit model the TML is subsectioned into  $N$  sections. Each section is  $L/N$  in length and electrically short. A transition matrix is calculated for each section. The relationship between the voltages and currents at each end of the TML is the cascaded circuits represented by the product of all  $N$  transition matrices  $\Phi_k$ , where  $k = 1, 2, \dots, N$ . If the TML itself is electrically short then one section can be used to represent the entire line.

The typical lumped-circuit TML models are lumped T, lumped  $\Gamma$ , lumped Pi, and lumped Tee, so named because of their associated equivalent circuit configurations [Paul, April 1976 (pages 71-74)]. For the two-wire case

$$\begin{bmatrix} I(kL/N) \\ V(kL/N) \end{bmatrix} = \Phi_k \begin{bmatrix} I((k-1)L/N) \\ V((k-1)L/N) \end{bmatrix} \quad (\text{A.1.3-5})$$

If  $I_s(x)$  and  $V_s(x)$  are the TML current and voltage excited by an incident field then their "lumped circuit" counterparts are, with  $\Phi$  as in (A.1.3-2),

$$\begin{bmatrix} I_s(kL/N) \\ V_s(kL/N) \end{bmatrix} = \int_{(k-1)L/N}^{kL/N} \begin{bmatrix} I_s(x') \\ V_s(x') \end{bmatrix} dx' \quad (A.1.3-6)$$

For very short sections  $\phi((kL/N)-x')$  is approximately constant over each section and thus removable from the integration. The total current and voltage at the end of the kth subsection are the sum of (A.1.3-5) and (A.1.3-6). The current and voltage at the end of the TML can be obtained by a recursive algorithm which uses as an input to subsection k+1 the output at the end of subsection k.

#### A.1.3.6 Weak Coupling TML (TML-WC-FD, TML-WC-FW-FD)

The TML weak coupling model involves an additional approximation to the above lumped circuit model. The weak coupling model assumes that the inductive and capacitive coupling exist independently of each other. If the TML is extremely short electrically, 1/20 of a wavelength or less, this assumption will usually bound the magnitude of coupling. This model also assumes that the receptor TML wire has no effect upon the voltage and current in the generator TML wire. The model is a lumped circuit model with all the self inductance  $L_m$  and capacitance  $C_m$  terms removed. For two wires above a ground plane (Figure A.1.3-1) the "cross talk" coupled current is given by [Paul, Feb. 1978 (RADC TR); Paul, ("A Summary of Models in IEMCAP")].

$$I_{rL} = \left( \left| \frac{j\omega L_m L}{Z_{rL} + Z_{ro}} \right| + \left| \frac{j\omega C_m LZ_{go} Z_{ro}}{Z_{rL} + Z_{ro}} \right| \right) I_{go} \quad (A.1.3-7)$$

The accuracy of this model increases when either the capacitive or inductive coupling predominates. If the capacitive and inductive coupling are of the same magnitude, this model tends to overpredict by a factor of 2. However, this model can be in great error even for very short lines ( $L \approx 0.01\lambda$  or less) if there are mismatches in termination impedances.

#### A.1.3.7 Transmission Line Per-Unit-Length Parameters

The accuracies of the different TML models are greatly affected by the accuracy to which values of the per-unit-length parameters (i.e., per unit length of TML capacitance, inductance, media conductance, and individual wire resistances) are known. The assumption of only the TEM mode of propagation reduces the problem of calculating the per-unit-length parameters to 2-dimensional static analyses.

A closed form solution for capacitance and inductance exists for two perfect conductors in an infinite homogeneous medium. The derivation of the per-unit-length capacitance for two identical wires is [Magnusson, 1970; Paris, 1969]

$$C = \pi\epsilon / \text{Cosh}^{-1}(b/2a) \quad (\text{A.1.3-8})$$

where  $b$  is the wire separation and  $a$  is the wire radius.

If the wires have different radii ( $a_1, a_2$ ) the per-unit-length capacitance is [Clements, March 1974]

$$C = 2\pi\epsilon / \text{Cosh}^{-1}((b^2 - a_1^2 - a_2^2)/(2a_1a_2)) \quad (\text{A.1.3-9})$$

With  $C$  known, the per-unit-length inductance and per-unit-length medium conductance can be obtained from  $LC=\mu\epsilon$  and  $LG=\mu\sigma$  [Paul, April 1976].

If the number of wires in the TML exceeds 2 and they are closely spaced, there exists no closed form solution for the per-unit-length parameters. Moment method techniques (Section A.1.1.3) can then be used to calculate the per-unit-length capacitance [Clements, March 1974; Paul, Nov. 1976]. The level of difficulty in applying a moment method here depends upon the spacing of the wires and the presence of shields or dielectric coatings [Paul, April 1976; Paul, Nov. 1976; Liu, Sept. 1977].

A.2

Time Domain

A.2.1

Radiation and Scattering

A.2.1.1

Singularity Expansion Method (SEM)

The Singularity Expansion Method (SEM) [Baum, 1976] deals with the Laplace transform or complex frequency representation of electromagnetic systems. Thus, it is restricted to linear media. Through SEM the transient behavior of antennas and scatterers can be essentially characterized by relatively few numbers, called natural frequencies, which are independent of excitation. This trait facilitates designing antennas or scatterers through modification of shape or loading. Also, for transient analysis SEM appears faster than conventional Fourier transform techniques. For example, only about 3 or 4 natural frequencies (poles) are needed to describe the "late" time behavior of currents on a dipole of length L excited by a step plane wave which grazes the dipole axis. For broadside incidence, even fewer poles are needed. Late time refers to the time  $t$  for which  $ct/L \geq 3$  where  $c = \text{speed of light}$ .

At present the SEM model has been developed only for specialized shapes such as the straight wire [Tesche, January 1973], crossed wires [Crow, July 1975], crossed wires over a ground plane [Crow, March 1979], bodies of revolution ( $n = 0$  mode only) [Marin, March 1974], and loops [Wilton, April 1979].

The locations of the natural frequencies in the complex plane are determined much in the same manner as in classical circuit theory. For example beginning with the moment method formulation for thin wires (A.1.1-7)  $j\omega$  is replaced with the complex frequency  $s$  resulting in [Tesche, January 1973]

$$[Z(s)] \vec{I}(s) = \vec{V}(s) \quad (A.2.1-1)$$

The natural frequencies  $s_a$  are those satisfying  $[Z(s)] \vec{I}(s) = 0$  for nontrivial  $\vec{I}$ , or, equivalently, determinant of  $[Z(s)] = 0$ . From the latter condition they can be determined by an iterative method similar to Newton-Raphson [Tesche, January 1973]. Residue matrices corresponding to the poles can then be computed, either numerically [Tesche, January 1973] or via relationships between poles and their residues [Wilton, April 1979]. Analytic function theory can also be used to expedite pole computation [Crow, March 1979]. These residue matrices and natural frequencies provide an expression for the time-domain wire current in terms of damped sinusoids.

An efficient method for determining poles from a short segment of time response obtained, perhaps, from experimental data is Prony's method [Poggio, January 1978; Brittingham, April 1976]. Knowledge of dominant poles alone is often useful in designing potential scatterer configurations such as cable routing, "box" locations, conduit bending, and even aircraft fuselage shape in order to suppress EMI.

#### A.2.1.2 Time-Marching: Finite Difference (FE-TD)

The model FE-TD is a finite difference solution to Maxwell's equations as is FE-BOR-FD (Section A.1.1.5) but in the time domain. Also FE-TD is not limited to special shapes such as BORs. Since the time dependence is solved via time marching (successive initial value problems) FE-TD is applicable to the most general type of media -- anisotropic, non-linear, inhomogeneous, etc.

An example of this model based on the cubic-cell lattice work of Yee [Yee, May 1966] has been coded and successfully applied to steady state problems [Taflove, August 1975; Taflove, June 1978]. This model incorporates a far-field simulator (approximate) lattice truncation condition and a surface condition for simulating a plane wave excitation. Both modifications reduce the lattice size originally required by Yee's method. However, for typical EMC problems the lattice size still required results in computer storage excessive for all but the largest computers such as the CDC STAR system. Also the large number of time intervals required to arrive at a steady state solution is not tractable by all but the fastest computers (e.g., CDC Star System). A means for combining FE-TD with "exterior" methods in order to alleviate these difficulties is currently under investigation under contract with RADC.

A.2.1.3      Time-Marching: Current Expansion (TW-TD, SPE-TD, SPH-TD)

The models TW-TD, SPE-TD, and SPH-TD in Table 7.2-1 are time-marching as is FE-TD. However, conductor currents are the unknowns rather than fields. Thus, considerably larger problems can be handled than with FE-TD, but the radiating media cannot be nearly as complex. The details of these models are available in [Bennett, September 1977; Bennett, July 1974; Miller, September 1972; Landt, May 1974].

A.2.2      Transmission Line (TML-DP-TD)

Solutions to the time domain transmission line equations

$$\frac{\partial \vec{V}(x, t)}{\partial x} = -[L] \frac{\partial \vec{I}(x, t)}{\partial t}$$

$$\frac{\partial \vec{I}(x, t)}{\partial x} = -[C] \frac{\partial \vec{V}(x, t)}{\partial t}$$

for an  $n+1$  wire line are available [Marx, July 1973] where  $[L]$  and  $[C]$  are  $n \times n$  inductance and capacitance (per unit length) matrices and  $\mathbf{V}(x, t)$  and  $\mathbf{I}(x, t)$  are  $n$  dimensional column vectors of line voltage and current. The  $[L]$  and  $[C]$ matrices can be obtained as for the frequency domain model [Paul, November, 1976] or by time domain reflectivity measurements [Carey, September 1969; Agrawal, February 1979].

## APPENDIX B

### Combined Coupling Models

Combined coupling models are discussed here. Of course, there are many conceivable ways of combining basic coupling models, such as those discussed in Appendix A, but it was not possible to consider them all in this limited effort. Thus only those combined models summarized in Table 7.2-2 are dealt with here. These models have been chosen because (a) they are deemed of particular interest to an IAP designer, and (b) they are either already available in some form of computer code or expected to be shortly.

#### B.1 Low to Medium Frequency Radiation and Scattering

##### B.1.1 Thin Wires and Surfaces-Frequency Domain (TW-FD/SPH-FD, TW-FD/SPE-FD, TW-FD/BOR-FD)

Scattering and radiation from conducting surfaces with nearby or attached wires can be analyzed with moment methods by simply choosing as expansion functions the combined set  $N$  of wire segment functions (Section A.1.1.1) and surface patch functions (Section A.1.1.2). Also  $N$  equations are obtained by requiring that the surface and wire boundary conditions at each surface patch and wire segment be satisfied. The resulting matrix equation can be "partitioned" to identify submatrices identical to the thin wire matrices and the surface patch matrices. In addition 1) "interaction" matrices appear which involve computing the surface fields due to wire expansion functions and vice versa, and 2) "junction" matrices may need be computed. The latter arise from the need to satisfy continuity of current at a surface-to-wire junction. This may require a third type of expansion function.

The combined model TW-FD/SPH-FD employs the MFIE (A.1.1-29) for surfaces and the thin-wire equation (A.1.1-4) or (A.1.1-6 for wires. The applicabilities and limitations of each were discussed in their respective sections. This combined model employs a moment derived matrix equation that, for  $N_s$  surface expansion functions and

$N_w$  wire expansion functions, may be expressed as

$$\begin{bmatrix} [Z] & [ZB] \\ [BZ] & [B] \end{bmatrix} \begin{bmatrix} \vec{I} \\ \vec{J} \end{bmatrix} = \begin{bmatrix} \vec{V} \\ \vec{H} \end{bmatrix} \quad (B.1.1-1)$$

where the  $N_w \times N_w$   $[Z]$  and  $N_w \times 1$  column vectors  $\vec{I}$  and  $\vec{V}$  are the same as in (A.1.1-7) and the  $N_s \times N_s$   $[B]$  and  $N_s \times 1$  column vectors  $\vec{J}$  and  $\vec{H}$  are as given in (A.1.1-31). The elements of the surface-wire  $N_w \times N_s$  interaction matrix  $[ZB]$  are determined by computing the symmetric product (Section A.1.1.1.3) of a surface patch expansion function field with a wire testing function. Similarly, the elements of the  $N_s \times N_w$  wire-surface interaction matrix  $[BZ]$  are determined by computing the symmetric product of a wire expansion function field with a surface patch testing function. In the AMP and NEC codes [AMP, July 1972; Burke, July 1977] a TW-FD/SPH-FD model is implemented with pulse-like expansion functions and impulse weighting (testing) used in treating surfaces. A forerunner to these codes [Albertsen, Sept. 1973] has been extensively applied to satellite antenna analysis. A typical satellite model is depicted in Figure B.1.1-1. The main body was subdivided into quadrilateral surface patches and the wire antenna into pulse segments. The conducting solar panel was wire grid modeled since, as pointed out in Section A.1.1.2, open surfaces cannot be treated with the MFIE. For the dimensions indicated in Figure B.1.1-1 and a frequency of 609.0 MHz the model was divided into  $N_p = 60$  ( $N_s = 2N_p$ ) surface patches and  $N_w = 75$  wire segments. All wire radii were  $10^{-3}$  m. With the solar panel absent ~3dB agreement in radiation patterns resulted in comparison with an idealized experimental model. This agreement tended to worsen with inclusion of the panel. The execution time equated to 5 to 10 minutes on a Honeywell 6000 system for a single radiation pattern of 72 points. The dimensioning of the code

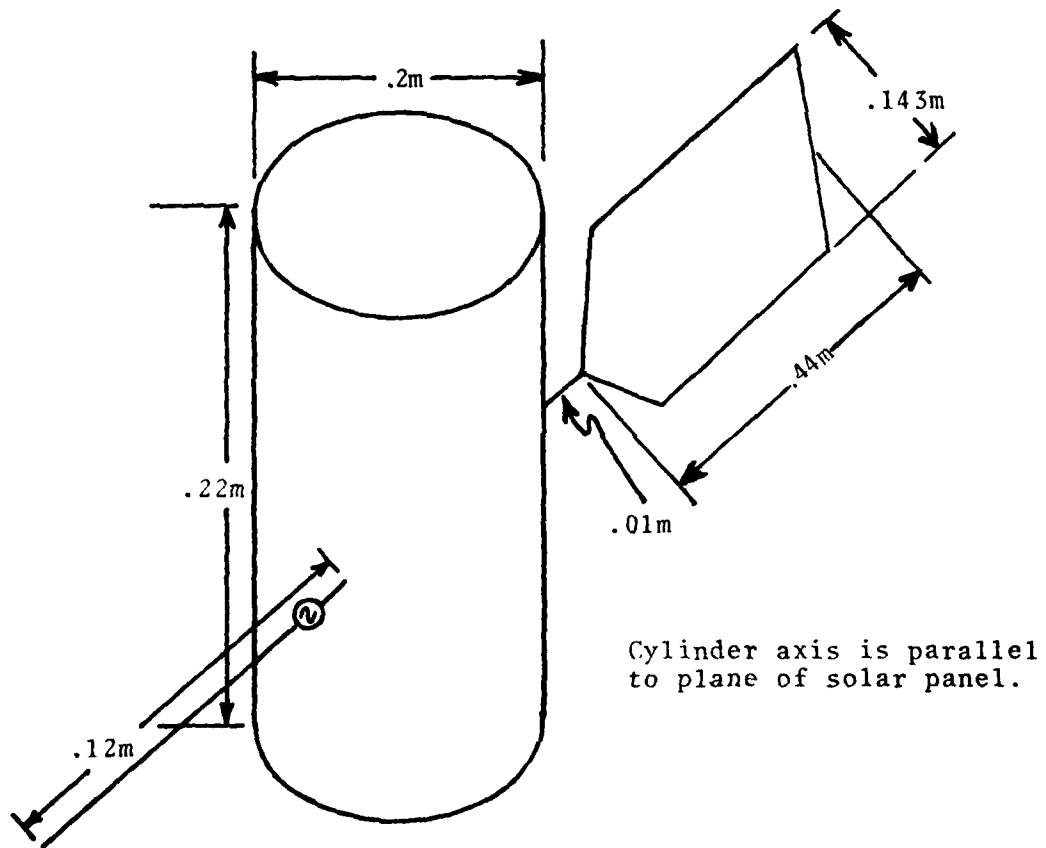


Figure B.1.1-1. Satellite Model with a Circular Cylinder Main Body, a Wire Antenna Monopole, and a Conducting "Solar" Panel.

(when used separately and not as a part of AMP or NEC) for  $N_p = 78$  and  $N_w = 85$  required ~120K computer words. Agreement with measurements on a real-world model (not idealized) was 5 to 10 dB or worse. Large radiation pattern effects could be predicted such as approximate pattern maxima and minima but not absolute levels [Albertsen, Sept. 1973].

A subsectional basis moment method treatment of the electric field integral equation EFIE (A.1.1-30) combined with the thin-wire equation (A.1.1-4) or (A.1.1-6) results in the combined model TW-FD/SPE-FD. Characteristics of TW-FD and SPE-FD applied separately were discussed in Section A.1.1.2. A TW-FD/SPE-FD model with piecewise sinusoidal expansion functions on rectangular patches (A.1.1-32) for surfaces and on one-dimensional subsections (A.1.1-14) for wires has been developed [Newman, Nov. 1978]. The resulting matrix equation in partitioned form is

$$\begin{bmatrix} [Z] & [ZS] & [ZA] \\ [SZ] & [Z^S] & [SA] \\ [AZ] & [AS] & [Z^A] \end{bmatrix} \begin{bmatrix} \vec{i} \\ \vec{j} \\ \vec{J}_A \end{bmatrix} = \begin{bmatrix} \vec{V} \\ \vec{V}^S \\ \vec{V}^A \end{bmatrix} \quad (B.1.1-2)$$

where  $[Z]$ ,  $\vec{i}$ , and  $\vec{V}$  are as defined for (A.1.1-7) and  $[Z^S]$ ,  $\vec{j}$ , and  $\vec{V}^S$  are as defined for (A.1.1-33). The wire-to-surface and vice versa interactions are contained in  $[SZ]$  and  $[ZS]$ . The remaining matrices arise from the need for a special expansion function at each wire-to-surface junction. This is to insure continuity of current and the expected behavior of surface current flow away from the junction ( $\frac{1}{\rho}$  where  $\rho$  is the distance to the junction along the surface). Agreement with experiment was within 2 dB for input impedances of (a) monopoles over a square ground plane with and without parasitic elements and also with and without an additional reflecting plate and (b) a T-bar fed, rectangular, cavity-backed slot antenna. Approximately ten

times smaller CPU times over a wire gridded method were observed with approximately ten times fewer unknowns and appreciably better accuracy [Newman, Nov. 1978]. A significant limitation is the inability to efficiently fit rectangular patches to many curved surfaces and surfaces with curved edges.

Another useful conducting body model is formed by combining the BOR model BOR-FD (Section A.1.1.3) with the thin wire model TW-FD (Section A.1.1.1). The resulting combined model TW-FD/BOR-FD is applicable to radiation and scattering from arbitrarily oriented wires in the vicinity of conducting bodies of revolution. If the BOR model is based on the EFIE then the BOR, as well as the wires, may be impedance loaded. Also the BOR may then have edges as in aperture coupling problems.

Generally, wires in the vicinity of a BOR destroy the rotational symmetry upon which the desirable BOR modal decoupling is based. However, the small-matrix computational advantages of BOR techniques are still applicable through the concept of "computational Green's functions." In this case a generalized impedance matrix  $[Z_w]$  for the wires, which accounts for the presence of the BOR, is found by exciting the BOR with each wire expansion function and observing the scattered field along the wire surfaces. This can be accomplished with a conventional BOR code. With  $[Z_w]$  known, the wire currents due to an applied excitation can be determined by simply inverting  $[Z_w]$ . Then the BOR can be excited mode by mode, and all electromagnetic quantities can be obtained from the resulting currents. This method can also be described in terms of matrix partitioning [Mautz, Jan. 1974].

A TW-FD/BOR-FD code has been developed [Medgyesi-Mitschang, July 1976] based on piecewise linear (overlapping triangles) expansion functions for the thin wires and piecewise linear variation along the generating curve for the BOR expansion functions. Good pattern agreement with experiment for radiation from loop antennas on helicopters taking, in particular,

rotor blades into account was observed. This code has since been improved to better model the junctions of wires connected to BORs [Schaeffer, June 1979]. Good radiation pattern agreement with experiment for "cone-spheres", spheres, and cylinders with attached dipole and loop scatterers resulted.

B.1.2 Material Bodies-Frequency Domain  
(UM-BOR-FD, BOR-FD/ESC-BOR-FD, TW-FD/VC-FD)

Combined coupling models for analyzing radiation and scattering from penetrable (dielectric, permeable, finitely conductive, etc.) bodies, including partially perfectly conducting and partially penetrable bodies, are discussed here. Applications include partially composite aircraft, dielectric radomes, ferrites, missile plumes, etc.

The model UM-BOR-FD is the unimoment method [Mei, Nov. 1974] applied to rotationally symmetric bodies. As brought out in Section 7.1 this model is, in essence, a combined model. It divides the media into essentially two regions: an interior region containing the multiple inhomogeneous material bodies and an exterior region containing only free (or homogeneous) space. The internal "problem" is modeled via a finite element technique such as FE-BOR-FD (Section A.1.1.5) and the external "problem" via infinite space radiating modes. In the unimoment method the region-dividing surface is always chosen to be spherical so that the radiating modes become the well-known spherical harmonics. However, the close relationship between this method and the generalized network formulation for apertures [Harrington, Nov. 1976], as mentioned in Section 7.1, suggests that spherical surfaces may not be necessary. Thus structures that do not well fit a spherical region may be more efficiently analyzed by suitable modification of the unimoment method [Schuman, August 1978].

In the unimoment method interior and exterior techniques are effectively combined by solving the interior problem N times so that N linear independent solutions are generated. The linear combination of these solutions which best satisfies the continuity conditions at the spherical interface is then determined by solving a matrix equation of order proportional to N.

In the model UM-BOR-FD [Morgan, March 1979] a body of revolution BOR of inhomogeneity with, perhaps, a homogeneous spherical core of radius  $r_1$  is enclosed in a sphere of radius  $r_2$ . Spherical modes are used to expand the fields in regions  $r > r_2$  and  $r < r_1$ . Then the finite element coupled azimuthal potential (CAP) formulation (Section A.1.1.5) is solved such that the tangential components of E- and H-fields are continuous across the  $r = r_1$  and  $r = r_2$  interfaces. This is accomplished by solving the CAP formulation for specified boundary conditions (at  $r = r_1$  and  $r = r_2$ ) for each spherical mode in the  $r < r_1$  region expansion and  $r > r_2$  region expansion. A highly solvable banded sparse matrix results for each case. The coefficients of the scattered field modes are then obtained by specifying continuous fields across  $r = r_1$  and  $r = r_2$  by a least squares fit.

A computer code for UM-BOR-FD is available [Morgan, March 1979]. For a number of penetrable spheres, cylinder cones, and composite shapes, with and without hollow cores, about 5 dB agreement in scattering pattern comparison with experiment was achieved. Typical encompassing radii were  $\sim 2.5\lambda_0$  (free space wavelengths) and CPU run time  $\sim 20$  minutes on a CDC 7600 for computing scattering patterns from ten incident fields.

Since boundary conditions are inherent in the finite-element formulation, a single mesh is often adequate for many problems. A user then need only change the media electrical parameters ( $\epsilon$  and  $\mu$ ) at mesh points in solving different problems. This code is thus fairly user-oriented. However, thin conductors, wires, etc., currently present problems [Tesche, March 1979].

The CPU time and memory constraints can be approximated for the UM-BOR-FD base which employs a Riccati transformation in solving the interior problem. Consider a lattice between  $r_1$  and  $r_2$  composed of  $M$  colatitudes and  $\sim K$  nodes (mesh points) per colatitude. Also for within  $\sim 5$  dB accuracy in field assume  $N$  BOR modes, mesh density  $\delta = 116 \text{ elements}/\lambda_i^2 (= 116 |\epsilon_r \mu_r|/\lambda_0^2)$ , and  $2r_2 = D$  where  $\lambda_i$  = average media wavelength, and  $\epsilon_r$ ,  $\mu_r$  are the corresponding relative permittivity and permeability. Then for large  $N$  the CPU time  $\tau$  is limited by the matrix inversions. Thus for a Honeywell 6000 system

$$\tau = 10^{-4} (M(2K)^3 + N(2N')^3)$$

where  $N' = 2\sqrt{2\epsilon_r \mu_r} N$  [Morgan, March 1979]. In this equation, the  $2K$  reflects the need to consider both electric and magnetic CAP modes, and  $2N'$  reflects the need to consider both  $\phi$  and  $\psi$  components of spherical waves. For  $N = \pi D$ ,  $M = \pi K$ , and the total number of nodes on a  $\phi = \text{constant}$  half cross section =  $2\pi D^2 \delta$ , it follows that

$$r = D^4 (2.1|\epsilon_r \mu_r|^2 + 1.75|\epsilon_r \mu_r|^{3/2})$$

The required matrix storage in real computer words (one complex word = two real words) is

$$\begin{aligned} \text{Matrix storage} &= 2(2K)^2 + (2N')^2 \\ &= 500D^2|\epsilon_r \mu_r| \end{aligned}$$

Another combined model for rotationally symmetric inhomogeneous body problems is BOR-FD/ESC-BOR-FD. The conducting BOR model BOR-FD is described in Section A.1.1.3 and the equivalent surface current BOR model ESC-BOR-FD in Section A.1.1.5. The latter model treats inhomogeneous penetrable bodies as layers of homogeneous media. This combined model has been successfully applied to missile plume problems [Wilton, April 1979] and a report is forthcoming.

A third combined model for inhomogeneous media is formed from the thin wire model TW-FD (Section A.1.1.1) and the volume current model VC-FD (Section A.1.1.6). The applicabilities and limitations of these models have already been discussed in their respective sections. The combined model TW-FD/VC-FD [Newman, July 1978] is applicable to lossy and loaded thin-wire antennas and scatterers in the presence of isotropic, inhomogeneous, and lossy dielectrics/ferrites. As with VC-FD it is limited to electrically small inhomogeneous bodies. Specific applications include ferrite loaded loops, manpack transceiver antennas, and radome covered antennas.

## B.2 High Frequency

### B.2.1 Curved Surfaces with Edges (GO/GTD)

Currently available high frequency computer codes of wide applicability are based on ray theory (Section A.1.2.2.1) and generally combine geometrical optics GO (Section A.1.2.2) with the geometrical theory of diffraction GTD (Section A.1.2.3) [Marhefka, March 1978; Back, September 1975]. They are usually restricted to problems involving conducting scatterers which are typically prevalent when analyzing aircraft and satellite based systems as well as many others. With GO, incident and reflected rays are computed. This accounts for reflections from curved surface scatterers, as well as direct transmissions, in arriving at the "coupling" between emitters and field points of interest, such as receptor locations. With GTD, diffraction from scatterer edges and diffraction around smooth convex scatterer surfaces are included in this coupling. The combined model is denoted GO/GTD.

Rarely is a computer code written for GTD that does not also include GO. This is because the dominant terms comprising the total field are usually the direct and reflected rays - a result of their attenuating less rapidly with ray path distance than do the diffracted rays. In shadow regions, however, the direct and reflected rays are absent. Thus field levels are typically low in shadow regions.

A principal difficulty with applying GO/GTD to complicated geometries formed by a number of edges and surfaces in relatively close proximity is in determining which of the higher order (multiple) diffractions and reflections need be considered in arriving at the total field. For example, diffracted rays may become incident rays on surfaces (edge-surface reflection), diffracted rays may become incident rays on other edges (edge-edge diffraction), and so on. Long computer processing times may be required in accounting for all significant rays, especially if the edges are other than straight and/or the surfaces other than flat or simply curved (cylindrical, spherical, etc.). For arbitrarily shaped edges and/or surfaces a determination of diffraction and/or reflection points via Fermat's Principle (Sections A.1.2.2, A.1.2.3.1) usually requires a time-consuming search procedure.

The absence of significant higher order reflections and/or diffractions in an analysis usually shows up as discontinuities in radiation pattern in the vicinity of affected shadow or reflection boundaries (Section A.1.2.2.1). Although the solution is not accurate near these discontinuities (a neighborhood of a few degrees or so) the fields outside these regions often remain accurate [Marhefka, May 1978].

For typical engineering accuracy with GTD, exciting antennas should be at least a quarter wavelength from any edges or curved surfaces [Marhefka, March 1978].

### B.2.2 Combined GTD Moment Methods (GTD/MOM)

An accurate antenna analysis cannot ignore nearby electrically large conducting bodies. For example, a monopole antenna on a satellite formed by a patch work of flat conducting plates will exhibit impedance as well as gain dependence on diffraction from the interconnecting edges of the plates. However, a moment method (Section A.1.1.1.3) representation of the entire satellite is likely to result in a forbiddingly large generalized impedance matrix [Z] at, e.g., microwave frequencies. Thus a technique which combines a moment method treatment of the antenna with a ray theory (GO/GTD model) treatment of the neighboring scatterers is of interest. This has been shown feasible [Thiele, January 1975]. Such a model is denoted here as GTD/MOM. Although the following discussion is in terms of wire type antennas, it can be straightforwardly recast, via moment methods, in terms of antennas of arbitrary structure.

In the application of GTD/MOM to wire type antennas, only the wire current  $I$  is expanded in typical moment method fashion as expressed by (A.1.1-8). However, the resulting matrix equation (A.1.1-7), which is usually solved for the current expansion coefficients  $I_n$ , is modified to reflect scattering from nearby surfaces and edges. This is done by modifying the operator  $L$  in (A.1.1-2) such that  $L$  now represents not only the tangential component along the antenna surface of free-space field radiated by  $I$  but also the reflected and/or diffracted fields from the scattering surfaces as well. With  $I$  expanded by (A.1.1-8) the reflected and/or diffracted fields are determined by application of GO/GTD. In general, each  $I_n$  will "excite" a different set of reflected and/or diffracted rays. These rays, in addition to the free-space field radiated by each  $I_n$ , result in the total field radiated by each  $I_n$ . In accordance with (A.1.1-1) and appropriate expansion and testing functions (Section A.1.1.1.3), the resulting matrix equation replacing (A.1.1-7) that need be solved is

$$([Z] + [Z^G]) \vec{I} = \vec{V} \quad (\text{B.2.2-1})$$

where the elements of  $[Z^G]$  are the diffracted and/or reflected ray contributions between expansion and testing function segments for  $I$ . In (B.2.2-1)  $[Z]$ ,  $\vec{I}$ , and  $\vec{V}$  are the same as in (A.1.1-7).

Note that the order of the matrix equation (B.2.2-1) is no greater than the number of antenna current expansion functions even though scattering from electrically large nearby structures (finite ground planes, curved aircraft fuselages, aircraft wings, satellite solar panels, etc.) are largely accounted for. Thus with GTD/MOM an electrically very large problem can be accurately solved via solution to a reasonably sized matrix equation.

Once (B.2.2-1) is solved and  $I$  is determined, near and far radiated fields can be obtained by straightforward application of GO/GTD.

This method has treated a number of problems [Thiele, January 1975]. Results for monopoles at the centers of four-sided, eight-sided, and circular flat plates all compared favorably with experiment. Also computed were the impedances of a monopole near a conducting wedge and near a conducting step for various step heights.

### B.3 Time Domain (TW-TD/SPH-TD, SPE-TD/SPH-TD, TDA)

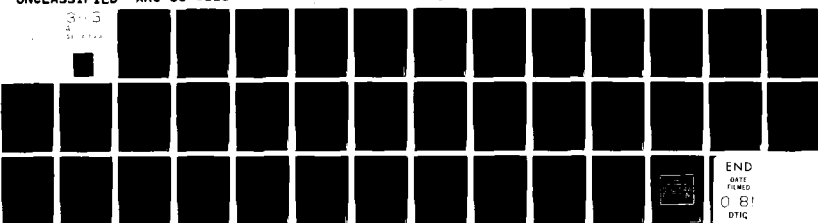
The combined models TW-TD/SPH-TD, SPE-TD/SPH-TD and TDA all employ time-marching with conducting wire or surface currents as unknowns. The time-domain augmentation technique TDA, in addition, includes high frequency diffraction theory to significantly extend the applicable frequency range without prohibitive computer effort. Pertinent references include [Miller, September 1972; Bennett, June 1970].

AD-A103 899

ATLANTIC RESEARCH CORP ALEXANDRIA VA  
INTRASYSTEM ANALYSIS PROGRAM (IAP) STRUCTURAL DESIGN STUDY (U)  
JUN 81 W G DUFF, L D THOMPSON, H K SCHUMAN F30602-77-C-0150  
UNCLASSIFIED ARC-53-6111 RADC-TR-81-133 NL

F/G 20/3

3-5  
2  
MAY 1981



END  
DATE  
FILED  
0 81  
DTIC

## B.4

Branched Transmission Line (TML-FD/N, TML-WC-FD/S)

Present models for analyzing multiple transmission line cables which interconnect at junction "networks" (TML-FD/N) are of the admittance parameter type [Paul, October 1979] or of the scattering parameter type [Liu, September 1977; Baum, November 1978; Tesche, no date]. The former generally requires fewer simultaneous equations to solve. However, since admittance parameters for certain degenerate situations (e.g., half wavelength shorted cable) do not exist, a general purpose computer code may need to be constructed in a manner that recognizes and solves these degenerate situations separately. This is not necessary for the scattering parameter model.

A weak coupling model (Section A.1.3.6), useful for electrically very short lines, that is extended to account for a lossy ground return of a transmission line bundle, is currently an IEMCAP model (TML-WC-FD/S) [Paul, no date].

## APPENDIX C

### SYSTEMS EQUATIONS - DERIVATIONS

Derivations of the systems equations discussed in Section 4 are given here.

#### C.1 Waveform Systems Equations

The waveform systems equations appearing in Table 4.1-1 are derived below. First considered are those corresponding to aperiodic emissions. These are followed by the periodic emission cases. An aperiodic waveform is assumed to have a continuous frequency spectrum whereas the periodic waveform spectrum is assumed discrete. Terms appearing in the derivations are listed in Section 4.1 for reference. In all cases, linear processes and deterministic waveforms are assumed.

##### C.1.1 Continuous Spectrum

Convolution, sometimes appropriately referred to as the "superposition integral", relates the input and output time domain quantities of a linear process. Thus

$$v_o(t) = \int_{-\infty}^{\infty} v_i(\tau)h(t-\tau)d\tau \quad (\text{time invariant}) \quad (\text{C.1-1})$$

$$v_o(t) = \int_{-\infty}^{\infty} v_i(\tau)h_g(t-\tau, t)d\tau \quad (\text{general time variant}) \quad (\text{C.1-2})$$

$$v_o(t) = \int_{-\infty}^{\infty} a(t)v_i(\tau)h(t-\tau)d\tau \quad (\text{time and frequency separable}) \quad (\text{C.1-3})$$

where  $v_i(t)$  and  $v_o(t)$  are the time dependent emission and response respectively,  $h(t)$  is the time-invariant process impulse response,  $h_g(y, t)$  is the general time variant process response, measured at time  $t$ , to a unit impulse applied at time  $t-y$ , and  $a(t)h(t-\tau)$  is the frequency separable process response, measured at time  $t$ , to a unit impulse applied at time  $\tau$ .

In the frequency domain it is well known that (C.1-1) becomes, through Fourier transformation as defined by (4.1-1),

$$V_o(f) = H(f) V_i(f) \quad (C.1-4)$$

where  $V_o(f)$ ,  $H(f)$ , and  $V_i(f)$  are the Fourier transforms of  $v_o$ ,  $h$ , and  $v_i$  respectively. It can readily be shown that  $e^{j2\pi ft} H(f)$  is the time domain response of a time invariant process to  $e^{j2\pi ft}$ . Generalizing upon this, a convenient frequency domain representation of (C.1-2) is found by first denoting the response of a general time variant process to  $e^{j2\pi ft}$  by  $e^{j2\pi ft} H_g(f,t)$ . Thus from (C.1-2) after an appropriate change of variable of integration, one gets

$$H_g(f,t) = \frac{\int_{-\infty}^{\infty} h_g(y,t) e^{j2\pi f(t-y)} dy}{e^{j2\pi ft}}$$

$$H_g(f,t) = \int_{-\infty}^{\infty} h_g(y,t) e^{-j2\pi fy} dy \quad (C.1-5)$$

Hence, for fixed  $t$ ,  $h_g(y,t)$  is the inverse Fourier transform of  $H_g(f,t)$ , i.e.,

$$h_g(y,t) = \int_{-\infty}^{\infty} H_g(f,t) e^{j2\pi fy} df$$

After substitution into (C.1-2) and interchange of integrations one gets

$$v_o(t) = \int_{-\infty}^{\infty} \int_{-\infty}^{\infty} v_i(\tau) e^{j2\pi f(t-\tau)} d\tau H_g(f,t) df$$

$$v_o(t) = \int_{-\infty}^{\infty} V_i(f) H_g(f,t) e^{j2\pi ft} df \quad (C.1-6)$$

Since

$$V_o(f) = \int_{-\infty}^{\infty} v_o(t) e^{-j2\pi ft} dt$$

it follows that, in combination with (C.1-6),

$$\begin{aligned} V_o(f) &= \int_{-\infty}^{\infty} V_i(f') \int_{-\infty}^{\infty} H_g(f'; t) e^{-j2\pi(f-f')t} dt df' \\ &= \int_{-\infty}^{\infty} V_i(f') H_{gg}(f'; f-f') df' \end{aligned} \quad (\text{C.1-7})$$

Equation (C.1-7) is the general time variant process frequency domain representation where  $H_{gg}(f', f)$  is, for fixed  $f'$ , the Fourier transform of  $H_g(f', t)$ .

The response  $v_o(t)$  to the time and frequency separable process (C.1-3) is the product of  $a(t)$  and  $b(t)$  where

$$b(t) = \int_{-\infty}^{\infty} v_i(\tau) h(t-\tau) d\tau$$

Since multiplication in the frequency domain is convolution in the time domain and vice versa it follows that the Fourier transform of  $b(t)$  is  $V_i(f)H(f)$  and

$$V_o(f) = A(f) * (V_i(f)H(f)) \quad (\text{C.1-8})$$

where the asterisk indicates convolution. Equation (C.1-8) is the time and frequency separable process frequency domain representation.

### C.1.2 Discrete Spectrum

A periodic emission of period T can be expressed as

$$\text{where } v_i(t) = \frac{1}{T} \sum_{n=-\infty}^{\infty} v_n^i e^{j \frac{2\pi n}{T} t} \quad (\text{C.1-9})$$

$$v_n^i = \int_{-T/2}^{T/2} v_i(t) e^{-j \frac{2\pi n}{T} t} dt$$

Thus, for linear processes

$$v_o(t) = \frac{1}{T} \sum_{n=-\infty}^{\infty} H\left(\frac{n}{T}\right) v_n^i e^{j \frac{2\pi n}{T} t} \quad (\text{time invariant}) \quad (\text{C.1-10})$$

$$v_o(t) = \frac{1}{T} \sum_{n=-\infty}^{\infty} H_g\left(\frac{n}{T}, t\right) v_n^i e^{j \frac{2\pi n}{T} t} \quad (\text{general time variant}) \quad (\text{C.1-11})$$

$$v_o(t) = \frac{a(t)}{T} \sum_{n=-\infty}^{\infty} H\left(\frac{n}{T}\right) v_n^i e^{j \frac{2\pi n}{T} t} \quad (\text{Time and frequency separable}) \quad (\text{C.1-12})$$

Equations (C.1-10) and (C.1-11) follow directly from superposition, (C.1-9), and the definitions of  $H(f)$  and  $H_g(f, t)$  (previous section). Equation (C.1-12) is determined from superposition, (C.1-9), and by noting that the response S of a time and frequency separable process to  $e^{j \frac{2\pi n}{T} t}$  is expressible by

$$S = \int_{-\infty}^{\infty} a(t) h(t-\tau) e^{j \frac{2\pi n}{T} \tau} d\tau$$

$$S = a(t) H\left(\frac{n}{T}\right) e^{j \frac{2\pi n}{T} t}$$

Frequency domain counterparts to (C.1-11) and (C.1-12) are determined by Fourier transforming  $v(t)$ . Since  $H_{gg}\left(\frac{n}{T}, f\right)$  is the Fourier transform of  $H_g\left(\frac{n}{T}, t\right)$  then for the general time variant process

$$v_o(f) = \frac{1}{T} \sum_{n=-\infty}^{\infty} v_n^i \int_{-\infty}^{\infty} H_g\left(\frac{n}{T}, t\right) e^{-j 2\pi (f - \frac{n}{T}) t} dt$$

$$= \frac{1}{T} \sum_{n=-\infty}^{\infty} v_n^i H_{gg}\left(\frac{n}{T}, f - \frac{n}{T}\right) \quad (\text{C.1-13})$$

The time and frequency separable case is determined by transforming (C.1-12) into

$$V_o(f) = \frac{1}{T} \sum_{n=-\infty}^{\infty} H\left(\frac{n}{T}\right) V_n^i (A(f) * \delta(f - \frac{n}{T}))$$

The convolution operation is evaluated as

$$\begin{aligned} A(f) * \delta(f - \frac{n}{T}) &= \int_{-\infty}^{\infty} A(\tau) \delta(f - \frac{n}{T} - \tau) d\tau \\ &= A(f - \frac{n}{T}) \end{aligned}$$

Thus

$$V_o(f) = \frac{1}{T} \sum_{n=-\infty}^{\infty} H\left(\frac{n}{T}\right) V_n^i A(f - \frac{n}{T}) \quad (C.1-14)$$

## C.2 Parameter System Equations

The susceptibility margins tabulated in Table 4.2-1 are derived here. Various terms appearing in the discussion are, for reference, included in the list at the end of Section 4.2. Also the receptor model of Figure 4.2-1 is assumed throughout.

### C.2.1 Average Power - Deterministic Waveform

The average receptor input power (on a 1-ohm basis) is given by

$$P_r = \lim_{T \rightarrow \infty} \frac{1}{T} \int_{-T/2}^{T/2} i_r^2(t) dt \quad (C.2-1)$$

where  $i_r(t)$  is the receptor input waveform. If  $i_r(t)$  is of finite duration then  $P_r = 0$  and a total energy consideration is more appropriate. If  $i_r(t)$  is deterministic and of infinite extent then  $i_r(t)$  is assumed to be periodic with period  $T_0$ . Then the limit in (C.2-1) can be removed if  $T = T_0$ . Since

$$i_r(t) = \sum_{n=-\infty}^{\infty} I_r\left(\frac{n}{T_0}\right) e^{jn\omega_0 t}$$

where

$$I_r(nT_o) = \frac{1}{T_o} \int_{T_o/2}^{T_o/2} i_r(t) e^{-j n \omega_o t} dt$$

and  $\omega_o = 2\pi/T_o$ , it follows that [Hancock, 1961 (pp 16, 17)]

$$P_r = \sum_{n=-\infty}^{\infty} |I_r(n/T_o)|^2 = \int_{-\infty}^{\infty} G_r(f) df$$

where

$$G_r(f) = \sum_{n=-\infty}^{\infty} |I_r(n/T_o)|^2 \delta(f - n/T_o)$$

Thus  $G_r(f)$  is a superposition of impulses when representing the average power of a periodic waveform.

The average power at the detector is given by

$$\begin{aligned} P_d &= \int_{f_a}^{f_b} G_r(f) |B_r(f)|^2 df \\ &= 2 \int_{f_a}^{f_b} G_r(f) |B_r(f)|^2 df \end{aligned} \quad (C.2-2)$$

where  $B_r(f)$  is the receptor input-to-detector linear transfer function and  $f_a$  and  $f_b$  are the lower and upper frequencies defining the common frequency band between  $G_r(f)$  and  $B_r(f)$ .

Note that  $G_r(-f) = G_r(f)$  and  $|B_r(-f)|^2 = |B_r(f)|^2$ .

The detector interference threshold power  $K^P$  (on a 1-ohm basis) is related to a receptor input sinusoidal waveform amplitude  $2|I_r^S(f)|$  by

$$\begin{aligned} K^P &= \frac{1}{2} |B_r(f) 2I_r^S(f)|^2 \\ &= 2|B_r(f)|^2 |I_r^S(f)|^2 \end{aligned} \quad (C.2-3)$$

Now, equations (C.2-2) and (C.2-3) determine the average power susceptibility margin for deterministic waveforms as

$$\frac{P_d}{P} = \int_{f_a}^{f_b} \frac{G_r(f)}{|I_r^s(f)|^2} df$$

This is presently the IEMCAP susceptibility margin if  $G_r(f)$  is replaced by  $|T_{re}(f)|^2 G_e(f)$  where  $T_{re}(f)$  is a linear coupling model between the waveform source and the receptor with an emitter with output power spectral density  $G_e(f)$ .

#### C.2.2 Average Power - Stochastic Waveform

The receptor average power for a stationary stochastic waveform is given by

$$P_r = \int_{-\infty}^{\infty} G_r(f) df$$

where  $G_r(f)$  is the Fourier transform of the autocorrelation of the waveform. Also [Papoulis, 1965, pg. 346]

$$\begin{aligned} P_d &= \int_{-\infty}^{\infty} G_r(f) |B_r(f)|^2 df \\ &= 2 \int_{f_a}^{f_b} G_r(f) |B_r(f)|^2 df \end{aligned} \quad (C.2-4)$$

Thus the average power susceptibility margin for stochastic stationary waveforms is the same as for deterministic waveforms.

#### C.2.3 Total Energy - Deterministic Waveform

The total energy of a periodic waveform is infinite. Thus such a waveform will always cause interference to an energy sensitive receptor. However, in practice this interference cannot occur unless the average power exceeds the average rate of energy dissipation (e.g., heat loss due to environmental cooling). Thus for periodic waveforms appropriate average power susceptibility criteria should be used even for "total energy" sensitive

receptors. The above average power margins are then applicable.

If a waveform is not periodic, it is assumed to have finite energy. Then the total energy at the detector input (on a 1-ohm basis) is given by [Hancock, 1961 (pg. 17)].

$$E_d = \int_{-\infty}^{\infty} |I_d(f)|^2 df$$

where  $I_d(f)$  is the Fourier transform of the detector input waveform  $i_d(t)$ . Note that  $|I_d(f)|^2$  is an energy density function.

Since  $I_d(f) = B_r(f)I_r(f)$  where  $I_r(f)$  is the Fourier transform of the receptor input waveform  $i_r(t)$  then

$$\begin{aligned} E_d &= \int_{-\infty}^{\infty} |B_r(f)|^2 |I_r(f)|^2 df \\ &= 2 \int_{f_a}^{f_b} |B_r(f)|^2 |I_r(f)|^2 df \end{aligned} \quad (C.2-5)$$

The detector interference threshold energy level  $K^E$  can be related to the receptor input energy for a sinusoidal waveform if an appropriate time interval  $\Delta_r$  is defined for the receptor and the discussion regarding (C.2-3) is noted. Thus

$$K^E = 2 \Delta_r |B_r(f)|^2 |I_r^s(f)|^2 \quad (C.2-6)$$

and a total energy susceptibility margin for deterministic, finite energy waveforms becomes

$$\frac{E_d}{K^E} = \frac{1}{\Delta_r} \int_{f_a}^{f_b} \frac{|I_r(f)|^2}{|I_r^s(f)|^2} df$$

Note that the measurable quantities are transferred to the receptor input.

C.2.4      Total Energy - Stochastic Waveform

As with periodic deterministic waveforms, a stationary stochastic waveform is of infinite duration and, hence, has infinite energy. Therefore, an average power susceptibility margin is then appropriate in order to predict whether dissipation (e.g., heat loss due to environmental cooling) exceeds energy buildup. The energy buildup is necessary for interference to occur.

However, certain emitters may be considered sources of "switched" stochastic waveforms in that an otherwise stationary process is turned on and turned off at regular intervals. For example, consider a rotating reflector antenna that is emitting narrowband Gaussian noise within a receptor bandwidth. The total energy at the detector of the receptor can be determined from

$$E_d = \Delta P_d \quad (C.2-7)$$

where  $P_d$  is given by (C.2-4) and  $\Delta$  is the "dwell" time for which the mainbeam of the antenna illuminates the receptor. With  $K^E$  given by (C.2-6) it follows that a total energy susceptibility margin for "switched" stochastic waveforms is

$$\frac{E_d}{K^E} = \frac{\Delta}{\Delta_r} \int_{f_a}^{f_b} \frac{G_r(f)}{|I_r^s(f)|^2} df$$

The use of (C.2-7) for computing stochastic waveform total energy may also provide a "total energy" computation for those periodic deterministic waveforms which are on-off switched at a much slower rate than is inherent in the waveform's bandwidth.

### C.2.5 Peak Current - Deterministic Waveform

Some receptors (e.g., many digital devices) are sensitive to the peak value of a waveform (e.g., voltage or current). An upper bound to this peak can be given in terms of amplitude spectral density frequency domain data [Pearlman, Sept. 1977 (Appendix B)]. This bound can be used to define a conservative estimate of a peak current (or voltage) susceptibility margin for deterministic waveforms in terms of receptor input quantities. Consider the detector current given by

$$i_d(t) = \int_{-\infty}^{\infty} I_r(f) B_r(f) e^{j\omega t} df \quad (C.2-8)$$

Note that  $I_r(f)$  is a superposition of impulses for periodic (infinite-duration) waveforms and a continuous function for finite-energy (finite-duration) waveforms.

Now from (C.2-8) it follows that

$$\begin{aligned} |i_d(t)| &\leq \int_{-\infty}^{\infty} |I_r(f)| |B_r(f)| df \\ |i_d(t)| &\leq 2 \int_{f_a}^{f_b} |I_r(f)| |B_r(f)| df \end{aligned} \quad (C.2-9)$$

Also, the detector interference threshold peak current level  $K$  is given in terms of the amplitude of a CW receptor input phasor  $2I_r^S(f)$  by

$$K = 2 |B_r(f)| |I_r^S(f)|$$

Hence,

$$\frac{|i_d(t)|}{K} \leq \int_{f_a}^{f_b} \frac{|I_r(f)|}{|I_r^S(f)|} df$$

and a peak current susceptibility margin for deterministic waveforms is given by

$$\int_{f_a}^{f_b} \frac{|I_r(f)|}{|I_r^s(f)|} df$$

The problem with this margin is that it may be too conservative and predict interference when, in fact, the peak value of  $|i_d(t)|$  is far less than K. This situation occurs, for example, if  $B(f)$  is off-tune for a pulse-like  $i_r(t)$ . Far-out lobes of  $I_r(f)$  will then be within the passband of  $B(f)$ . The lack of phase information in the right-hand side of (C.2-9) prevents accounting for the adding and subtracting of these lobes. The result is too conservative an upper bound.

#### C.2.6 Peak Current - Stochastic Waveform

The peak of a stochastic waveform cannot be given precisely. Therefore, the peak waveform susceptibility of a receptor must include, along with K, an estimate of the fraction of time that a stochastic waveform peak at the detector input must exceed K in order for interference to occur. This estimate is denoted  $\alpha$ .

Let  $i_r(t)$  be a stationary stochastic process which is adequately described by first and second order statistics (means and autocorrelations). Then the same holds for  $i_d(t)$ . For simplicity also assume  $i_r(t)$  has zero mean. (This is always the case in antenna reception. However, it may not be the case in "direct wire" coupling where a dc component is possible.) Then  $i_d(t)$  also has zero mean. The variance of  $i_d(t)$  is given by [Papoulis 1965 (pp. 346 - 348)].

$$\sigma_d^2 = \int_{-\infty}^{\infty} G_r(f) |B_r(f)|^2 df = 2 \int_0^{\infty} G_r(f) |B_r(f)|^2 df \quad (C.2-10)$$

Now, from Chebyshev's inequality [Papoulis, 1965 (pg. 150)] the probability of  $|i_d(t)|$  exceeding  $K$  is bounded by

$$p(|i_d| > K) < \frac{\sigma_d^2}{K^2}$$

Therefore, an indication that a stochastic waveform is compatible, i.e., does not cause interference, is given by

$$\frac{\sigma_d^2}{\alpha K^2} < 1 \quad (C.2-11)$$

It is desirable to "transfer" the computation of (C.2-11) to the receptor input. The variance of  $i_r$  is given by

$$\sigma_r^2 = \int_{-\infty}^{\infty} G_r(f) df = 2 \int_0^{\infty} G_r(f) df \quad (C.2-12)$$

Hence,

$$\sigma_d^2 < |B_r(f_p)|^2 \sigma_r^2 \quad (C.2-13)$$

where  $f_p$  is the frequency at which  $B_r(f)$  is maximum. Thus

$$\frac{\sigma_d^2}{K^2} < \frac{|B_r(f_p)|^2}{K^2} \sigma_r^2$$

Also

$$2|I_r^s(f_p)| = \frac{K}{|B_r(f_p)|} \quad (C.2-14)$$

From the above two equations it follows that  $\frac{\sigma_r^2}{4|I_r^s(f_p)|^2}$   
is an upper bound to  $\frac{\sigma_d^2}{K^2}$ . Hence, a requirement for compatibility is

$$\frac{\sigma_r^2}{4\alpha|I_r^s(f_p)|^2} < 1$$

and  $\frac{\sigma_r^2}{4\alpha|I_r^s(f_p)|^2}$  is an attractive peak current susceptibility

margin for stationary stochastic processes. Note that  $\sigma_r^2$  is computed from a spectral density as indicated by (C.2-12) which is usually measurable.

Another peak current susceptibility margin applicable to normal, zero-mean, stationary waveforms is given by

$$\frac{\sqrt{2}}{\alpha} \int_K^{\infty} \frac{1}{\sigma_d \sqrt{\pi}} e^{-x^2/(2\sigma_d^2)} dx$$

which, if less than unity, indicates compatibility.

From (C.2-13) it follows that

$$\frac{\sqrt{2}}{\alpha} \int_K^{\infty} \frac{1}{\sigma_d \sqrt{\pi}} e^{-x^2/(2\sigma_d^2)} dx <$$

$$\frac{\sqrt{2}}{\alpha} \int_K^{\infty} \frac{1}{|B_r(f_p)| \sigma_r \sqrt{\pi}} e^{-x^2/(2|B_r(f_p)|^2 \sigma_r^2)} dx$$

Hence, the right-hand side of the above inequality is also a suitable susceptibility margin. After a change of variable of integration and noting (C.2-14) this margin becomes

$$\frac{\sqrt{2}}{\alpha} \int_0^{\infty} \frac{1}{\sigma_r \sqrt{\pi}} e^{-x^2/(2\sigma_r^2)} dx \\ 2 |I_r^s(f_p)|$$

where all quantities are defined at the receptor input as preferred.

A peak current EMI margin applicable to narrowband Gaussian waveforms expressed by

$$i_r(t) = x_r(t) \cos(2\pi f_o t) + y_r(t) \sin(2\pi f_o t)$$

where  $x_r(t)$  and  $y_r(t)$  are stationary, normal, independent zero-mean processes with identical autocorrelations can be derived in a similar manner. The result is (Rayleigh statistics)

$$\frac{1}{\alpha} \int_0^{\infty} \frac{x}{\sigma_r^2} e^{-x^2/(2\sigma_r^2)} dx \\ 2 |I_r^s(f_o)|$$

If a sinusoid of amplitude  $s$  is added to the waveform to form

$$i_r(t) = (x_r(t)+s)\cos(2\pi f_0 t) + y_r(t)\sin(2\pi f_0 t)$$

then the corresponding susceptibility margin becomes (Rician statistics)

$$\frac{1}{\alpha} \int_{-\infty}^{\infty} \frac{x}{\sigma_r} e^{-(x^2+s^2)/(2\sigma_r^2)} J_0(\frac{xs}{\sigma_r}) dx$$
$$2\sqrt{s(f_0)}$$

where  $J_0(x)$  is the modified Bessel function of order zero.

#### C.2.7 Rise Time

A receptor said to be sensitive to the "rise time" of a waveform is also sensitive to the "inverse of rise time" which

can be defined as the peak value of  $\left| \frac{di_d(t)}{dt} \right|$ . Since

$$\left| \frac{di_d(t)}{dt} \right| \leq \int_{f_a}^{f_b} 2\omega |I_r(f)| |B_r(f)| df$$
$$\leq 4\pi f_b \int_{f_a}^{f_b} |I_r(f)| |B_r(f)| df$$

it follows that an upper bound to  $\left| \frac{di_d(t)}{dt} \right|$  is proportional to  $f_b$  or "bandwidth". Thus a bandwidth susceptibility margin for both deterministic and stochastic waveforms is given by

$$\frac{\beta_r}{\beta_r^s}$$

where  $\beta_r$  is the portion of the receptor input waveform bandwidth within the pass band of  $B_r(f)$ , and  $\beta_r^s$  is the receptor input waveform bandwidth which induces the interference threshold bandwidth at the detector.

## APPENDIX D

### SYSTEM LEVEL AND IAP CODES

The IAP structural design presented in this report centers on the concept of a procedure. Many different combinations of systems equations and emitter, receptor, and coupling models can be formed, each serving a different purpose and each relating to a different procedure. A highly flexible structure results whereby either procedures can be easily created on demand or areas in need of development can be readily recognized.

Previously developed "system level codes" are closely related to procedures; several of these codes are introduced here. Other, less encompassing codes, currently supported by the IAP, also are discussed. Characteristics of some of these codes are summarized in Table D-1. Although this table is far from complete, it identifies several important models that underlie these codes.

Table D-1. Summary of EMC Analysis Models to be Considered for IAP

Model	Source	Remarks
<b>System Models</b>		
Linear	IEMCAP	Use for continuous signals and average power receptors.
	SEMCAP	Use for transient signals and threshold devices.
Nonlinear	IPP-1 SEMCA COSAM	These programs use system level models for intermodulation, cross modulation, and desensitization. Required inputs may be obtained from measured data.
<b>Emitter Models (Transmitters)</b>		
Modulation Envelope	IEMCAP	Models are standard ones used in EMC analysis. They are widely accepted and easily implemented with minimum nominal input data and computer main memory.
Noise	SEMCA	Models based on measured data on shipboard transmitters. Should be modified for aerospace transmitters.
Intermodulation, Cross Modulation, & Desensitization	NCAP	May be used for analysis at the circuit and component level to determine equipment EMI characteristics resulting from nonlinearities. Requires detailed input data at the circuit and component level.
Harmonics	IEMCAP	Models based on MIL-STD or user defined. Appropriate for system level analysis and may be implemented with minimum of input data and computer main memory.
	IPP-1	Models based on measured data. Appropriate for system level analysis and may be implemented with minimum input data and computer main memory.
<b>Emitter Models (Signal &amp; Control)</b>		
Required and Nonrequired	IEMCAP SEMCAP	Use power spectral density for continuous signal devices. Use voltage spectra for transients or signals with high peak power.
<b>Coupling Models-Antenna Coupled</b>		
Friis	IEMCAP	Basis for many EMI analyses. Easy to implement.
Intravehicle	IEMCAP	Validated and provides good results. Appropriate detail for system level analysis
Crowded Cosite	SEMCA	Based on shipboard measurements. May be applicable to other crowded cosite situations.

Table D-1. (Continued)

Model	Source	Remarks
Cosite	COSAM	Easily implemented model applicable to certain cosite situations.
Ground Wave	IEMCAP	Standard model. Easily implemented. Applicable to ground wave propagation.
Complex Systems	GEMACS	May be used to analyze antenna coupling. Requires detailed input data. Computer memory requirements and run times excessive for application in system level analysis. Could be used off line to generate coupling data for input to system level analysis.
<b>Coupling Models-Field</b>		
Aperture	IEMCAP	Easily implemented simple model appropriate for system level analyses.
	GEMACS	Require detailed input data and considerable computer main memory and run time.
	GRD	May be used off line to generate internal field data for system level analysis.
<b>Wire, Case, Antenna</b>		
	IEMCAP	Easily implemented simple models appropriate for system level analysis.
	GEMACS , GRD	May be used off line to generate data for system level analysis.
<b>Coupling Models-Wires</b>		
Wire-to-Wire	IEMCAP	Models are appropriate for system level analysis. Require minimum input, main memory and run time. Provide reasonable results. Have been subject to extensive analysis and validation.
	GEMACS	Could be used off-line to analyze specific situations involving unusual geometries or requiring more accuracy than can be obtained with IEMCAP models.
<b>Transfer Models-Filter</b>		
Filter Models	IEMCAP	Provides analytical models for certain filter types.

D.1            SYSTEM LEVEL CODES

D.1.1        IEMCAP

The Intrasystem Electromagnetic Compatibility Analysis Program (IEMCAP) [Paul, no date] is a system-level EMC analysis program. IEMCAP is a link between equipment and subsystem EMC performance and total system EMC characteristics. It provides the means for tailoring EMC requirements to the specific system, whether it is ground-based, airborne, or a space/missile system. This is accomplished in IEMCAP by detailed modeling of the system elements and the various mechanisms of electromagnetic transfer to perform the following tasks:

1. Provide a data base that can be continuously maintained and updated to follow system design changes,
2. Generate EMC specification limits tailored to the system,
3. Evaluate the impact of granting waivers to the tailored specifications,
4. Survey a system for incompatibilities,
5. Assess the effect of design changes on system EMC, and
6. Provide comparative analysis results on which to base EMC tradeoff decisions.

IEMCAP is designed to predict interference in a population of receptors due to a population of emitters. The basic medium for modeling signals is the frequency domain. Each emitter's emission characteristics are represented by its power output, tuned frequency, emission spectrum in the vicinity of the tuned frequency, and spurious emission levels and frequencies. The model assumes that harmonic spurious output levels can be approximated by one or more straight line

segments. Spurious output frequencies are determined by the user as harmonics of the tuned frequency or, when applicable, are generated by the computer code.

The receptor representation is similar to that of the emitter; receptor characteristics are represented by its sensitivity, tuned frequency, selectivity curve, spurious response levels, and spurious frequencies. It is assumed that spurious response levels can be approximated by one or more straight lines. Spurious response frequencies are either generated by the code or determined by the user external to the program using available techniques; e.g., the superheterodyne conversion process.

The gains of low-gain antennas are determined by preprogrammed equations; medium- and high-gain antennas are represented by multilevel patterns in which each level is specified by a gain and associated azimuth and elevation beam width.

Various models of coupling or transfer functions are included in the program. Single tuned, transformer coupled, Butterworth tuned, low pass, high pass, band pass, and band reject filter models are employed. The filter transfer models calculate the "insertion loss" (in dB) provided by a filter at a given frequency; i.e., the reduction in delivered power due to insertion of a filter.

Two antenna-to-antenna propagation models are available. For ground systems, the propagation model is a simplified theoretical ground wave model that assumes a smooth earth surface and a 4/3 earth radius that accounts for atmospheric refraction. An intravehicular propagation model calculates the propagation loss associated with an electromagnetic coupling path when both emitter and receptor are located on the same system. Power received is related to power transmitted, free

space transmission (Friis equation), and a shading factor due to the presence of the vehicle whose bulk may be interposed in the region emitter and receptor.

Environmental electromagnetic field interaction with the system wiring is determined by the program. External fields enter a vehicle through dielectric apertures in the system's skin and couple onto wires immediately adjacent. The coupled RF energy is a function of the aperture size and location. A lumped parameter transmission line model is used to compute the currents induced in the wire loads. Artificial apertures are required for ground systems to determine certain field-to-wire conditions.

Coupling between wires in a common bundle comprises capacitive coupling (due to the interwire capacitance) and inductive coupling (due to the mutual inductances between the wires). Total coupling is approximated by summing the capacitive and inductive coupling (computed separately). Relatively complex wire configurations can be accommodated; e.g., shielded (single or double shield), unshielded, twisted pair, balanced, or unbalanced.

The equipment case model treats each case as though it were a dipole. The source model assumes a falloff of  $1/R^3$ , where R equals the distance between cases for both the electric and magnetic fields.

#### D.1.2 SEMCAP

The Specification and Electromagnetic Compatibility Analysis Program (SEMCAP) [SEMCAP, Aug. 1973; Biber, no date; Johnson, no date; Thomas, 1968; Johnson, 1968] is a computer program that performs system level compatibility analysis based upon the functional signal requirements of the system. It also develops the electromagnetic compatibility specification limits for interference generation and susceptibility applicable to the

subsystem or black box level equipments to be employed on the system, and contains waiver evaluation capability to evaluate lack of specification compliance.

SEMCAP is similar in many respects to IEMCAP. Both programs divide the system into a generator or emitter of energy, a transfer or coupling function which alters the emitted energy spectrum to account for the transmission medium, and a receptor response or susceptibility function. Although both SEMCAP and IEMCAP use similar models for emitters, transfer functions, and receptors, the programs utilize different systems equations for describing the interaction of these basic elements. The SEMCAP systems equations appear appropriate for transient or impulsive signals and threshold type devices, whereas the IEMCAP systems equations appear more suitable for continuous signals and devices that respond to average power.

#### D.1.3      SEMCA

The Shipboard Electromagnetic Compatibility Analysis (SEMCA) [SEMCA, no date] model consists of a set of computer routines or algorithms that enables one to conduct a comprehensive analysis regarding the compatibility of a ship's radiating and receiving equipments.

SEMCA is primarily used to assess equipment performance in the VLF/LF/HF and VHF/UHF ranges, but can be extended to include the microwave region. Though originally designed on a "cosite" model to address intraship problems, the model has been expanded to include signals emanating from "off-ship" sources.

SEMCA is tailored to shipboard environments; for example, intraship coupling is "tied" to ship topside modeling. The degradation outputs from SEMCA are primarily tied to communication systems; i.e., the articulation score or index for voice systems or bit-error-rate for TTY.

D.1.4        COSAM

The Cosite Analysis Model (COSAM) [Minor, July 1969; Lustgarten, 1970; Lustgarten, July 1970] is a system model used to evaluate the electromagnetic compatibility of a single site where a large number of transmitting and receiving communication equipments are employed. This "cosite" EMC analysis must take into account the close distance between antennas and the high level of undesired signals present at receiver inputs and transmitter outputs.

D.1.5        IPP-1

The Interference Prediction Process, Version 1 (IPP-1) [Duff, Jan. 1972] is a versatile computer code designed to assess transmitter-to-receiver interference and to provide useful parameters and data for optimizing compatibility in electromagnetic environments. IPP-1 may be used to assess interaction between equipments over a broad frequency span ranging from VLF through microwave systems. Although both pulse and nonpulse systems are within the capability of IPP-1, many of the submodels were generated to handle the special interaction mechanisms of nonpulse systems.

IPP-1, operating under the control of an "executive routine," can, through user options, "order" several basic types of analyses to be performed; e.g.,

1. EMC analysis,
2. Data base management,
3. Power density/field strength analysis,
4. Frequency/distance analysis,
5. Frequency band analysis,
6. Intermodulation analysis, and
7. Adjacent signal analysis.

IPP-1 initially involved only the EMC analysis. The other options were added later for special types of applications.

D.1.6        TRED

The Transmitter and Receiver Equipment Development (TRED) [Chase, Sept. 1971] model does not deal with EMC analysis of existing systems but, using EMC constraints and atmospheric noise considerations, specifies how a communication receiver system should be configured to obtain optimum communication performance in the presence of interference and noise. This model operates with the high frequency (2- to 30-MHz) band.

D.2        OTHER IAP CODES

D.2.1        GEMACS

The General Electromagnetic Model for the Analysis of Complex Systems (GEMACS) [Balestri, April 1977] is a user-oriented general purpose code for electromagnetic analysis of complex systems. The code supports all of the functions necessary for using one thin-wire method of moments (MOM) formulation. The GEMACS code uses a high-level language and provides flexibility of control over the computational sequence.

D.2.2        NCAP

The Nonlinear Circuit Analysis Program (NCAP) [Spina, 1979] allows determination of the nonlinear transfer functions of an electronic circuit. NCAP utilizes standard circuit elements and can analyze interconnecting networks of these elements.

NCAP is written in FORTRAN IV, has been implemented on the Honeywell 6180, can directly analyze networks containing up to 500 nodes, has a free-field format for input data, has capabilities to allow the user to build device models in addition to the several stored models, and has a user-oriented format.

NCAP solves the nonlinear network problem by forming both the nodal admittance matrix (Y matrix) for the entire network, and the first-order generator (current-source) excitation vector for all of the linear sources in the network. The generators can

be located at any node in the network and can have any desired frequency, amplitude, and phase. The usual procedure of premultiplying the generator vector by the inverse Y matrix results in the first-order nodal voltage vector for the network, the elements of which are the first-order transfer functions at all nodes in the network at the given excitation frequency. In the event that there is more than one generator at a given frequency, the first-order transfer function (which is linear) is the total transfer function due to the superposition of the generators. The higher-order transfer functions are solved iteratively.

#### D.2.3      PSTAT

The computer code Precipitation Charging, Noise Generation, and Coupling (PSTAT) [Nanevicz, Oct. 1974] is a computer code that predicts the effects of precipitation-static ("p-static") noise in aircraft systems. The computer code allows the EMC engineer, or systems designer, to determine the effects of p-static charging on a wide variety of aircraft types under a wide variety of flight situations. The code is based on the results of both experiment and analysis. The accuracy of PSTAT depends on the modeling and on the extent to which the experimental data represent the true picture of p-static noise. It is believed that PSTAT is accurate to within a few percent for KC-135 type aircraft, decreasing to tens of percent for widely divergent aircraft types (delta wing fighters, for example). The present program cannot be applied for helicopters or rockets because their geometries are radically different from aircraft.

#### D.2.4      XTALK, XTALK2, FLATPAK, FLATPAK2

Four transmission line codes are supported by the IAP: XTALK, XTALK2, FLATPAK, and FLATPAK2 [Paul, July 1977]. XTALK analyzes three configurations of transmission lines: (1) N+1 bare wires, (2) N bare wires above an infinite ground plane, and (3) N wires within a cylindrical shield filled with a homogeneous dielectric. All conductors are assumed to be perfect. XTALK2

analyzes the same three structural configurations as XTALK except that the conductors are permitted to be imperfect. FLATPAK analyzes ( $N+1$ ) wire ribbon cables; all wires are assumed to be perfect. FLATPAK2 analyzes the same configuration as FLATPAK except that the wires are permitted to be imperfect. In all four codes, the medium surrounding the conductors is assumed lossless. Sinusoidal steady-state excitation is assumed.

The four codes form an initial library of analysis capabilities for wire-coupled interference problems. A fifth transmission line code applicable to twisted wire pairs [Paul, Feb. 1978] also is supported by the IAP.

APPENDIX E  
REFERENCES

1. A. T. Adams, C. B. Varnado, and D. E. Warren, "Aperture Coupling by Matrix Methods", 1973 IEEE EMC Symposium Record, pp 226-240, June 1973.
2. A. K. Agrawal, H. M. Fowles, L. D. Scott, "Experimental Characterization of Multiconductor Transmission Lines in Inhomogeneous Media Using Time Domain Techniques", IEEE Trans. on Electromagnetic Compatibility, Vol. EMC-21, No. 1, pp 28-32, February 1979.
3. N. C. Albertsen, J. E. Hansen, and E. N. Eilskow Jensen, Computation of Spacecraft Antenna Radiation Patterns, Report ESRO CR-207, Technical Univ., Lyngby, Denmark, September 1973.
4. AMP (Antenna Modeling Program) Engineering Manual, M. B. Associates, ONR Contract, IS-R-72/10, July 1972. (See associated User Manual and Systems Manual for AMP code description.)
5. H. Bach, Description of and Manual for Polyhedral Satellite Program, Electromagnetic Inst., Technical Univ., Lyngby, Denmark, R 129, Sept. 1975.
6. C. A. Balanis and Y. B. Cheng, "Antenna Radiation Modeling for Microwave Landing System", IEEE Trans. on Antennas and Propagation, Vol. AP-24, No. 4, pp 490-497, July 1976.
7. R. J. Balestri, T. R. Ferguson, and E. R. Anderson, General Electromagnetic Model for the Analysis of Complex Systems, Vol. 2 - Engineering Manual, RADC-TR-77-137, Rome Air Development Center, Griffiss AFB, NY, April 1977. (See Vol. 1 - User's Manual for code description.)
8. C. E. Baum, "The Singularity Expansion Method", Topics in Applied Physics, Vol. 10, L. B. Felson, Ed., 1976.
9. C. E. Baum, T. K. Liu, and F. M. Tesche, On the Analysis of General Multiconductor Transmission-Line Networks, AFWL Interaction Note 350, Nov. 1978.
10. C. L. Bennett, J. D. DeLorenzo, and A. M. Auckenthaler, Integral Equation Approach to Wideband Inverse Scattering, RADC-TR-70-177, Rome Air Development Center, Griffiss AFB, NY, June 1970.
11. C. L. Bennett, et.al., Space Time Integral Equation Approach for Targets with Edges, AFWL Interaction Note 234, July 1974.
12. C. L. Bennett, R. Hieronymus, and H. Mieras, Impulse Response Target Study, RADC-TR-77-273, Rome Air Development Center, Griffiss AFB, NY, Sept. 1977.
13. R. G. Bergland, "Comparing Network Architectures", Datamation, Feb. 1978.
14. R. M. Bevensee, S3F-SYR/LLL1, The Syracuse Computer Code for Radiation and Scattering from Bodies of Revolution, Extended for Near-Field Computations, Report No. UCRL-51622, prepared for U.S. Atomic Energy Commission under Contract No. W-7405-Eng-48 with the Lawrence Livermore Laboratory, of California, Livermore, CA, May 1974.
15. R. M. Bevensee, Ed., Electromagnetic Computer Code Newsletter, Vol. 3, No. 1, Lawrence Livermore Laboratory, Univ. of California, Livermore, CA, 1976.

16. R. M. Bevensee, et.al., "Computer Codes for EMP Interaction and Coupling", IEEE Trans. on Electromagnetic Compatibility, Vol. EMC-20, No. 1, pp 156-165, February 1978. (Or see IEEE Trans. on Antennas and Propagation, Vol. AP-26, No. 1, January 1978.)
17. K. W. Biber, and A. K. Thomas, "Computer Assisted EMC Program on Pioneer F&G", SEMCAP Selected Technical Papers, TRW Systems Group, Redondo Beach, CA.
18. J. Boersma, "Computation of Fresnel Integrals", Math. Comp., Vol. 14, pg 380, 1960.
19. J. N. Brithingham, E. K. Miller, and J. L. Willows, Derivation of Simple Poles in a Transfer Function from Real-Frequency Information, Lawrence Livermore Laboratory Report UCRL-52050, April 1976.
20. D. Buchanan, et.al., Assessment of MOM Techniques for Shipboard Applications, RADC-TR-77-14, Rome Air Development Center, Griffiss AFB, NY, January 1977.
21. G. Burke and A. Poggio, Numerical Electromagnetic Code (NEC) - Method of Moments, NOSC/TD 116, Naval Ocean Systems Center, San Diego, CA, July 1977.
22. G. J. Burke, Lawrence Livermore Laboratory, Univ. of California, Livermore, CA, March 1979.
23. W. D. Burnside, M. C. Gilreath, R. J. Marhefka, and C. L. Yu, "A Study of KC-135 Aircraft Antenna Patterns", IEEE Trans. on Antennas and Propagation, Vol. AP-23, No. 3, pp 309-316, May 1975.
24. V. L. Carey, T. R. Scott, W. T. Weeks, "Characterization of Multiple Parallel Transmission Lines Using Time Domain Reflectometry", IEEE Trans. on Instrumentation and Measurements, Vol. IM-18, No. 3, September 1969.
25. J. P. Castillo, K. CA Chen, B. K. Singagaragu, Calculation of Currents Induced on a Disk by a Wire Grid Code, AFWL Interaction Note 230, Feb. 1975.
26. H. H. Chao and B. J. Strait, Computer Programs for Radiation and Scattering by Arbitrary Configurations of Bent Wires, Scientific Report No. 7 on Contract F19628-68-C-0180, AFCRL-70-0374, Syracuse Univ., Syracuse, NY, September 1970.
27. W. M. Chase and C. W. Tirrell, TRED HF Communication System Analysis, Naval Electronics Laboratory Center, San Diego, CA, September 1971.
28. J. C. Clements and C. R. Paul, Computation of the Capacitance Matrix for Dielectric Coated Wires, RADC-TR-74-59, Rome Air Development Center, Griffiss AFB, NY, March 1974.
29. P. Clemmow, "Edge Currents in Diffraction Theory", IRE Trans. on Antennas and Propagation, Vol. AP-4, pp 282-287, July 1956.
30. S. Coen, T. K. Liu, and F. M. Tesche, Calculation of the Equivalent Capacitance of a Rib Near a Single Wire Transmission Line, AFWL-TR-77-60, 1977.

31. T. T. Crow, B. D. Graves, and C. D. Taylor, "The Singularity Expansion Method as Applied to Perpendicular Crossed Wires", IEEE Trans. on Antennas and Propagation, Vol. AP-23, No. 4, pp 540-546, July 1975.
32. T. T. Crow, C. D. Taylor and M. Kumbale, "The Singularity Expansion Method Applied to Perpendicular Crossed Wires Over a Perfectly Conducting Ground Plane", IEEE Trans. on Antennas and Propagation, Vol. AP-27, No. 2, pp 248-251, March 1979.
33. G. A. Deschamps, "Ray Techniques in Electromagnetics", Proc. IEEE, Vol. 60, pp 1022-1035, September 1972.
34. W. G. Duff, et.al., Adjacent Channel Interference Analysis, RADC-TR-68-595, Rome Air Development Center, Griffiss AFB, NY, March 1969.
35. W. G. Duff, et.al., IPP-1 User's Manual, RADC-TR-71-300, Rome Air Development Center, Griffiss AFB, NY, January 1972. (See also IPP-1 Program Improvements, Atlantic Research Corp., Alexandria, VA. 1972.)
36. G. C. Feth, "Memories: Smaller, Cheaper, and Faster", IEEE Spectrum, June 1976.
37. D. J. Frediani, Jr., F. C. Lang, and B. F. LaPage, "A Comparison of Measured Radar Cross Sections of Solid and Mesh Ogives", IEEE Trans. on Antennas and Propagation, Vol. AP-22, No. 3, pp 427-432, May 1974.
38. E. Freeman, IEMCAP Implementation Study, RADC-TR-77-374, Rome Air Development Center, Griffiss AFB, NY, 1977.
39. D. V. Giri, S. K. Chang, and F. M. Tesche, A Coupling Model for a Pair of Skewed Transmission Lines, AFWL Interaction Note 349, September 1978.
40. A. W. Glisson, Jr., On the Development of Numerical Techniques for Treating Arbitrarily-Shaped Surfaces, PhD Dissertation, Electrical Engineering Dept., Univ. of Mississippi, Oxford, MS. June 1978. (Or see Simple and Efficient Numerical Techniques for Treating Bodies of Revolution, RADC-TR-79-22, Rome Air Development Center, Griffiss AFB, NY, March 1979.)
41. J. C. Hancock, An Introduction to the Principles of Communication Theory, McGraw-Hill, 1961.
42. R. F. Harrington, Field Computation by Moment Methods, The MacMillan Company, 1968.
43. R. F. Harrington and J. R. Mautz, Radiation and Scattering from Bodies of Revolution, Final Report, prepared for Air Force Cambridge Research Laboratories, Bedford, MA, under Contract F19628-67-C-0233, July 1969.
44. R. F. Harrington and J. R. Mautz, "An Impedance Sheet Approximation for Thin Dielectric Shells", IEEE Trans. on Antennas and Propagation, Vol. AP-23, No. 4, pp 531-534, July 1975.
45. R. F. Harrington and J. R. Mautz, "A Generalized Network Formulation for Aperture Problems", IEEE Trans. on Antennas and Propagation, pp 870-873, November 1976.
46. R. F. Harrington, Electrical and Computer Engineering Department, Syracuse Univ., Syracuse, NY, Private Communication, February 1979.

47. Interference Notebook, Volume I, RADC-TR-66-1, Rome Air Development Center, Griffiss AFB, NY, July 1967.
48. Intrasytem Electromagnetic Compatibility Analysis Program (IEMCAP), (4 Volumes), in particular, Volume I, (User's Manual, Engineering Section) and Volume II (User's Manual, Usage Section), RADC-TR-74-342, Rome Air Development Center, Griffiss AFB, NY, December 1974.
49. P. Isaacson, "Personal Computing", Datamation, July 1978.
50. G. James, Geometrical Theory of Diffraction for Electromagnetic Waves, Peter Peregrinus Ltd, 1976.
51. W. R. Johnson, "Computerized Electromagnetic Compatibility Specification Development for Space Vehicles", 1968 IEEE EMC Symposium Record.
52. W. R. Johnson, J. A. Spagon, A. K. Thomas, "Application of Computer Technology to the Implementation of EMC Programs", SEMCAP Selected Technical Papers, TRW Systems Group, Redondo Beach, CA.
53. D. S. Jones, "Numerical Methods for Antenna Problems", Proc. IRE, Vol. 121, No. 7, pp 573-582, July 1974.
54. J. b. Keller, "Geometrical Theory of Diffraction", Journal of the Optical Society of America, 52, pp 116-130, February 1962.
55. R. W. P. King, R. B. Mack, and S. S. Sandler, Arrays of Cylindrical Dipoles, New York, Cambridge Univ. Press, 1968.
56. C. Klein and R. Mittra, "Stability of Matrix Equations Arising in Electromagnetics," IEEE Trans. on Antennas and Propagation, Vol. AP-21, No. 6, pp 902-905, November 1973.
57. C. A. Klein and R. Mittra, "An Application of the Condition Number Concept in the Solution of Scattering Problems in the Presence of the Interior Resonant Frequency", IEEE Trans. Antennas and Propagation, Vol. 23, No. 3, pp 431-435, May 1975.
58. E. Knott and T. B. A. Senior, "Comparison of Three High-Frequency Diffraction Techniques", Proc. IEEE, Vol. 62, pp 1468-1474, Nov. 1974.
59. R. G. Kouyoumjian and Pathak, "A Uniform Geometrical Theory of Diffraction for an Edge in a Perfectly Conducting Surface", Proc. IEEE, Vol. 62, pp 1448-1461, November 1974.
60. R. G. Kouyoumjian, "The Geometrical Theory of Diffraction and its Applications", Numerical and Asymptotic Techniques in Electromagnetics, Springer-Verlog, NY, 1975.
61. D. C. Kuo and B. J. Strait, Improved Programs for Analysis of Radiation and Scattering by Configurations of Arbitrarily Bend Thin Wires, Scientific Report No. 15, Contract No. F19628-68-C-0180 with Air Force Cambridge Research Laboratories, Bedford, MA, January 1972. (Or see D. C. Kuo, H. H. Chao, J. R. Mautz, B. J. Strait, and R. F. Harrington, "Analysis of Radiation and Scattering by Arbitrary Configurations of Thin Wires", (computer program description), IEEE Trans. on Antennas and Propagation, Vol. AP-23, No. 3, pp 450-451, May 1975. A program listing is available from NAPS as document 01798.)

62. J. A. Landt, E. K. Miller, and M. VanBlaricum, WT-MBA/LLL1B: A Computer Program for the Time-Domain Electromagnetic Response of Thin-Wire Structures, Report UCRL-51585, Lawrence Livermore Laboratory, Univ. of California, Livermore, CA, May 1974.
63. C. P. Lecht, The Waves of Change, Advanced Computer Techniques, Inc., 1977.
64. K. S. Lee, "Two Parallel Terminated Conductors in External Fields", IEEE Trans. on Electromagnetic Compatibility, Vol. EMC-20, No. 2, May 1978.
65. S. W. Lee, "Electromagnetic Reflection from a Conducting Surface: GO Solution", IEEE Trans. on Antennas and Propagation, Vol. AP-23, March 1975.
66. S. W. Lee, "Uniform Asymptotic Theory of Electromagnetic Edge Diffraction: A Review", Univ. of Illinois, Technical Report 77-1, 1977.
67. S. W. Lee, Differential Geometry for GTD Applications, Univ. of Illinois, Technical Report 77-21, October 1977.
68. S. W. Lee, "Geometric Optics", Univ. of Illinois, Technical Report 78-2, May 1978.
69. T. L. Lin, W. L. Curtis, and M. C. Vincent, "Radar Cross Sections of a Rectangular Conducting Plate by Wire Mesh Modeling", IEEE Trans. on Antennas and Propagation, Vol. AP-22, No. 5, pp 718-720, September 1974.
70. Y. T. Lin, "Computation of Low Frequency Scattering from Airplanes", Electroscience Laboratory Report 2768-9, Ohio State University, Columbus, Ohio, September 1972. (See also IEEE Trans. on Antennas and Propagation, pp 53-56, January 1975).
71. T. K. Liu, Electromagnetic Coupling Between Multiconductor Transmission Lines in a Homogeneous Medium, AFWL Interaction Note 309, December 1976.
72. T. K. Liu, F. M. Tesche, and S. K. Chang, Numerical Results for Multi-Conductor Transmission-Line Networks, AFWL EMP Interaction Note 322, September 1977.
73. "Look Ahead", Datamation, July 1978.
74. M. Lustgarten, Air Force Project #649E, Contract F 19628-69-C-0073, IIT Research Institute, Annapolis, MD, 1970.
75. M. Lustgarten, "Cosite Analysis Model (COSAM)", 1970 IEEE International Symposium, July 1970.
76. P. C. Magnusson, Transmission Lines and Wave Propagation, Allyn and Bacon, 1970.
77. R. J. Marhefka, User's Manual for Plates and Cylinder Computer Code, Ohio State Univ., Electroscience Laboratory Technical Report 4508-8, March 1978.
78. R. J. Marhefka, Ohio State Univ. Electroscience Laboratory, Private Communication, May 1978.
79. L. Marin, "Natural - Mode Representation of Transient Scattering from Rotationally Symmetric Bodies", IEEE Trans. on Antennas and Propagation, Vol. AP-22, No. 2, pp 266-274, March 1974.

80. K. D. Marx, "Propagation Modes, Equivalent Circuits, and Characteristics Terminations for Multiconductor Transmission Lines with Inhomogeneous Dielectrics", IEEE Trans. on Microwave Theory and Technique, Vol. MTT-21, No. 7, July 1973.
81. J. R. Mautz, Scattering from Loaded Wire Objects Near a Loaded Surface of Revolution, Report No. SURC TN 74-030, Space and Missile System Organization, Air Force Systems Command, Los Angeles, CA, under Contract F 04801-71-C-0056, January 1974.
82. J. R. Mautz and R. F. Harrington, H-Field, E-Field, and Combined Field Solutions for Bodies of Revolution, (with computer program), TR-77-2 and TR-77-3, Syracuse Univ., Electrical and Computer Engineering Dept., Syracuse, NY, February and May 1977.
83. J. R. Mautz and R. F. Harrington, Electromagnetic Scattering From a Homogeneous Body of Revolution, TR-77-10, Electrical and Computer Engineering Dept., Syracuse Univ., Syracuse, NY, November 1977.
84. L. N. Medgyesi-Mitschang, "Analysis of Extended Off-Surface Radiators", IEEE International Symposium on Electromagnetic Compatibility, Washington, D.C., pp 308-311, July 1976.
85. L. N. Medgyesi-Mitschang, "A Method of Moments Formulation for Bodies of Translation", IEEE Antennas and Propagation Symposium Digest, pp 122-125, Washington, D.D., May 1978.
86. K. K. Mei "Unimoment Method of Solving Antenna and Scattering Problems", IEEE Trans. on Antennas and Propagation, Vol. AP-22, pp 760-766, November 1974.
87. E. K. Miller, Some Computational Aspects of Transient Electromagnetics, Report UCRL-51276, Lawrence Livermore Laboratory, Univ. of California, Livermore, CA, September 1972.
88. E. K. Miller, et.al., An Evaluation of Computer Programs Using Integral Equations for the Electromagnetic Analysis of Thin-Wire Structures, Report UCRL-75566 Rev. 1, Lawrence Livermore Laboratory, Univ. of California, Livermore, CA, March 1974.
89. E. K. Miller and F. J. Deadrick, Some Computational Aspects of Thin-Wire Modeling, Lawrence Livermore Laboratory, Report UCRL 74818, Univ. of California, Livermore, CA, June 1973. (See also Numerical and Asymptotic Techniques in Electromagnetics, Chapt. 4, R. Mittra, Ed., NY:Springer-Verlag, 1975.)
90. E. K. Miller and A. J. Poggio, "Moment-Method Techniques From an Applications Viewpoint", Proc. Nat. Conf. on Electromagnetic Scattering, Univ. of Illinois at Chicago Circle, June 15-18, 1976.
91. L. Minor, E. Neham, and J. Wilson, Cosite Analysis Model, ECAC Report R-189, July 1969.
92. R. Mittra, Y. Rahmat-Samii, and W. L. Ko, "Spectral Theory of Diffraction", Applied Physics, Vol. 10, pp 1-13, 1976.

93. M. A. Morgan, S. K. Chang, and K. K. Mei, "Coupled Azimuthal Potentials for Electromagnetic Field Problems in Inhomogeneous Axially Symmetric Media", IEEE Trans. on Antennas and Propagation, Vol. AP-25, No. 3, pp 413-417, May 1977.
94. M. A. Morgan and F. M. Tesche, "Basic Statistical Concepts for Analysis of Random Cable Coupling Problems", IEEE Trans. on Electromagnetic Compatibility, Vol. 20, No. 1, pp 185-187, February 1978.
95. M. A. Morgan and K. K. Mei, "Finite Element Computation of Scattering by Inhomogeneous Penetrable Bodies of Revolution", IEEE Trans. on Antennas and Propagation, Vol. AP-27, No. 2, pp 202-214, March 1979.
96. P. D. Moulton, and R. C. Sander, "Another Look at SNA", Datamation, March 1977.
97. J. E. Nanevicz and D. G. Douglas, Static Electricity Analysis Program, Vols. I and II, SAMS0-TR-75-44, Stanford Research Institute, Oct. 1974.
98. E. H. Newman and P. Tulyathan, "Wire Antennas in the Presence of a Dielectric/Ferrite Inhomogeneity", IEEE Trans. on Antennas and Propagation, Vol. AP-26, No. 4, pp 587-593, July 1978.
99. E. H. Newman and D. M. Pozar, "Electromagnetic Modeling of Composite Wire and Surface Geometries", IEEE Trans. on Antennas and Propagation, Vol. AP-26, No. 6, pp 784-789, November 1978.
100. Nonlinear System Modeling and Analysis with Applications to Communications Receivers, RADC-TR-73-178, Rome Air Development Center, Griffiss AFB, NY, June 1973.
101. D. T. Paris and F. K. Hurd, Basic Electromagnetic Theory, McGraw-Hill, 1969.
102. A. Papoulis, Probability, Random Variables, and Stochastic Processes, McGraw-Hill, 1965.
103. C. R. Paul, "On Uniform Multimode Transmission Lines", IEEE Trans. on Microwave Theory and Technique, No. 8, August 1973.
104. C. R. Paul, Multiconductor Transmission Line Theory, RADC-TR-76-101, Vol. I, Rome Air Development Center, Griffiss AFB, NY, April 1976.
105. C. R. Paul and A. E. Feather, "Computation of Transmission Line Inductance and Capacitance Matrices from the Generalized Capacitance Matrix", IEEE Trans. on Electromagnetic Compatibility, Vol. EMC-18, No. 4., November 1976.
106. C. R. Paul and A. G. Feather, "Application of Moment Methods to the Characterization of Ribbon Cables", Computer and Electronic Engineering, Vol. 4, pp 173-184, Pergamon Press, Great Britain, 1977.
107. C. R. Paul, Applications of Multiconductor Transmission Line Theory to the Prediction of Cable Coupling, RADC-TR-76-101, Volume VII, Rome Air Development Center, Griffiss AFB, NY, July 1977.

108. C. R. Paul, "Applications of Multiconductor Transmission Line Theory to the Prediction of Cable Coupling", RADC-TR-76-101, Volume VI, Rome Air Development Center, Griffiss AFB, NY, February 1978.
109. C. R. Paul, "Solution of the Transmission Line Equations for Three Conductor Lines in Homogeneous Media", IEEE Trans. on Electromagnetic Compatibility, Vo.. EMC-20, No. 1, pp 216-222, February 1978.
110. C. R. Paul, Univ. of Kentucky, Private Communication, 1979.
111. C. R. Paul, Analysis of Electromagnetic Coupling in Branched Cables, Technical Report soon to be published by RADC under Contract F30602-79-C-0011, 1979.
112. C. R. Paul, "Analysis of Electromagnetic Coupling in Branched Cables", IEEE Electromagnetic Compatibility Symposium, San Diego, CA. Oct. 1979.
113. C. R. Paul, A Summary of Models in IEMCAP, prepared for Intrasystem Analysis Program Course, Rome Air Development Center.
114. R. A. Pearlman, Intrasystem Electromagnetic Compatibility Analysis Program (IEMCAP) F-15 Validation-Interpretation of the Integrated Margin, RADC-TR-77-290, Part II, Rome Air Development Center, Griffiss Air Force Base, NY, September 1977.
115. J. Perini and H. K. Schuman, Method of Moment Thin Wire Computer Program Comparisons for Complex Structures and Coarse Accuracy, RADC-TR-78-106, Rome Air Development Center, Griffiss Air Force Base, NY, May 1978.
116. E. I. Piatkowski, et.al., "Field Penetration Into a Spherical Cavity by Wire Mesh Modeling", IEEE Antennas and Propagation Symposium Digest, Univ. of Illinois, Urbana, IL, pp 67-70, June 1975.
117. A. J. Poggio, M. L. Van Blaricum, E. K. Miller, and R. Mittra, "Evaluation of a Processing Technique for Transient Data", IEEE Trans. on Antennas and Propagation, Vol. AP-26, No.1, pp 165-173, January 1978.
118. R. J. Pogorzelski, "Scattering from Inhomogeneous and/or Composite Bodies of Arbitrary Shape", IEEE Antennas and Propagation International Symposium, Amherst, MA, pp 429-431, October 1976.
119. A. Ralston, A First Course in Numerical Analysis, McGraw-Hill, 1965.
120. S. S. M. Pao and D. R. Wilton, Electrical Engineering Dept., Univ. of Mississippi, Oxford MS, Private Communication, April 1979.
121. J. H. Richmond, "Computer Program for Thin-Wire Structures in a Homogeneous Conducting Medium", Ohio State Electroscience Laboratory, No. Date. (For brief code description see: IEEE-Trans. on Antennas and Propagation, Vol. AP-22, No. 2, pg 365, March 1974, and NAPS Document 02223.)
122. J. H. Richmond, D. M. Pozar, and E. H. Newman, "Rigorous Near-Zone Field Expressions for Rectangular Sinusoidal Monopole", IEEE Trans. on Antennas and Propagation, Vol. AP-26, pp 509-510, May 1978.
123. C. E. Ryan, Assessment of Geometrical Theory of Diffraction for Shipboard Applications, Georgia Institute of Technology, Engineering Experiment Station Interim Report At1736, August 1975.

124. T. K. Sarkar and B. J. Strait, Analysis of Arbitrarily Oriented Thin-wire Antennas Over a Plane Imperfect Ground, Syracuse Univ. Report TR-75, December 1975.
125. T. K. Sarkar and D. D. Weiner, "Scattering Analyses of Nonlinearly Loaded Antennas", IEEE Trans. on Antennas and Propagation, pp 125-131, March 1976.
126. T. F. Sarkar, "Analysis of Radiation by Arrays of Arbitrarily Oriented Wire Antennas Over Plane Imperfect Ground (Reflection-Coefficient Method)", IEEE Trans. on Antennas and Propagation, Vol. AP-29, pg 546, July 1976.
127. T. F. Sarkar, D. D. Weiner, and R. F. Harrington, "Analysis of Nonlinearly Loaded Multiport Antenna Structures Over an Imperfect Ground Plane Using the Volterra-Series Method", IEEE Trans. on Electromagnetic Compatibility, Vol. EMC-20, No. 2, pp 278-287, May 1978.
128. J. F. Schaeffer and L. N. Medgyesi-Mitschang, "Junction Treatment for BOR-Wire Geometrics", International IEEE Antennas and Propagation Society Symposium, Seattle, Washington, June 1979.
129. H. H. Schenck, "Improved Integral Formulation for Radiation Problems", J. Acoust. Soc. Am., Vol. 44, pp 41-58, 1968.
130. H. K. Schuman and R. F. Harrington, "Body of Revolution Modeling and Applications to EMC", IEEE Electromagnetic Compatibility Symposium, Washington, D.C., pp 295-300, July 1976.
131. H. K. Schuman, The Analysis of Aperture Coupling in Bodies of Revolution by Combining Methods Optimum for Internal and External Regions, Atlantic Research Corporation, August 1978.
132. H. K. Schuman and D. E. Warren, "Aperture Coupling in Bodies of Revolution", IEEE Tran. on Antennas and Propagation, AP-26, pp 778-783, November 1978.
133. SEMCA V; Volumes C, XA, and XB, General Electric Company, Daytona Beach, FL.
134. SEMCAP Program Description, Version 7.3 TRW Systems Group, Redondo Beach, CA, 1973.
135. SIGGRAPH, "Status Report of the Graphics Standards Planning Committee", Computer Graphics, Vol. 11, No. 3, Fall 1977.
136. SIGGRAPH, Computer Graphics, Vol. 12, Nos. 1-2, June 1978.
137. A. A. Smith, Coupling of External Electromagnetic Fields to Transmission Lines, Wiley and Sons, 1977.
138. J. Spina, et.al., "Nonlinear Circuit Analysis Program (NCAP) Documentation", RADC-TR-79-245, Vol. 1 - Engineering Manual; Vol. 2 - User's Manual; Vol. 3 - Programmer's Manual, Rome Air Development Center, Griffiss Air Force Base, NY, 1979.
139. A. Taflove and M. E. Brodwin, "Numerical Solution of Steady-State Electromagnetic Scattering Problems Using the Time-Dependent Maxwell's Equations", IEEE Trans. on Microwave Theory and Technique, Vol. MIT-23, No. 8, pp 623-630, August 1975.

140. A. Taflove, Time Domain Solutions for Electromagnetic Coupling, RADC-TR-78-142, Rome Air Development Center, Griffiss AFB, NY, June 1978.
141. F. M. Tesche, "On the Analysis of Scattering and Antenna Problems Using the Singularity Expansion Techniques", IEEE Trans. on Antennas and Propagation, Vol. AP-21, No. 1, pp 53-62, January 1973.
142. F. M. Tesche, M. A. Morgan, B. Fishbine, and E. R. Parkinson, Internal Interaction Analysis: Topological Concepts and Needed Model Improvements, AFWL Interaction Note 248, July 1975.
143. F. M. Tesche, An Electromagnetic Model for a Cable Clamp on a Single Wire Transmission Line, AFWL Interaction Note 107, December 1976.
144. F. M. Tesche, T. K. Liu, S. K. Chang, and D. V. Girk, Field Excitation of Multiconductor Transmission Lines, AFWL Interaction Note 351, September 1978.
145. F. M. Tesche, Private Communication, March 1979.
146. F. M. Tesche, "Analysis of Transmission Line Networks", soon to be included in AFWL EMC Handbook.
147. D. J. Theis, "An Overview of Memory Technologies", Datamation, Jan. 1978.
148. G. A. Thiele, Computer Techniques for Electromagnetics, Edited by R. Mittra, Pergamon Press Ltd., 1973.
149. G. Thiele and T. Newhouse, "A Hybrid Technique for Combining Moment Methods with the Geometric Theory of Diffraction", IEEE Trans. on Antennas and Propagation, Vol. AP-23, No. 1, pp 62-69, January 1975.
150. A. K. Thomas, "Math Modeling Techniques for a Computerized EMC Analysis", SEMCAP Selected Technical Papers, TRW Systems Group, Redondo Beach CA, 1968 IEEE EMC Symposium Record.
151. P. Ya. Ufimtsev, "Method of Edge Waves in the Physical Theory of Diffraction", FTD-4C-23-259-71, Foreign Tech Division, Air Force Systems Command, NTIS AD No. 733203, September 1971. (Translated from the Russian)
152. D. E. Warren, "Eear Electric and Magnetic Fields of Wire Antennas", IEEE Trans. on Antennas and Propagation, (Computer program description) Vol. AP-22, No. 2, p. 364, March 1974. (See also NAPS document 02221 D. E. Warren, "A User Manual for Program WRSMOM", available from the author, Rome Air Development Center, Air Force Systems Command, Griffiss AFB, New York 13441.)
153. N. Weizer, "Distributed System of the 1980s", Information Systems in the 1980s, Arthur D. Little, Inc. 1978.
154. J. J. Whalen, "Predicting RFI Effects in Semiconductor Devices at Frequencies Above 100 MHz", IEEE Trans. on Electromagnetic Compatibility, Vol. EMC-21, No. 4, pp 281-282, November 1979.
155. D. R. Wilton and C. M. Butler, "Efficient Numerical Techniques for Solving Pocklington's Equation and Their Relationships to Other Methods", IEEE Trans. on Antennas and Propagation, Vol. AP-24, pp 83-86, January 1976.

156. D. R. Wilton, Electrical Engineering Dept., Univ. of Mississippi, Oxford, MS, Private Communication, April 1979.
157. F. G. Withington, "IBM's Future Large Computers", Datamation, July 1978.
158. K. S. Yee, "Numerical Solution of Initial Boundary Value Problems Involving Maxwell's Equations in Isotropic Media", IEEE Trans. on Antennas and Propagation, Vol. AP-14, pp 302-307, May 1966.

THE  
LAW  
OF  
NATURE  
AND  
GRATITUDE  
TO  
THE  
AMERICAN  
PEOPLES  
BY  
JOHN  
ADAMS  
1776